Lipid Extraction and Bionanocomposites Synthesis from Spent Hens

by

Muhammad Safder

A thesis submitted in partial fulfillment of the requirements for the degree of

Doctor of Philosophy

in

Bioresource & Food Engineering

Department of Agricultural, Food and Nutritional Science
University of Alberta

ABSTRACT

Spent hen, a poultry industry by-product with little market value and high lipid content, can be used as a new and sustainable biomass source for lipid production. This study focused on environmentally benign extraction methods, i.e., the microwave-assisted and supercritical CO_2 extraction of lipids from the spent hen and conversion of extracted lipid into bionanocomposites.

First, over 95% of the lipids were recovered within 10 min using microwaves. Factors affecting the lipid extraction yield, including extraction time, temperature, and the solvent-to-feed ratio were studied using response surface methodology. To account for the low sample size, parametric bootstrapping was used with a replacement approach. Data in all combinations were bootstrapped 10,000 times, which showed a decrease in standard deviation. Fatty acid profiles of extracts obtained under different conditions were investigated using gas chromatography equipped with mass spectrometry and a flame ionization detector for qualitative and quantitative analysis, respectively. The lipids predominantly contained oleic (46%), linoleic (~22%), and palmitic (~23%) acids. Proton nuclear magnetic resonance spectroscopy (^{1}H NMR) and Fourier transform infrared spectroscopy were used to characterize different functional groups in the lipids. The phase transitions and thermal degradation behavior of lipids were determined using differential scanning calorimetry and thermogravimetric analysis, respectively.

Second, lipids were extracted using supercritical carbon dioxide (SC-CO_2) at 50−70 °C, 30−50 MPa, and constant CO_2 flow rate of 1 L/min (measured at ambient conditions). The maximum yield of total lipid 37$\pm$0.4% (w/w) with 92% recovery was obtained at 50 MPa/70 °C. Fatty acid compositional analysis was performed using gas chromatography with flame ionization detector (GC-FID). Helium ion microscopy (HIM) was used to assess the morphological changes before and after extraction. Furthermore, epoxidation of the extracted lipids was conducted with

and without the use of a solvent, where the solvent-free epoxidation was completed within 20 min. The reaction progress was monitored by attenuated total reflectance-Fourier transform infrared (ATR-FTIR) and ^{1}H NMR spectroscopy analysis, which showed the conversion rates of 59.8, 84.2 and 100% at 5, 10, and 20 min, respectively. The findings suggest that an alternative bio-epoxy can be produced using SC-CO_2 extraction and solvent-free epoxidation of extracted lipids from poultry industry waste/by-product.

Third, a monomer was synthesized using the mixture of fatty acids obtained through the hydrolysis of triglycerides extracted from spent hens. The reaction conditions of temperature and time were studied to obtain a high molecular weight biopolymer using bulk polymerization. The bionanocomposites were then prepared with different ratios of nanoclay (0, 3, 5, and 10%) using *in situ* polymerization. The bionanocomposite films were prepared using compression molding and the effect of nanoparticle addition, in terms of their dispersion and impact on the final material properties, was investigated by different characterization techniques. Results indicated improved thermal stability for nanoreinforced biocomposites. The flammability test showed substantial improvements in the flame retardancy of bionanocomposites compared to the neat biopolymer. These results suggest that high-performance bionanomaterials can be developed from spent hen lipids through *in situ* dispersion of nanoclay during polymerization.

Finally, a novel unsaturated macromonomer containing both saturated and unsaturated fatty acids was synthesized from spent hen lipids and its chemical structure was characterized by FTIR, ^{1}H NMR, and gel permeation chromatography (GPC). The monomer was synthesized via epoxidation of spent hen lipids, followed by grafting nanocellulose groups and acrylic groups subsequently onto spent hen lipid molecules. The bionanocomposites were prepared by *in situ* addition of modified nanoclay in different proportions. Also, the nanocomposites were synthesized

by copolymerization of spent hen lipid monomer and styrene. The obtained spent hen lipid monomer possessed a highly polymerizable C═C functionality, consequently resulting in rigid bioplastics. The synthesized cross-linked biomaterial from spent hen lipids provide an environmentally friendly material showing potential for use in structural plastics.

In summary, lipids were extracted from the whole carcass of spent hens with high yields by microwave-assisted and SC-CO_2 extraction and converted to bioepoxy materials. Furthermore, the extracted lipids were converted to bionanocomposites with enhanced thermal stability and flame retardancy properties. Moreover, environmentally friendly technologies such as microwave-assisted extraction and SC-CO_2 extraction not only helped to reduce the lipid extraction time, but also minimized the use of toxic organic solvents. Overall, in addition to several environmental advantages, this research would benefit poultry, packaging, food and plastics industries.

PREFACE

This thesis contains original work done by Muhammad Safder and has been written according to the guidelines for a paper format thesis of the Faculty of Graduate Studies and Research at the University of Alberta. The concept and idea of this work originated from Muhammad Safder and his supervisor, Dr. Aman Ullah and co-supervisor Dr. Feral Temelli. The whole thesis is composed of seven chapters: Chapter 1 presents an introduction to this project and the objectives of the thesis. Chapter 2 is a literature review regarding spent hens, lipid extraction methods, and lipid-based bionanocomposites.

Chapter 3 has been published as Muhammad Safder, Feral Temelli, and Aman Ullah, "Extraction, optimization, and characterization of lipids from spent hens: An unexploited sustainable bioresource" Journal of Cleaner Production 206 (2019) 622-630. In this chapter, Muhammad Safder was responsible for the experimental design and conducting the experiments, data analysis and writing the first draft of the manuscript. Dr. Aman Ullah is the corresponding author and Dr. Ullah and Dr. Temelli were responsible for the experimental design, data interpretation, correction and submission of the manuscript.

Chapter 4 has been published as Muhammad Safder, Feral Temelli, and Aman Ullah, "Supercritical CO_2 extraction and solvent-free rapid alternative bio epoxy production from spent hens" Journal of CO_2 Utilization 34 (2019) 335-342. In this chapter, Muhammad Safder was responsible for designing and conducting the experiments, data analysis and writing the first draft of the manuscript. Dr. Ullah and Dr. Temelli are the corresponding authors and were responsible for the experimental design, data interpretation, correction and submission of the manuscript.

Chapter 5 is to be submitted for consideration for publication as Muhammad Safder, Feral Temelli, and Aman Ullah, "Lipid-derived hybrid bionanocomposites from spent hens". In this

chapter, Muhammad Safder was responsible for designing and conducting experiments, data analysis and writing the first draft of the manuscript. Dr. Ullah is the corresponding author and Dr. Ullah and Dr. Temelli were responsible for the experimental design, data interpretation, correction and submission of the manuscript.

Chapter 6 is to be submitted for consideration for publication as Muhammad Safder, Feral Temelli, and Aman Ullah, "CNC grafted nanoclay reinforced bionanocomposites from spent hens". In this chapter, Muhammad Safder was responsible for designing and conducting experiments, data analysis and writing the first draft of the manuscript. Dr. Ullah is the corresponding author and Dr. Ullah and Dr. Temelli were responsible for the experimental design, data interpretation, correction and submission of the manuscript.

This dissertation is dedicated to my beloved family

ACKNOWLEDGMENTS

First and foremost, I would like to express my sincere gratitude to my supervisor Dr. Aman Ullah for giving me an opportunity to be part of his group and provided me with enormous support, encouragement, and guidance throughout my Ph.D. study. His excellent supervision, humbleness, and patience enabled me to acquire considerable valuable experience. I am deeply grateful to my co-supervisor Dr. Feral Temelli for her invaluable motivation and intellectual support, which enabled me to develop my abilities as a researcher with critical thinking, organization of thoughts, and academic writing during my Ph.D. study.

I would like to thank Dr. Thava Vasanthan for being in my supervisory committee and all of his valuable feedback during my Ph.D. program. Special thanks to Dr. Prashant Waghmare from the Department of Mechanical Engineering to be in my examining committee and Dr. Hom Nath Dhakal from the School of Engineering of University of Portsmouth, England as my external examiner, and all of their feedback for my Ph.D. defense.

I would also like to express my sincere gratitude to my excellent colleagues and friends, Dr. Muhammad Arshad, Muhammad Zubair, Dr. Ricardo Tomas Do Couto, Dr. Karina Araus, Reza Ahmadi, Dr. Altaf Hussain, Rehan Ali, for their help and suggestions in my experimental work. Special thanks to Ereddad Kharraz for assisting in the use of a variety of instruments.

I am also grateful to the financial support of the Canadian Poultry Research Council (CPRC), Alberta Livestock and Meat Agency Ltd (ALMA), and Natural Sciences and Engineering Research Council (NSERC). Special thanks to Kelly Berdahl for all the arrangements for my defense.

Ultimately, I would like to thank my parents, wife, children, brothers, and sisters for their unconditional love, support, and encouragement throughout my Ph.D. program, which gave me

continuous motivation, energy, and courage to overcome any challenges in the pursuit of my career goals. Thanks to all my friends located around the world especially Dr. Ishtiaq Ahmed Khan for encouragement, help, and support, which are cherished by me as memories of good times we shared together.

TABLE OF CONTENTS

LIST OF TABLES

LIST OF FIGURES

LIST OF ABBREVIATIONS

AFM	Atomic force microscopy
AIBN	Azobisisobutyronitrile
ANOVA	Analysis of variance
ATR-FTIR	Attenuated total reflectance - Fourier transform infrared spectroscopy
CNC	Cellulose nanocrystals
DCC	Dicyclohexylcarbodiimide
DCM	Dichloromethane
DMA	Dynamic mechanical analysis
DMAP	4-(Dimethylamino) pyridine
DSC	Differential scanning calorimetry
EtOAc	Ethyl acetate
FTIR	Fourier transform infrared spectroscopy
GC-FID	Gas chromatography-flame ionization detector
GC-MS	Gas chromatography-mass spectrometry
GPC	Gel permeation chromatography
H NMR	Proton nuclear magnetic spectroscopy
HIM	Helium ion microscope
KOH	Potassium hydroxide
MAE	Microwave-assisted extraction
MeOH	Methanol
MU	Moisture uptake
RSM	Response surface methodology

SC-CO_2	Supercritical carbon dioxide
SD	Standard deviation
SDB	Standard deviation bootstrap
SDE	Standard deviation experimentally
SEM	Scanning electron microscopy
sem	Standard error of the mean
SFE	Supercritical fluid extraction
SPE	Solid phase extraction
TAGs	Triacylglycerols
TEM	Transmission electron microscopy
TGA	Thermogravimetric analysis
THF	Tetrahydrofuran
TLC	Thin layer chromatography
XRD	X-ray diffraction

CHAPTER 1 - INTRODUCTION AND THESIS OBJECTIVES

In the last few decades, the use of fossil fuel-derived polymers has tremendously increased in various applications including packaging, clothing, automobiles, space technology, buildings, adhesives, cosmetics, medical devices, electronics, diagnostics and other industrial fields. Worldwide, the consumption of plastics has been growing continuously over the past 50 years with an annual increase rate of over 5%, with the total annual utilization exceeding over 300 million metric tons in 2016 (Brockhaus et al., 2016). Generally, fossil resources are the main precursors for the production of monomers on industrial scale and as a result over 7% of the global oil and gas production goes into making plastics (Zhang et al., 2017), yet there are numerous environmental apprehensions associated with their use and sustainability (Jambeck et al., 2015). These fossil fuel reservoirs are not renewable and in the long term will not meet the needs of our society. In addition, the majority of petroleum-derived plastic items can last for several hundred years in landfills and do not degrade (Schneiderman and Hillmyer, 2017). Only 9% of the global plastics are recycled and about 60% are landfilled (Lambert and Wagner, 2017) but the landfill sites are decreasing. About five million tonnes of plastic waste is dumped into the ocean annually (Miller, 2013; Tuck et al., 2012), and consequently, the amount of plastic in the ocean is expected to be more than the number of fish by 2050 (Mohanty et al., 2018). Although there is no rapid solution for such complex environmental concerns, the development of polymers from renewable resources can mitigate some of these issues and provide sustainable alternatives to produce materials that are suitable for recycling and/or biodegradable (Zhu et al., 2016). Consequently, there has been a tremendous research interest both in academia and industry on the production and use of biodegradable and sustainable materials. “Biobased” sustainable materials are currently considered as the most suitable alternatives in the future as petroleum resources become limited

(Dietrich et al., 2017; He et al., 2017; Malinconico, 2017; Wróblewska-Krepsztul et al., 2018).

An eco-friendly and sustainable alternative for the plastic production is the utilization of monomers from renewable resources (proteins, carbohydrates, lipids) as starting materials to replace some or all of the synthetic plastics in many applications. Compared to proteins and carbohydrates, lipid-derived monomers and biopolymers, being hydrophobic in nature, have the potential to provide functionally equivalent, renewable and environmentally friendly replacements for these finite petroleum-based raw materials, provided that they can be transformed into monomers and subsequently to polymers according to the end-use requirements, and that they can be produced in large scale to meet the current and growing industrial demand.

Consequently, much attention has been focused on the utilization of lipids as a raw material to produce chemicals, energy, monomers and biopolymers. The main components of all lipids are triacylglycerols (TAGs), which are esters of glycerol and free fatty acids. The lipids contain hydrocarbon chains, which are structurally like those commonly found in materials derived from petroleum. Therefore, lipids are considered as alternative natural materials to petroleum-based materials with potential applications in various industrial sectors. For the production of bio-based plastic materials the use of lipids from industrial by-products is highly desirable because it not only reduces utilization of food-grade lipids such as plant oils but also diverts waste from landfills. One such potential source of lipids is spent laying hens, which are mostly disposed of according to the restrictions identified by, for instance, the international Landfill Directive (Muise et al., 2016; Ullah and Wu, 2013; Wu, 2012).

Keeping in mind the stated issues, this PhD research aims to exploit a poultry industry byproduct (spent hens) as a potential source of lipids and develop nanoreinforced composite materials. There are no reports available in the literature on the utilization of lipids from spent hens

to develop biomaterials and or packaging materials. Therefore, this study aims to harvest this huge bioresource and develop bionanocomposites for a variety of applications.

It was hypothesized that lipid-derived polymers can lead to new high performance bionanocomposite materials through nanoparticle reinforcement. The overall objective of the proposed research was to use rapid and environmentally benign methods of lipid extraction using the spent hen as a raw material and to utilize the extracted lipids for the preparation of bionanocomposites. The specific objectives were:

(1) To extract the lipids from spent hens using microwave-assisted extraction and to optimize different extraction parameters, i.e., temperature, time, and solvent-to-feed ratio (Chapter 3),

(2) To extract the lipid from spent hens using supercritical CO_2 technology, and to study the effect of different extraction factors, i.e. pressure, time and temperature on lipid extraction yield and to transform the extracted TAGs into epoxidized lipid (Chapter 4),

(3) To prepare monomer and bionanocomposites from the fatty acids of the extracted lipids and reinforce them by the addition of nanoparticles, i.e., nanoclay (Chapter 5), and

(4) To produce bionanocomposites from the extracted lipids, i.e., epoxidation followed by cellulose nano crystals (CNC), monomer preparation, copolymerization with styrene and nanoreinforcement by the addition of nanoclay (Chapter 6).

References:

Fauziah, S., Liyana, I., Agamuthu, P. 2015. Plastic debris in the coastal environment: The invincible threat? Abundance of buried plastic debris on Malaysian beaches. *Waste Management & Research*, **33**(9), 812-821.

Muise, I., Adams, M., Côté, R., Price, G. 2016. Attitudes to the recovery and recycling of agricultural plastics waste: A case study of Nova Scotia, Canada. *Resources, Conservation and Recycling*, **109**, 137-145.

Passos, M.L., Ribeiro, C.P. 2016. *Innovation in food engineering: New techniques and products*. CRC Press.

Philp, J.C., Bartsev, A., Ritchie, R.J., Baucher, M.-A., Guy, K. 2013. Bioplastics science from a policy vantage point. *New Biotechnology*, **30**(6), 635-646.

Ullah, A., Vasanthan, T., Bressler, D., Elias, A.L., Wu, J. 2011. Bioplastics from feather quill. *Biomacromolecules*, **12**(10), 3826-3832.

Ullah, A., Wu, J. 2013. Feather fiber-based thermoplastics: effects of different plasticizers on material properties. *Macromolecular Materials and Engineering*, **298**(2), 153-162.

Wu, C.-S. 2012. Characterization and biodegradability of polyester bioplastic-based green renewable composites from agricultural residues. *Polymer Degradation and Stability*, **97**(1), 64-71.

Zhang, B., Wang, Q. 2012. Development of highly ordered nanofillers in zein nanocomposites for improved tensile and barrier properties. *Journal of Agricultural and Food Chemistry*, **60**(16), 4162-4169.

CHAPTER 2 - LITERATURE REVIEW

Currently, one of the main pivots of industry and academia is to find sustainable raw materials for the chemical manufacturing industries due to concerns related to the environment and decreasing fossil fuel reservoirs (Loh, 2017; Zubair and Ullah, 2019). To address these concerns and fulfill the industry requirements, utilization of industrial wastes or by-products has been evaluated (Arshad et al., 2016b; Kaur et al., 2018; Stephen and Periyasamy, 2018). One such potential, inexpensive and renewable bioresource, which has not been explored previously, is spent hens.

2.1. Spent hen composition and disposal problems

Spent hens are the old egg laying birds, which have surpassed their laying cycle of up to one year. Then, they are considered as poultry industry waste or by-product with minimal market value. Approximately, over 2.6 billion spent hens are produced every year around the world, of which 150 million are in North America (Kondaiah and Panda, 2007; Wang et al., 2013). The annual production of spent hens in Canada is over 26 million. Each spent hen has ~1.8 kg meat and on average the whole carcass contains about 60.1% moisture, 21.4% crude protein, 2.2% ash and 16.3% lipid, which represents about 42-45 kilotons of lipids only in North America (Tactacan et al., 2009). Ideally, these birds should be considered as food but due to their higher processing cost, low meat quality and yield, this is not feasible for the poultry industry (Kersey and Waldroup, 1998). As a result, egg producers have to euthanize the birds followed by composting or dumping into the landfills, which are not only expensive but also causing serious environmental concerns (Bernhart and Fasina, 2009).

2.2. Lipid extraction methods

Several lipid extraction methods are being used, and some of the common methods, which are reported in the literature are shown in Figure 2.1. Lipids are recovered from a variety of sources with and without the use of solvents (Ranjith Kumar et al., 2015). The solvent method of lipid extraction generally uses organic solvents, e.g. Soxhlet (De Castro and Priego-Capote, 2010), Folch (Folch, Jordi et al., 1957), and Bligh and Dyer (Jensen, 2008) methods and the enzymatic method of lipid extraction includes lytic (Gerken et al., 2013) and autolysis (Pueyo et al., 2000) methods. Furthermore, the lipids can be extracted using supercritical CO_2 technology (Temelli, 1992). The supercritical CO_2 technology is sustainable and environmentally friendly. Physical method of lipid recovery includes microwave-assisted extraction (Eskilsson and Björklund, 2000). Lipids can also be recovered using mechanical methods e.g., compression-decompression (Lee et al., 2012), high pressure (Cho et al., 2012), bead milling (Zheng et al., 2011), homogenization (Bligh and Dyer, 1959), hydrodynamic cavitation (Lee and Han, 2015), and ultrasonication (Zheng et al., 2011). The microwave-assisted and supercritical CO_2 extractions are the environmentally friendly, sustainable and rapid methods as compared to the solvent extraction where huge amounts of time, energy and toxic organic solvents are used (Carrapiso and García, 2000).

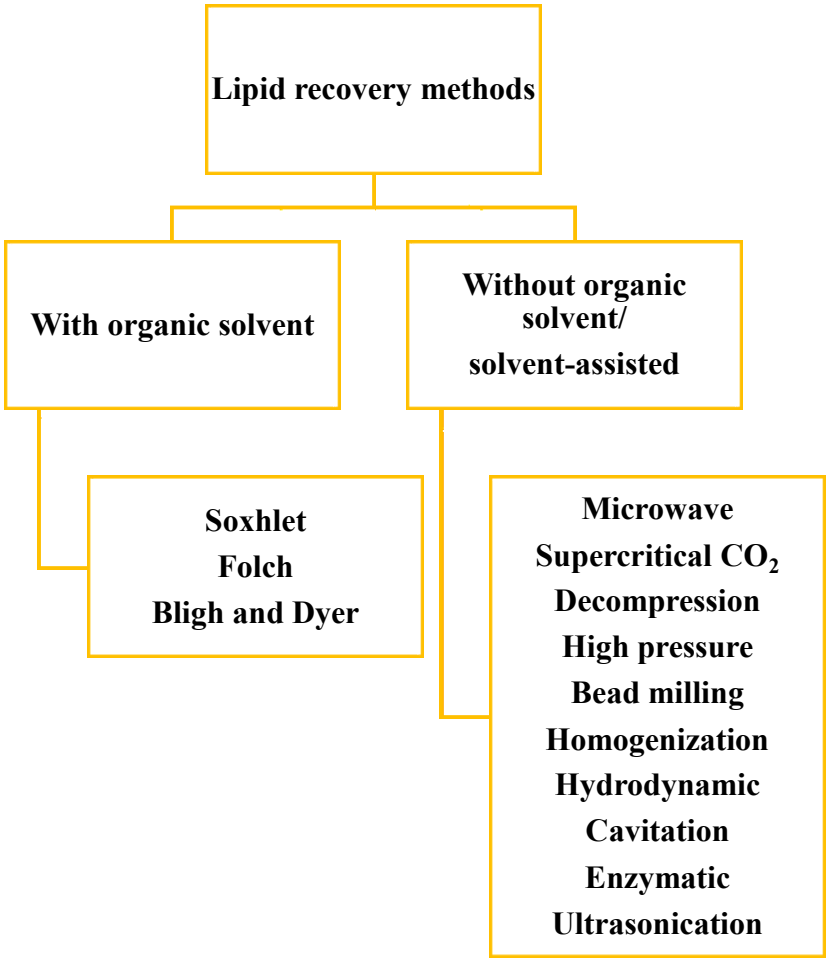

Figure 2.1: Schematic representation of common lipid recovery methods.

2.2.1. Microwave-assisted extraction (MAE)

MAE is an extraction technique that combines the use of microwave energy and traditional solvent extraction. In MAE, microwave energy is used to heat solvents in contact with solid samples or liquid samples (or to heat samples, e.g., fresh tissues) promoting partition of the compounds of interest from the sample into the solvent. In contrast to conventional heating, microwaves heat the solution directly. As a result, temperature gradients are minimal and the heating rate using microwave radiation is faster (Camel, 2000).

MAE offers several advantages, such as shorter extraction time, low level or no use of organic solvents and low extraction cost (Wahidin et al., 2014). During the microwave irradiation

process, rapid temperature increase, homogeneous heating, and high heating rates are responsible for short extraction times (Meullemiestre et al., 2016).

2.2.2. Supercritical CO_2 extraction (SC-CO_2)

Supercritical fluid extraction (SFE) is a modern separation technique where the solutes are dissolved in a fluid, whose dissolving capacity can be modified under conditions above its critical temperature and pressure. The characteristics of a supercritical fluid are applied to extract selectively a compound or to fractionate mixtures by modifying the temperature and pressure. A supercritical fluid shows physicochemical properties between those of a gas and a liquid. The dissolving capacity of a supercritical fluid depends on its density, which can be as good as liquid or as weak as gas by changing pressure and temperature (Raventós et al., 2002).

Supercritical carbon dioxide (SC-CO_2) is considered to be an alternative to organic solvents, which is abundant, nontoxic, nonflammable, cheap, sustainable and also has tunable physico-chemical properties (Brennecke, 1997; Leitner, 2000; Temelli, 2009). The inherent properties of CO_2, i.e., density, viscosity and diffusivity can be adjusted by altering temperature and pressure (Brunner, 2013; Soh and Zimmerman, 2011). Because of the solvent properties of CO_2, it is not only used for extractions but also as a reaction medium. This modern extraction technology has been used for the extraction of lipids from a variety of sources, including meat and poultry feed with excellent lipid recovery (King et al., 1989; Orellana et al., 2013).

2.3. Oil-derived bionanocomposites and their applications

The extracted oils from plant and animal sources can undergo a variety of chemical modifications, which lead to a plethora of sustainable materials. Typically, oils are comprised of up to 98% triglycerides (TAG), which are triesters of fatty acids and glycerol, and a typical structure is shown in Figure 2.2 (Barnwal and Sharma, 2005). The fatty acid part could be saturated

or unsaturated. Other than triglycerides, the oils also contain diglycerides, monoglycerides, phospholipids and free fatty acids (Srivastava and Prasad, 2000). Around 90% of the chemical transformations take place at carboxyl functionalities of oils and the rest of the chemical modifications are done at the double bonds of the fatty acid chains (Desroches et al., 2012).

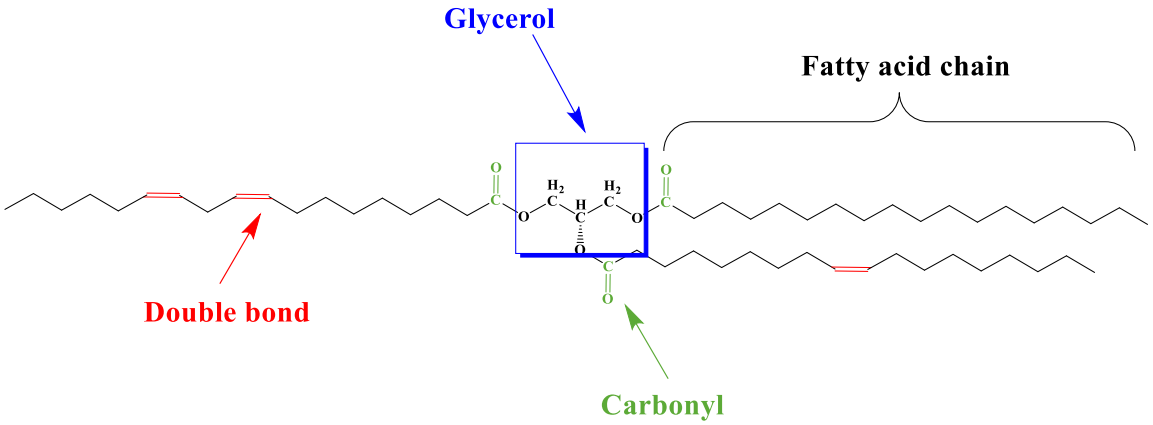

Figure 2.2: A representative structure of triglyceride showing reactive sites.

The major applications of chemically modified oils are in coatings and their tendency to form films depends on the extent of unsaturation in the fatty acid chains (Alam et al., 2014). The transformation of oils is completed by the incorporation of different groups into the oil backbone, such as hydroxyls, acrylics and acrylic co-polymers. Several such chemical modifications of the oils are reported, for example, mono and diglycerides are considered as raw materials to produce alkyds (Molina-Gutiérrez et al., 2019; Sharmin et al., 2015; Wu, Y. et al., 2012). Polyesteramides and polyetheramides are produced by the amidation transformation of oils (Indumathi and Rajarajeswari, 2019; Patil et al., 2019). The epoxides and polyols are produced by the oxidation of oils (Okieimen et al., 2005; Rwahwire et al., 2019). Similarly, some of the examples reported on double bond modifications are maleinization, and hydrohalogenation. Figure 2.3 summarizes some common transformations of the oils (Aigbodion et al., 2003; Rastegari et al., 2019; Xia and Larock, 2010) and a few specific examples of chemical modifications of oils are discussed next.

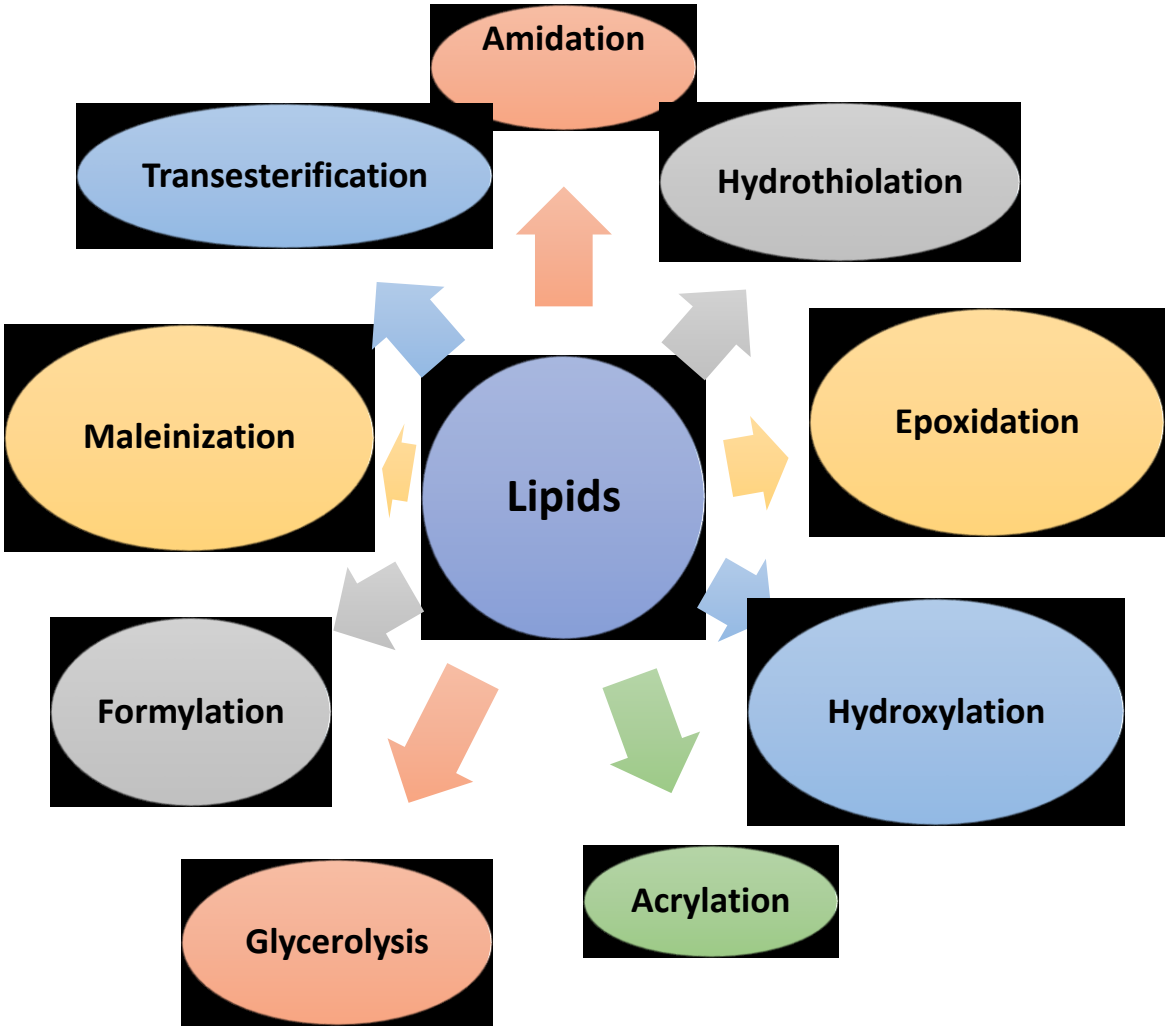

Figure 2.3: Common transformations of oils.

Epoxides are three membered highly strained rings, which serve as a precursor in the synthesis of numerous materials. Several studies have reported the epoxidation of oils from different sources, e.g., Zhang et al. (2018) reported an alternative and sustainable epoxidation method to acid-catalyzed epoxidations of soybean oil with 100% yields in the absence of any organic solvents. Similarly, Ahn et al. (2011) synthesized epoxidized soybean oil in a single step and at moderate reaction conditions at 50 °C and 5 min of reaction time, resulting in a thermally stable, transparent, biodegradable and pressure sensitive material as shown in Figure 2.4.

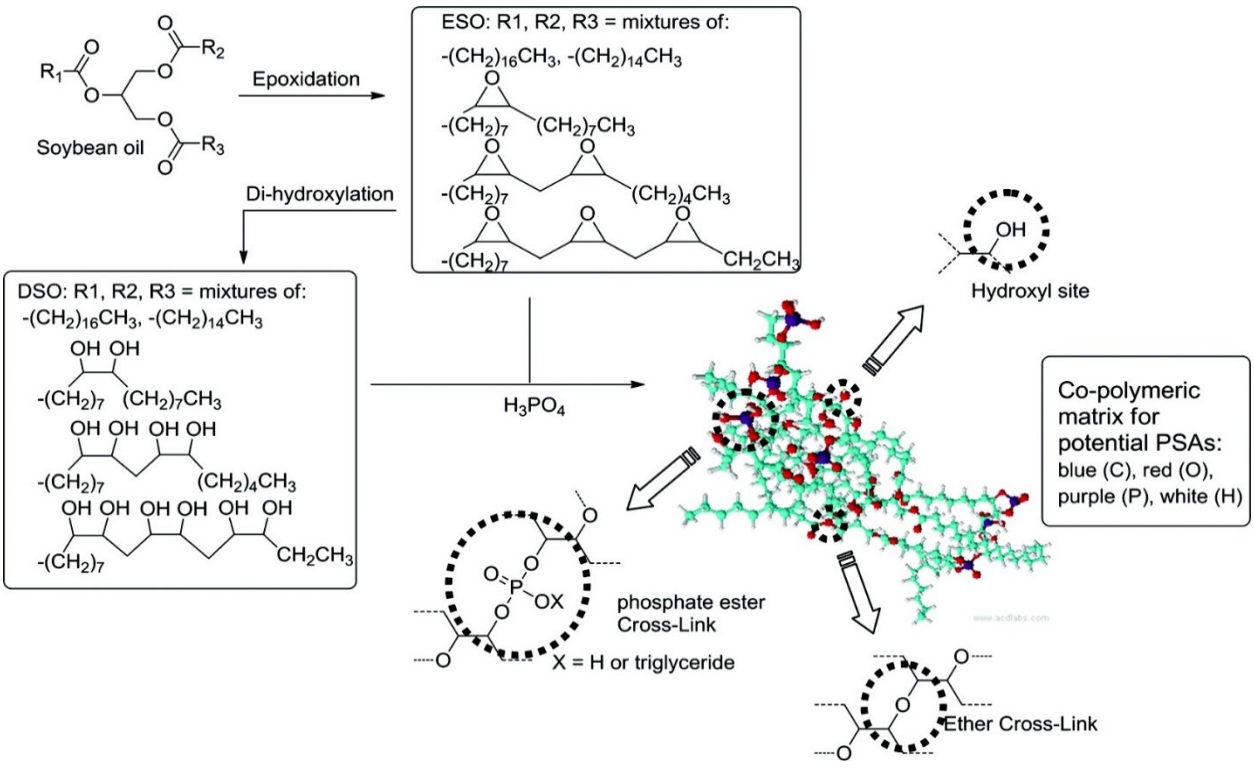

Figure 2.4: Epoxidation and hydroxylation of soybean oil for the production of thermally stable, transparent and pressure sensitive material (Reprinted with permission from ACS (Ahn et al., 2011)).

Several other studies have reported the epoxidation of oils from different sources, mainly from soybean, castor, tung, corn, linseed, and sunflower oils (Benaniba et al., 2003; Huang et al., 2013; Khundamri et al., 2019; Lligadas et al., 2006; Sinadinović-Fišer et al., 2012; Sun et al., 2011). Another study to modify linseed oil into coating was recently reported by Maurin et al. (2019) where they successfully modified the epoxidized linseed oil in solvent and catalyst free conditions with aminosilane. The plausible mechanism was ring opening of epoxide and transamidation of triglycerides and the prepared hydrophobic material could be used as a coating on cellulose and glass (Maurin et al., 2019). Another example of site selective epoxidation of oil from a non-edible source was reported from the algae specie *Botryococcus braunii.* The extracted oil was epoxidized by Prilezaev reaction using the oxidizing agent metachloroperbenzoic acid at

0 °C with up to 88% epoxide yield. The oil only showed epoxidation at the C2, 6, 11, 17, 21 positions, giving pentaepoxide in high yield (Kawashima and Kijima, 2018). Similarly, talapia oil was epoxidized by hydrogen peroxide in the presence of formic acid and toluene at room temperature for 16 h with a yield of 94% and the reaction took place as transesterification followed by epoxidation with the production of side products as ring opening of the epoxide. The epoxized talapia oil could be used as a precursor to oleochemicals as well as lubricants (Do Valle et al., 2018). Another example of epoxidized oil to be used as a source of other chemicals and lubricants was reported with the addition of nano-sized CuO and CeO_2 particles (do Valle et al., 2018). Again, the epoxidation of the rapeseed oil was performed in the presence of hydrogen peroxide, formic acid, concentrated sulphuric acid, and diethyl ether. To improve their tribiological properties, the nano-sized CuO and CeO_2 particles in the range of 0.1 to 1 wt% were added to the modified rapeseed oil. It was concluded that the epoxidized rapeseed oil showed improved anti-wear and friction-reducing properties compared to the unmodified oil. Also, the addition of nano particles enhanced its friction reducing properties, which was due to the presence of polar groups that facilitated the adsorption of metals for better film preparation (Gupta and Harsha, 2017).

The modification of epoxidized soybean oil to bio-rubber toughener was reported by Yadav et al. (2018) and the rubber toughener was synthesized in a single step reaction of epoxidized soybean oil consuming hexanoic anhydride from a bio-resource, which showed significant improvement in their fracture toughness and reduction in glass transition temperature.

Through the amidation of oils polyamides can be synthesized, which have several applications. Ahmad et al. (2004) synthesized boron-filled polyesteramides from soybean oil and further modified the boron-filled polyesteramide to get polyesteramide urethane by the addition of tolylene-2,4-diisocyanate, which showed the highest anti-microbial, anti-fungal activity for use as

coating materials. Several other polyamides have been synthesized from soybean, castor, and linseed oils (Biswas et al., 2008; Meier, 2019; Mohamed et al., 2014).

Hydroxy oils are considered as a feedstock for biodegradable polymer synthesis and used as lubricants. For example, biodegradable polyurethane films were prepared from Mahua oil by the incorporation of different proportions of zinc oxide nanoparticles (Indumathi and Rajarajeswari, 2019). The composite with 5% zinc oxide nanoparticles showed enhanced antimicrobial activity, hydrophobicity, barrier properties, stiffness and tensile strength. Furthermore, the zinc oxide nanoparticle enhanced shelf life of carrots when wrapped in films up to 9 days (Indumathi and Rajarajeswari, 2019).

Esterification of vegetable oils by benzyl alcohol using H_2SO_4 as catalyst was reported at 100 °C for 3 h, which gave benzyl esters with 96% yield. These benzyl esters from coconut, palm, and soybean oils could be used as a lubricant, which consumed less energy during synthesis and showed improved carbon black dispersion as compared to conventional aromatic oils (Boontawee et al., 2017).

Acryl groups are introduced in the oils for the preparation of polymers. Ge et al. (2019) synthesized acrylated epoxidized soybean oil-based films for improved moisture permeability by ultraviolet initiation and as a result moisture permeability was decreased by 10 times. An unsaturated ester from tung oil was prepared containing acrylates and maleates (Liu, C. et al., 2016). Firstly, the maleic group was introduced followed by acrylic moiety onto the tung oil. The prepared monomer possessed highly polymerizable double bonds, which resulted in a rigid biopolymer with high cross linking, glass transition temperature of up to 127 °C and significantly high tensile strength and modulus (Liu, C. et al., 2016). A soybean oil-based thermosetting resin was synthesized by the reaction of isosorbide-methacrylate with acrylated epoxidized soybean oil

resulting in improved degree of unsaturation (Liu, W. et al., 2016). The thermoset resin showed high flexural strength, strain, storage modulus, glass transition and thermal stability. A monomethyl itaconate was prepared with itaconic acid and epoxidized soybean oil. Also, acrylated soybean oil was synthesized from acrylic acid and epoxidized soybean oil. The comparison of monomethyl itaconate with acrylated soybean oil showed that the monomethyl itaconate had extremely low volatility as high as 90 °C while acrylic acid volatilized at as low as 30 °C, which proposed that monomethyl itaconate potentially could be used as an environmentally friendly alternative to acrylic acid (Li et al., 2016).

Thiol-ene click reactions could be performed on bio-based oils through radical and nucleophilic routes, which provide new avenues for the production of oleo chemicals with targeted functionalities. Chemical modification of bio oils was reported to prepare polyols in one step by the thiol-ene chemistry at −10 °C to −20 °C, giving almost 100% conversion of double bonds to hydroxyl functionalization, which exhibited good transparency for use as films (Alagi et al., 2016). Another example of thiol-ene click chemistry was performed on castor oil in which the oil derived polyurethane acrylate was prepared by photo initiation (Chen et al., 2016). The highly efficient side functionalization of castor oil was completed with β-mercaptoethanol by photo click reaction, which showed significant improvement in UV curing rate and better film curing (Chen et al., 2016).

Solvent-free polyurethanes were prepared from soybean oil by thiol-ene click chemistry. Briefly, the soybean oil was mixed with several diisocynates, dibutyltindilaurate, and ethyl methyl ketone using a molar proportion of isocyanate to hydroxyl 1.05:1 at 70 °C for 3 h and then the temperature was increased to 80 °C for 12 h in a home-made oven to obtain poly urethane films (Feng et al., 2017). The prepared films showed significantly high glass transition temperatures of

up to 41.3 °C, 15.7 MPa tensile strength, and 470% elongation at break (Feng et al., 2017). By using the thiol-ene click chemistry, soybean oil-based supramolecules reinforced with nano cellulose were synthesized, which exhibited high storage modulus at 200 °C (Feng et al., 2017). The plan was to introduce hydroxyl and carboxyl moieties in the soybean oil using methacrylate, 2-mercaptoethanol and initiator and the polymer prepared in this way facilitated hydrogen bonding with the nano cellulose to enhance the compatibility of nanocomposite (Song et al., 2017). Similarly, a green plasticizer from tung oil was synthesized by thiol-ene click chemistry (Jia et al., 2018).

The grafting of oils on the surface of petroleum-based polymers has also been reported, which showed improvement in the microbial and gas barrier properties of films. An example of grafting of clove oil on the surface of linear low density polyethylene exhibited strong anti-bacterial activity against *Salmonella typhimurium* and *Listeria monocytogenes* for up to 21 days when the chicken samples were refrigerated (Mulla et al., 2017). Different types of chemical modifications of the oils are shown in Figure 2.5.

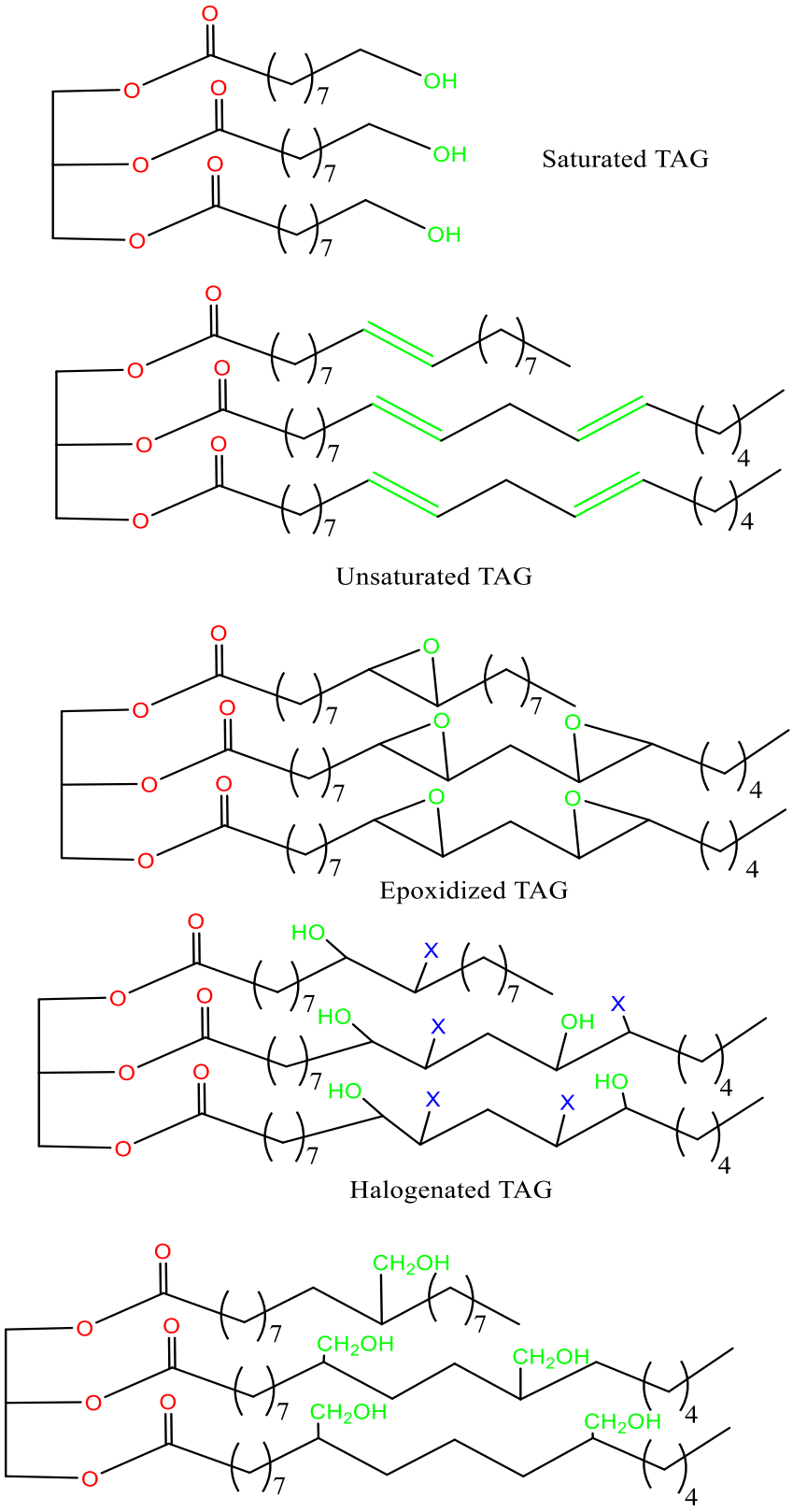

Figure 2.5: Chemical transformations of TAGs and fatty acids

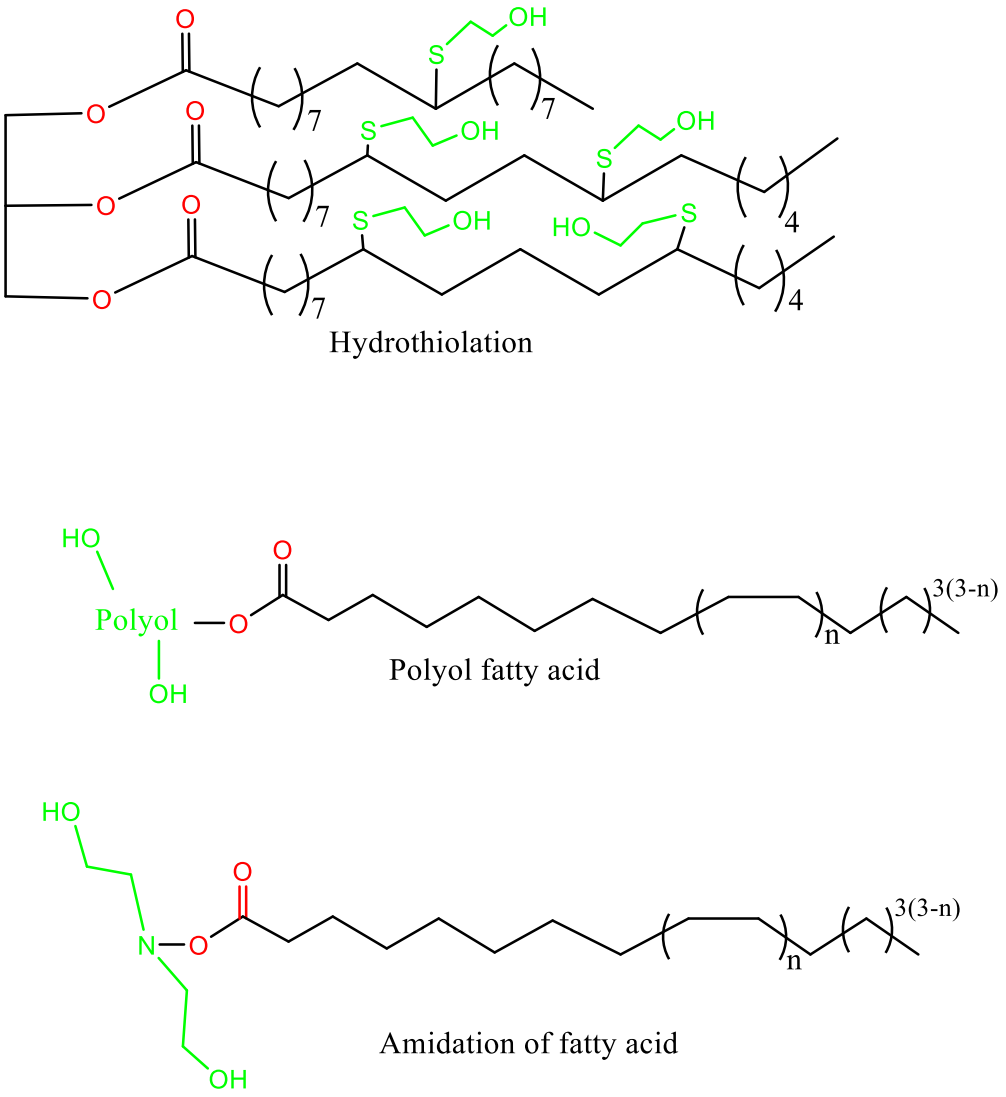

Figure 2.5: Chemical transformations of TAGs and fatty acids (continued)

2.4. Challenges with lipid-derived composites

Although bioplastics have a significant potential of replacing petroleum-based materials to help reduce environmental concerns, these materials still present a number of processing and property demerits that impede their utilization in many applications (Yu et al., 2006), in the food packaging field in particular. Lower barrier properties of bioplastics to gases and vapours, their lower thermal resistance, and strong water sensitivity, lower shelf-life stability due to ageing and

plasticizer migration are the issues associated with the use of bioplastics as food packaging materials (Satyanarayana et al., 2009). In this context, nanotechnology brings in significant opportunities to minimize these drawbacks (Lagaron and Lopez-Rubio, 2011).

Several attempts have been made to functionalize and crosslink TAGs from vegetable sources to develop thermosets and in some cases polymerization of functionalized TAGs to develop thermoplastic polymeric materials. However, bioplastics prepared from these independent biopolymers have intrinsic weaknesses such as low thermal stability, poor mechanical and other physical properties. These drawbacks can be overcome by exploiting biopolymer nanotechnology. Nanocomposites, with at least one dimension in nanometre scale, are regarded as a new generation of high-performance materials. Particularly, nanoclay and cellulose nano crystals (CNC) are considered to be emerging feedstocks for the preparation of nanoreinforced materials with enhanced properties (Floros et al., 2012).

2.3. Summary

The major goal of this PhD research is to utilize the poultry industry by-product (spent hen) as a starting material for the production of nanocomposites. The successful utilization of spent fowls would not only help to reduce the waste being sent to landfills but will also add value to poultry industry and benefit food industry through developing the composites from a renewable starting material. The use of environmentally friendly technologies such as microwave-assisted extraction and supercritical CO_2 extraction will not only help to reduce the lipid extraction time, but also minimize the use of toxic organic solvents. Overall, in addition to several environmental advantages, this research would benefit poultry, packaging, food and plastics industries.

2.4. References

Ahmad, S., Mahfuzul Haque, M., Ashraf, S.M., Ahmad, S. 2004. Urethane modified boron filled polyesteramide: a novel anti-microbial polymer from a sustainable resource. *European Polymer Journal*, **40**(9), 2097-2104.

Ahn, B.K., Kraft, S., Wang, D., Sun, X.S. 2011. Thermally stable, transparent, pressure-sensitive adhesives from epoxidized and dihydroxyl soybean oil. *Biomacromolecules*, **12**(5), 1839-1843.

Aigbodion, A., Okieimen, F., Obazee, E., Bakare, I. 2003. Utilisation of maleinized rubber seed oil and its alkyd resin as binders in water-borne coatings. *Progress in Organic Coatings*, **46**(1), 28-31.

Alagi, P., Choi, Y.J., Seog, J., Hong, S.C. 2016. Efficient and quantitative chemical transformation of vegetable oils to polyols through a thiol-ene reaction for thermoplastic polyurethanes. *Industrial Crops and Products*, **87**, 78-88.

Alam, M., Akram, D., Sharmin, E., Zafar, F., Ahmad, S. 2014. Vegetable oil based eco-friendly coating materials: A review article. *Arabian Journal of Chemistry*, **7**(4), 469-479.

Arshad, M., Kaur, M., Ullah, A. 2016. Green biocomposites from nanoengineered hybrid natural fiber and biopolymer. *ACS Sustainable Chemistry & Engineering*, **4**(3), 1785-1793.

Barnwal, B., Sharma, M. 2005. Prospects of biodiesel production from vegetable oils in India. *Renewable and Sustainable Energy Reviews*, **9**(4), 363-378.

Benaniba, M., Belhaneche-Bensemra, N., Gelbard, G. 2003. Stabilization of PVC by epoxidized sunflower oil in the presence of zinc and calcium stearates. *Polymer Degradation and Stability*, **82**(2), 245-249.

Bernhart, M., Fasina, O.O. 2009. Moisture effect on the storage, handling and flow properties of poultry litter. *Waste Management*, **29**(4), 1392-1398.

Biswas, A., Sharma, B., Willett, J., Erhan, S., Cheng, H. 2008. Soybean oil as a renewable feedstock for nitrogen-containing derivatives. *Energy & Environmental Science*, **1**(6), 639-644.

Bligh, E.G., Dyer, W.J. 1959. A rapid method of total lipid extraction and purification. *Canadian Journal of Biochemistry and Physiology*, **37**(8), 911-917.

Boontawee, H., Nakason, C., Kaesaman, A., Thitithammawong, A., Chewchanwuttiwong, S. 2017. Benzyl esters of vegetable oils as processing oil in carbon black–filled SBR compounding: Chemical modification, characterization, and performance. *Advances in Polymer Technology*, **36**(3), 320-330.

Carrapiso, A.I., García, C. 2000. Development in lipid analysis: some new extraction techniques and in situ transesterification. *Lipids*, **35**(11), 1167-1177.

Chen, G., Guan, X., Xu, R., Tian, J., He, M., Shen, W., Yang, J. 2016. Synthesis and characterization of UV-curable castor oil-based polyfunctional polyurethane acrylate via photo-click chemistry and isocyanate polyurethane reaction. *Progress in Organic Coatings*, **93**, 11-16.

Cho, S.-C., Choi, W.-Y., Oh, S.-H., Lee, C.-G., Seo, Y.-C., Kim, J.-S., Song, C.-H., Kim, G.-V., Lee, S.-Y., Kang, D.-H. 2012. Enhancement of lipid extraction from marine microalga, Scenedesmus associated with high-pressure homogenization process. *BioMed Research International*, **2012**.

De Castro, M.L., Priego-Capote, F. 2010. Soxhlet extraction: Past and present panacea. *Journal of Chromatography A*, **1217**(16), 2383-2389.

Desroches, M., Escouvois, M., Auvergne, R., Caillol, S., Boutevin, B. 2012. From vegetable oils to polyurethanes: synthetic routes to polyols and main industrial products. *Polymer Reviews*, **52**(1), 38-79.

do Valle, C.P., Rodrigues, J.S., Fechine, L.M.U.D., Cunha, A.P., Malveira, J.Q., Luna, F.M.T., Ricardo, N.M.P.S. 2018. Chemical modification of Tilapia oil for biolubricant applications. *Journal of Cleaner Production*, **191**, 158-166.

Eskilsson, C.S., Björklund, E. 2000. Analytical-scale microwave-assisted extraction. *Journal of Chromatography A*, **902**(1), 227-250.

Feng, Y., Liang, H., Yang, Z., Yuan, T., Luo, Y., Li, P., Yang, Z., Zhang, C. 2017. A solvent-free and scalable method to prepare soybean-oil-based polyols by thiol–ene photo-cick reaction and biobased polyurethanes therefrom. *ACS Sustainable Chemistry & Engineering*, **5**(8), 7365-7373.

Floros, M., Hojabri, L., Abraham, E., Jose, J., Thomas, S., Pothan, L., Leao, A.L., Narine, S. 2012. Enhancement of thermal stability, strength and extensibility of lipid-based polyurethanes with cellulose-based nanofibers. *Polymer degradation and stability*, **97**(10), 1970-1978.

Folch, J., Lees, M., Stanley, G.S. 1957. A simple method for the isolation and purification of total lipides from animal tissues. *Journal of biological chemistry*, **226**(1), 497-509.

Ge, X., Yu, L., Liu, Z., Liu, H., Chen, Y., Chen, L. 2019. Developing acrylated epoxidized soybean oil coating for improving moisture sensitivity and permeability of starch-based film. *International Journal of Biological Macromolecules*, **125**, 370-375.

Gerken, H.G., Donohoe, B., Knoshaug, E.P. 2013. Enzymatic cell wall degradation of *Chlorella vulgaris* and other microalgae for biofuels production. *Planta*, **237**(1), 239-253.

Gupta, R.N., Harsha, A. 2017. Antiwear and extreme pressure performance of castor oil with nano-additives. *Proceedings of the Institution of Mechanical Engineers, Part J: Journal of Engineering Tribology*, **232**(9), 1055-67.

Huang, K., Zhang, P., Zhang, J., Li, S., Li, M., Xia, J., Zhou, Y. 2013. Preparation of biobased epoxies using tung oil fatty acid-derived C21 diacid and C22 triacid and study of epoxy properties. *Green Chemistry*, **15**(9), 2466-2475.

Indumathi, M., Rajarajeswari, G. 2019. Mahua oil-based polyurethane/chitosan/nano ZnO composite films for biodegradable food packaging applications. *International journal of biological macromolecules*, **124**, 163-174.

Jensen, S.K. 2008. Improved Bligh and Dyer extraction procedure. *Lipid Technology*, **20**(12), 280-281.

Jia, P., Ma, Y., Xia, H., Zheng, M., Feng, G., Hu, L., Zhang, M., Zhou, Y. 2018. Clean synthesis of epoxidized tung oil derivatives via phase transfer catalyst and thiol–ene reaction: A detailed study. *ACS Sustainable Chemistry & Engineering*, **6**(11), 13983-13994.

Kaur, M., Arshad, M., Ullah, A. 2018. In-situ nanoreinforced green bionanomaterials from natural keratin and montmorillonite (MMT)/cellulose nanocrystals (CNC). *ACS Sustainable Chemistry & Engineering*, **6**(2), 1977-1987.

Kawashima, H., Kijima, M. 2018. Selective synthesis of botryococcene pentaepoxide-The chemical modifications of the algal biomass oil. *ChemistrySelect*, **3**(33), 9589-9591.

Kersey, J.H., Waldroup, P.W. 1998. Utilization of spent hen meal in diets for broiler chickens. *Poultry Science*, **77**(9), 1377-1387.

Khundamri, N., Aouf, C., Fulcrand, H., Dubreucq, E., Tanrattanakul, V. 2019. Bio-based flexible epoxy foam synthesized from epoxidized soybean oil and epoxidized mangosteen tannin. *Industrial Crops and Products*, **128**, 556-565.

Kondaiah, N., Panda, B. 2007. Processing and utilization of spent hens. *World's Poultry Science Journal*, **48**(3), 255-268.

Lagaron, J.M., Lopez-Rubio, A. 2011. Nanotechnology for bioplastics: opportunities, challenges and strategies. *Trends in Food Science & Technology*, **22**(11), 611-617.

Lee, A.K., Lewis, D.M., Ashman, P.J. 2012. Disruption of microalgal cells for the extraction of lipids for biofuels: processes and specific energy requirements. *Biomass & Bioenergy*, **46**, 89-101.

Lee, I., Han, J.-I. 2015. Simultaneous treatment (cell disruption and lipid extraction) of wet microalgae using hydrodynamic cavitation for enhancing the lipid yield. *Bioresource Technology*, **186**, 246-251.

Li, P., Ma, S., Dai, J., Liu, X., Jiang, Y., Wang, S., Wei, J., Chen, J., Zhu, J. 2016. Itaconic acid as a green alternative to acrylic acid for producing a soybean oil-based thermoset: synthesis and properties. *ACS Sustainable Chemistry & Engineering*, **5**(1), 1228-1236.

Liu, C., Shang, Q., Jia, P., Dai, Y., Zhou, Y., Liu, Z. 2016a. Tung oil-based unsaturated co-ester macromonomer for thermosetting polymers: synergetic synthesis and copolymerization with styrene. *ACS Sustainable Chemistry & Engineering*, **4**(6), 3437-3449.

Liu, W., Xie, T., Qiu, R. 2016b. Biobased thermosets prepared from rigid isosorbide and flexible soybean oil derivatives. *ACS Sustainable Chemistry & Engineering*, **5**(1), 774-783.

Lligadas, G., Ronda, J.C., Galià, M., Cádiz, V. 2006. Bionanocomposites from renewable resources: epoxidized linseed oil− polyhedral oligomeric silsesquioxanes hybrid materials. *Biomacromolecules*, **7**(12), 3521-3526.

Loh, S.K. 2017. The potential of the Malaysian oil palm biomass as a renewable energy source. *Energy Conversion and Management*, **141**, 285-298.

Maurin Pasturel, G., Lemor, A., Robin, J.J., Lapinte, V., 2019. Preparation and spectroscopic characterization of Si-coated vegetable oils and their application in in situ curing of hybrid coatings. *European Journal of Lipid Science and Technology* 121(4), 1800231.

Meier, M.A. 2019. Plant-oil-based polyamides and polyurethanes: Toward sustainable nitrogen-containing thermoplastic materials. *Macromolecular Rapid Communications,* **40***,* 1800524.

Mohamed, H., Badran, B., Rabie, A., Morsi, S. 2014. Synthesis and characterization of aqueous (polyurethane/aromatic polyamide sulfone) copolymer dispersions from castor oil. *Progress in Organic Coatings*, **77**(5), 965-974.

Molina-Gutiérrez, S., Ladmiral, V., Bongiovanni, R., Caillol, S., Lacroix-Desmazes, P. 2019. Radical polymerization of biobased monomers in aqueous dispersed media. *Green Chemistry,* **21**, 36-53.

Mulla, M., Ahmed, J., Al-Attar, H., Castro-Aguirre, E., Arfat, Y.A., Auras, R. 2017. Antimicrobial efficacy of clove essential oil infused into chemically modified LLDPE film for chicken meat packaging. *Food Control*, **73**, 663-671.

Okieimen, F.E., Pavithran, C., Bakare, I.O. 2005. Epoxidation and hydroxlation of rubber seed oil: one-pot multi-step reactions. *European Journal of Lipid Science and Technology*, **107**(5), 330-336.

Patil, C.K., Jirimali, H.D., Paradeshi, J.S., Chaudhari, B.L., Gite, V.V. 2019. Functional antimicrobial and anticorrosive polyurethane composite coatings from algae oil and silver doped egg shell hydroxyapatite for sustainable development. *Progress in Organic Coatings*, **128**, 127-136.

Pueyo, E., Martínez-Rodríguez, A., Polo, M.C., Santa-María, G., Bartolomé, B. 2000. Release of lipids during yeast autolysis in a model wine system. *Journal of Agricultural and Food Chemistry*, **48**(1), 116-122.

Ranjith Kumar, R., Hanumantha Rao, P., Arumugam, M. 2015. Lipid extraction methods from microalgae: a comprehensive review. *Frontiers in Energy Research*, **2**, 61.

Rastegari, H., Jazini, H., Ghaziaskar, H.S., Yalpani, M. 2019. Applications of Biodiesel By-products. in: *Biodiesel*, Springer, pp. 101-125.

Rwahwire, S., Tomkova, B., Periyasamy, A.P., Kale, B.M. 2019. Green thermoset reinforced biocomposites. in: *Green Composites for Automotive Applications*, Elsevier, pp. 61-80.

Satyanarayana, K.G., Arizaga, G.G., Wypych, F. 2009. Biodegradable composites based on lignocellulosic fibers—An overview. *Progress in Polymer Science*, **34**(9), 982-1021.

Sharmin, E., Zafar, F., Akram, D., Alam, M., Ahmad, S. 2015. Recent advances in vegetable oils based environment friendly coatings: A review. *Industrial Crops and Products*, **76**, 215-229.

Sinadinović-Fišer, S., Janković, M., Borota, O. 2012. Epoxidation of castor oil with peracetic acid formed in situ in the presence of an ion exchange resin. *Chemical Engineering and Processing: Process Intensification*, **62**, 106-113.

Song, L., Wang, Z., Lamm, M.E., Yuan, L., Tang, C. 2017. Supramolecular polymer nanocomposites derived from plant oils and cellulose nanocrystals. *Macromolecules*, **50**(19), 7475-7483.

Srivastava, A., Prasad, R. 2000. Triglycerides-based diesel fuels. *Renewable and Sustainable Energy Reviews*, **4**(2), 111-133.

Stephen, J.L., Periyasamy, B. 2018. Innovative developments in biofuels production from organic waste materials: A review. *Fuel*, **214**, 623-633.

Sun, S., Yang, G., Bi, Y., Liang, H. 2011. Enzymatic epoxidation of corn oil by perstearic acid. *Journal of the American Oil Chemists' Society*, **88**(10), 1567-1571.

Tactacan, G.B., Guenter, W., Lewis, N.J., Rodriguez-Lecompte, J.C., House, J.D. 2009. Performance and welfare of laying hens in conventional and enriched cages. *Poultry Science*, **88**(4), 698-707.

Temelli, F. 1992. Extraction of triglycerides and phospholipids from canola with supercritical carbon dioxide and ethanol. *Journal of Food Science*, **57**(2), 440-443.

Wang, H., Wu, J., Betti, M. 2013. Chemical, rheological and surface morphologic characterisation of spent hen proteins extracted by pH-shift processing with or without the presence of cryoprotectants. *Food Chemistry*, **139**(1), 710-719.

Wu, Y., Ni, G., Yang, F., Li, C., Dong, G. 2012. Modified maleic anhydride co-polymers as pour-point depressants and their effects on waxy crude oil rheology. *Energy & Fuels*, **26**(2), 995-1001.

Xia, Y., Larock, R.C. 2010. Vegetable oil-based polymeric materials: synthesis, properties, and applications. *Green Chemistry*, **12**(11), 1893-1909.

Yadav, S.K., Hu, F., La Scala, J.J., Palmese, G.R. 2018. Toughening anhydride-cured epoxy resins using fatty alkyl-anhydride-grafted epoxidized soybean oil. *ACS Omega*, **3**(3), 2641-2651.

Yu, L., Dean, K., Li, L. 2006. Polymer blends and composites from renewable resources. *Progress in Polymer Science*, **31**(6), 576-602.

Zheng, H., Yin, J., Gao, Z., Huang, H., Ji, X., Dou, C. 2011. Disruption of *Chlorella vulgaris* cells for the release of biodiesel-producing lipids: a comparison of grinding, ultrasonication, bead milling, enzymatic lysis, and microwaves. *Applied Biochemistry and Biotechnology*, **164**(7), 1215-1224.

Zubair, M., Ullah, A. 2019. Recent advances in protein derived bionanocomposites for food packaging applications. *Critical Reviews in Food Science and Nutrition*, 1-29.

CHAPTER 3 - EXTRACTION, OPTIMIZATION, AND CHARACTERIZATION OF LIPIDS FROM SPENT HENS: AN UNEXPLOITED SUSTAINABLE BIORESOURCE[1]

3.1. Introduction

To reduce the dependency on fossil fuels, there is an extensive ongoing search both in the industry and academia for new alternatives, which should be sustainable and environmentally friendly (Chen et al., 2013; Kumar et al., 2016). Compared to proteins and carbohydrates as renewable alternatives, much attention has been focused on the utilization of lipids to produce chemicals, fuels, monomers and biopolymers (Fang et al., 2016; Jin et al., 2017; Qadeer et al., 2017) because the hydrocarbon chains of fatty acids are structurally similar to those commonly found in petroleum. Therefore, lipid-derived materials are considered as an alternative to petroleum-based materials with potential applications in various industrial sectors (Katouzian et al., 2017; Tao, 2007).

Currently, the competitive potential of lipid-derived non-food products is limited because of the edible use and high cost of these lipids as a feedstock, i.e., soybean, canola, rapeseed, sunflower, palm, and coconut oils contributing up to 85% of the total lipid production (Piker et al., 2016). Microalgae as a potential source of lipid production (Álvarez-Díaz et al., 2017) also suffers from high production cost (da Silva et al., 2014). Consequently, alternative resources are needed to minimize cost (waste lipids or lipids from industrial by-products). It is possible to use non-edible waste lipids as a feedstock because large quantities of waste are produced on a daily basis, such as restaurant waste containing up to 30 wt% of lipids (Olkiewicz et al., 2014; Papanikolaou et al., 2011).

[1] A version of this chapter has been published: Safder, M., Temelli, F., Ullah, A. 2019. Extraction, optimization, and characterization of lipids from spent hens: An unexploited sustainable bioresource. Journal of Cleaner Production, 206, 622-630.

The use of lipids from industrial by-products is highly desirable because it will not only reduce the utilization of food-grade lipids but also divert waste from landfills. One such potential sustainable resource is spent hens, which are old egg-laying hens and are mostly disposed of in landfills (Bernhart and Fasina, 2009). Typically, the egg-laying period of hens lasts up to one year, and after that, they are referred to as spent hens as they are no longer satisfactory regarding their egg production and quality, as discussed in more detail in Chapter 2 (Section 2.1). This study aims to harvest this massive bioresource for the recovery of lipids with the ultimate goal of developing nanocomposites for food packaging applications.

Various techniques of lipid extraction from different substrates are being used, such as conventional (e.g., mechanical pressing and solvent extraction) and modern (e.g., supercritical fluid and microwave-assisted extraction) techniques. However, there are drawbacks associated with conventional techniques, including lengthy extractions and high usage of organic solvents (solvent extraction), as well as low extraction yield (mechanical pressing) (Amarni and Kadi, 2010; Cravotto et al., 2008; Orr et al., 2016). On the other hand, microwave-assisted extraction offers several advantages, such as shorter extraction time, low level or no use of organic solvents and low extraction cost (Wahidin et al., 2014). During the microwave irradiation process, rapid temperature increase, homogeneous heating, and high heating rates are responsible for short extraction times (Meullemiestre et al., 2016).

Recently, some work has been done to extract and use proteins from the spent hens (Hong et al., 2018; Wang et al., 2013; Yu et al., 2018), but to the best of my knowledge no work has been completed on the extraction of lipids from spent hens using conventional or microwave-assisted extraction techniques. Consequently, the objectives of this study were to explore microwave-assisted extraction as a rapid and environmentally benign method of lipid extraction, to evaluate

the effects of time, temperature and solvent-to-feed ratio on the lipid extraction yield and to characterize the extracted lipids from spent hens.

3.2. Materials and methods

Spent hens were obtained through Alberta Hatching Egg Producers (AHEP). The solvent n-hexane (95%) was purchased from Caledon Laboratory Chemicals (Georgetown, ON, Canada), while dichloromethane (DCM, 99.5%), chloroform (≥99%) methanol (99.9%), acetone (≥99.5%), ethyl acetate (EtOAc, 99.5%), potassium hydroxide (KOH, ≥85%), sodium chloride (NaCl, 99.9%), anhydrous sodium sulphate (Na_2SO_4, 99%), ferric chloride (≥99.8%), acetic acid (≥99%), sulphuric acid (98%) and formic acid (≥95%) were purchased from Sigma-Aldrich (St. Louis, MO, USA) and used as received.

3.2.1. Sample preparation

The spent hens were cut into small pieces manually followed by grinding at the Agri-Food Discovery Place (AFDP), South Campus, University of Alberta. Grinding of the birds was done using the Holly Mini-Matic Ergonomic Mixer/Grinder (Hollymatic Corporation, Countryside, IL, USA) with a 5 mm plate followed by the Stephan Microcut MC 10 (Stephan Machinery GmbH, Hameln, Germany) using the 1.8 mm cutting head. No water was added during the grinding process. The ground hen materials were kept at -20 °C until further use.

3.2.2. Proximate analysis of ground spent hens

The lipid, protein, ash, and moisture contents of the spent hen with bones were determined. Water and ash contents were estimated using the standard AOAC methods 935.29 and 942.05, respectively (Horwitz and Latimer, 2005). The total amount of crude protein of the spent hens was determined using LECO (Nitrogen/Carbon) analyzer (TruSpec®CN., Saint Joseph, MI, USA) and a conversion factor of 6.25 (Osen et al., 2014). Lipid extraction of the spent hen was carried out

using conventional methods, i.e., Folch (Folch, J. et al., 1957) and Soxhlet using dichloromethane-methanol at 2:1 (v:v) ratio (Binnington, 1932) and all the analysis were performed in triplicate.

3.2.3. Microwave-assisted lipid extraction

All extractions were conducted in a 80 mL sealed tube having a pressure maximum of 2 MPa with a built-in magnetic stirrer using a CEM-Discover unit (120 V, CEM Corporation, Matthews, NC, USA), equipped with a microwave radiation source having a maximum power of 300 W. The microwave power was adjusted by the unit to reach and sustain the fixed temperature. To monitor the internal temperature of the vessel contents, the instrument was switched to fiber optic mode.

3.2.3.1. Single factor extraction conditions

A sample of about 15 g whole ground spent hen was placed in the 80 mL vessel with a solvent-to-feed ratio ranging from 1.7-6.7 mL/g of dichloromethane-methanol (2:1, v:v) on a wet basis. The mixture was subjected to microwave irradiation at the range of temperatures from 60-100 °C for different time intervals (3-30 min) for the extraction of lipids, keeping solvent-to-feed ratio (v/wt) constant at 1.3 mL/g. Then, extractions without and with the addition of solvent were performed at 80 ºC over 30 min. In the last set of extractions, the solvent-to-feed ratio was varied from 0.7 to 2.6 mL/g at temperatures of 60, 80 and 100 ºC at a fixed time of 30 min. Crude spent hen lipids were obtained by filtration using Whatman filter paper (185 mm, GE Healthcare UK Limited, Amersham Place Little Chalfont, Buckinghamshire, UK), then the solvent was evaporated to get the extract using rotary evaporator under vacuum at 35 °C. The yield of extracted

lipids was calculated based on the starting weight of whole ground spent hen sample. All the experiments were conducted in duplicates and mean values were reported.

3.2.3.2. Response surface methodology (RSM)

Once the ranges of parameters were determined using the single factor experiments described above, RSM was used to determine the optimal condition for the microwave extraction of lipids from spent hen and to study the effects of input variables, i.e., temperature (A), extraction time (B), and solvent-to-feed ratio (v/wt) (C) on the extraction yield (Y). Temperature range of 60-100 °C, 3-10 min extraction time, and 0.7-2 mL/g solvent-to-feed ratio (10, 20, and 30 mL of solvent (DCM-methanol, 2:1, v:v) per 15 g of ground spent hen) were used as input variables. A total of seventeen experimental runs were performed with five repetitions of the center point according to Box-Behnken Design (BBD) using the Design-Expert software (Version 10.0, Stat-Ease, Inc., Minneapolis, MN, USA). Test variables and their ranges are shown in Table 3.1, while the designed experiments by the Box-Behnken method and their results are given in Table 3.2. The analysis of variance (ANOVA) was performed, and the regression coefficients of the model parameters were determined.

Table 3.1: The input factors and their ranges used.

Code	Variable	−1	0	1
A	Temperature (°C)	60	80	100
B	Time (min)	3	6.5	10
C	Solvent-to-feed ratio (mL/g)	0.7	1.3	2

Bootstrap statistical analyses were performed in R version 3.4.3 (R Core Team 2017). A total of 13 different combinations of input variables, i.e., temperature, time and solvent-to-feed ratio were used. All 13 combinations of the input variables were tested in triplicates, and the results for each combination were bootstrap 10,000 times to account for the low sample size.

Parametric bootstrapping with replacement approach was used. Differences among the groups were compared by conducting a three-way analysis of variance (ANOVA) (Bryant et al., 1987) using a linear model at an alpha level of 0.05.

Table 3.2: The Box-Behnken design for optimization of process parameters of time (min), temperature (°C), and the solvent-to-feed ratio (mL/g) and the resulting extraction yield % (wt/wt) on wet basis.

Entry	Temperature (°C)	Time (min)	Solvent-to-feed ratio (mL/g)	Yield (%)
1	80	6.5	1.3	12.7
2	80	3	0.7	10.1
3	80	3	2	11.0
4	60	10	1.3	13.0
5	80	6.5	1.3	11.1
6	60	6.5	2	11.3
7	60	6.5	0.7	10.4
8	80	10	0.7	12.5
9	80	6.5	1.3	13.1
10	100	3	1.3	11.4
11	80	6.5	1.3	11.2
12	80	10	2	15.9
13	60	3	1.3	11.0
14	100	6.5	0.7	12.0
15	100	6.5	2	14.0
16	100	10	1.3	14.9
17	80	6.5	1.3	12.0
18[b]	60	480	10	16.1
19[c]	25	60	20	16.3
20[d]	80	10	2	15.7

[b] Extraction of lipids by Soxhlet method
[c] Extraction of lipids by Folch method
[d] Extraction of lipids on a two fold scale-up process

3.2.3.3. Two fold scale-up of microwave-assisted extraction

All extractions were conducted in a CEM-Discover unit (120 V, CEM Corporation, Matthews, NC, USA). The optimized conditions for the lipid extraction from spent hen at a laboratory scale were used for two-fold scale-up of the process. A temperature of 80 °C, 10 min extraction time, and 2 mL/g solvent-to-feed ratio (60 mL of solvent (dichloromethane-methanol, 2:1, v:v per 30 g of ground spent hen) were used. The lipid extract was filtered using five folds of cheese cloth, an organic layer was separated by a separatory funnel and the organic solvents were removed using a rotary evaporator under vacuum at 35 °C. The yield of extracted lipids was calculated based on the initial feed weight. All experiments were conducted in triplicates.

3.2.4. Lipid analyses and characterization of extracts

The lipids extracted using optimized microwave extraction conditions were fractionated into different classes using previously reported solid phase extraction (SPE) protocol (Zhao et al., 2015) with some modifications. Briefly, the SPE cartridge packed with silica (Supelclean^{TM} ENVI-Carb^{TM}, Sigma-Aldrich, Oakville, ON, Canada) was conditioned with DCM, and then a solution of lipid (30 mg) in 2 mL of DCM was applied onto the cartridge. The cartridge was first eluted with DCM and then with acetone/methanol (9:1 v:v) followed by pure methanol to extract neutral lipids, glycolipids, and phospholipids, respectively. Solvents were evaporated and residues were weighed to determine the percentage of each lipid class. The SPE analyses were performed in triplicate.

3.2.4.1. Gas chromatography-mass spectrometry (GC-MS) and gas chromatography-flame ionization detector (GC-FID)

For the identification of fatty acid components, the lipid extract was transesterified with methanol according to the protocol reported by (Arshad et al., 2014) and their GC-MS analysis

was performed on Agilent 6890N gas chromatograph (Ramsey, MN, USA), equipped with a fused silica SP2560 capillary column (100 m length × 0.25 mm diameter × 0.2 mm film thickness) and detector (5975B inert XL MSD). The prepared sample (0.5 mg/mL in DCM (2 µL)) was injected at an injector temperature of 240 °C operating at a split mode of 20:1. Initially, the temperature of the oven was set at 45 °C and held for 4 min; the temperature was gradually raised to 175 °C with the average ramping rate of 13 °C/min. This temperature was kept constant for 27 min and further increased to 215 °C using a ramping rate of 4 °C/min, and held for 35 min. To measure the masses of different components in the sample, a scanning range of 30–1000 amu with a scan rate of 1.55 per second was used. The carrier gas used was helium with a flow rate of 1.3 mL/min.

To determine the fatty acid composition of the extracted samples, the GC-FID analysis was performed using a Perkin Elmer GC-FID Clarus 500 instrument (Alexandria, VA, USA) fitted with a flame ionization detector. The temperature of the detector was 280 °C, while the injector was set at 240 °C. Hydrogen was used as the carrier gas at the flow rate of 45 mL/min.

3.2.4.2. Proton nuclear magnetic spectroscopy (^{1}H NMR)

The structure elucidation of extracted lipids was performed by ^{1}H NMR spectroscopy and the spectra were recorded using deuterated chloroform at 400 MHz (Varian Inova instrument, Palo Alto, CA, USA).

3.2.4.3. Attenuated total reflectance - Fourier transform infrared spectroscopy (ATR-FTIR) analysis

ATR-FTIR spectra of extracted lipids were recorded using a Bruker Optics (Esslingen, Germany) unit with the help of single bounce diamond ATR crystal. All samples were scanned in

the wavenumber range of 450-3500 cm^{-1}, spectra were obtained using OPUS software 6.5 version from Bruker, and a total of 16 scans at a resolution of 4 cm^{-1} were recorded.

3.2.4.4. Differential scanning calorimetry (DSC) measurement

To investigate thermal transitions in the extracted lipid samples, DSC analyses were performed using a TA Instrument (2920 Modulated DSC, TA Instruments, New Castle, DE, USA), with a purge of nitrogen gas. Samples (2.0–5.0 mg) were weighed in a pan, which was sealed and placed in a DSC cell. The thermograms were recorded in the range of -50 to +50 °C, where the heating rate was set at 3 °C/min. To eliminate the thermal history, the 2nd heating cycle of DSC profiles was selected.

3.2.4.5. Thermogravimetric analysis (TGA)

The thermal degradation behavior of extracted lipids was investigated by thermal gravimetric analysis using a Q50 TGA instrument (TA Instruments, New Castle, DE, USA) in the presence of nitrogen gas. TGA measurements were conducted by heating the samples in the range of 30 to 600°C at the ramp rate of 10 ºC/min.

3.3. Results and discussion

Proximate analysis of the whole ground spent hen showed 60.1 ± 0.1% moisture, 21.4 ± 0.1% crude protein, 16.3 ± 0.2% lipid and 2.2 ± 0.2% ash content. In addition to the proximate analysis, different classes of crude lipids were estimated by the solid phase extraction technique with 86.2 ± 0.4%, 0.6 ±0.5% and 0.3 ± 0.2 % of neutral lipids, phospholipids, and glycolipids, respectively. In this study, the lipids extracted from the whole ground spent hen (containing 60.1 ± 0.1% moisture content), employing the conventional Folch method using dichloromethane and methanol (2:1 v/v) was considered as the total lipid in the sample. The lipids extracted using the Folch method were 1.6 g per 10 g of wet biomass spent hen (16.3% yield). Lipid extraction

efficiency (% recovery) was reported as the ratio of the total lipids extracted by microwave-assisted extraction and the lipids extracted by the Folch method.

3.3.1. Influence of extraction parameters based on single factor experiments

The effects of temperature, organic solvent addition and solvent-to-feed ratio on the lipid extraction yield were evaluated using single factor experiments as discussed below.

3.3.1.1. Temperature effect on lipid extraction yield

The influence of extraction temperature on lipid yield was studied while keeping solvent-to-feed ratio (v/wt) at 1.3 mL/g as depicted in Figure 3.1 (a). High temperature increases the solubility of lipids and their diffusion; however, there is a risk of thermal degradation at higher temperatures. An increase in the lipid extraction yield was observed by raising the temperature from 60 °C to 100 °C, where the yield of 13.1% at 60 °C and 30 min is increased to 16.0% at 80 °C and 16.1% at 100 °C (Figure 3.1 (a)). As expected, the temperature had a direct effect on the extraction yield. Generally, high mass transfer rates are achieved in microwave-assisted extractions at elevated temperatures. Overall, the rise of temperature increases the lipid extraction yield due to the weakening of intermolecular forces, i.e., hydrogen bonding, which leads to improved diffusion of the lipid molecules within the matrix and then into the solvent phase. Furthermore, the viscosities of the solvent and lipids drop at higher temperatures, which also increase the diffusion rates. At elevated temperatures, the thermal energy overcomes the cohesive and adhesive forces, which leads to improved capacity of solvents to dissolve lipids (Karlovic et al., 1992). With an increase in extraction time, the lipid yield was substantially improved only up to 10 min and then reached a plateau, which was in agreement with a report on olive pomace oil (Yanık, 2017). At higher temperatures and prolonged extraction times, the cell structure can break down, which could enhance the release of lipids (McMillan et al., 2013); however, the temperature

sensitive constituents could be damaged. It was clear from Figure 3.1 (a), that prolonged extraction times had no remarkable effect on the lipid yield. Considering a higher extraction yield, 80 °C was selected as the optimum temperature in the subsequent single-factor experiment. Considering the above results, extraction temperatures of 60 °C, 80 °C, and 100 °C and a time range of 3-10 min were employed in the RSM study to further optimize extraction conditions.

3.3.1.2. Effect of organic solvent addition on lipid extraction yield

In addition to the effect of temperature and time on lipid extraction yield, the effect of solvent addition was studied as depicted in Figure 3.1 (b). The microwave-assisted lipid extractions were performed without and with solvent (solvent-to-feed ratio, 1.3 mL/g) addition at 80 °C for up to 30 min. Solvent addition showed a substantial effect on lipid extraction yield (about 16.1%) as compared to the extraction performed without solvent, where the extraction yield was 5.6% at 10 min. It is apparent that the extraction of lipids using a solvent is more efficient as compared to the extraction of lipids without solvent.

3.3.1.3. Influence of solvent-to-feed ratio (v/wt) on lipid yield

The influence of solvent-to-feed ratio on the lipid extraction yield is shown in Figure 3.1 (c). The increase in the solvent-to-feed ratio (v/wt) from 0.7 to 2.0 resulted in a higher lipid yield. At a solvent-to-feed ratio of more than 2, the lipid extraction yield reached a plateau at 60 and 80 ^{o}C but declined at 100 °C, which is attributed to the large volume of low boiling point solvents creating more pressure inside the vessel causing some bleeding of the solvent and dissolved lipids out of the vessel, as was observed at the completion of extraction. Similar observations were recorded on flavonoids extraction (Xiao et al., 2008). Hence, 2 mL/g was adopted as the most appropriate solvent-to-feed ratio (v/wt). Also, it is desirable to keep the solvent-to-feed ratio small

to minimize the amount of solvent used. When using RSM to optimize the extraction factors, the solvent-to-feed ratio (v/wt) of 0.7, 1.3, and 2 mL/g were employed for further analysis.

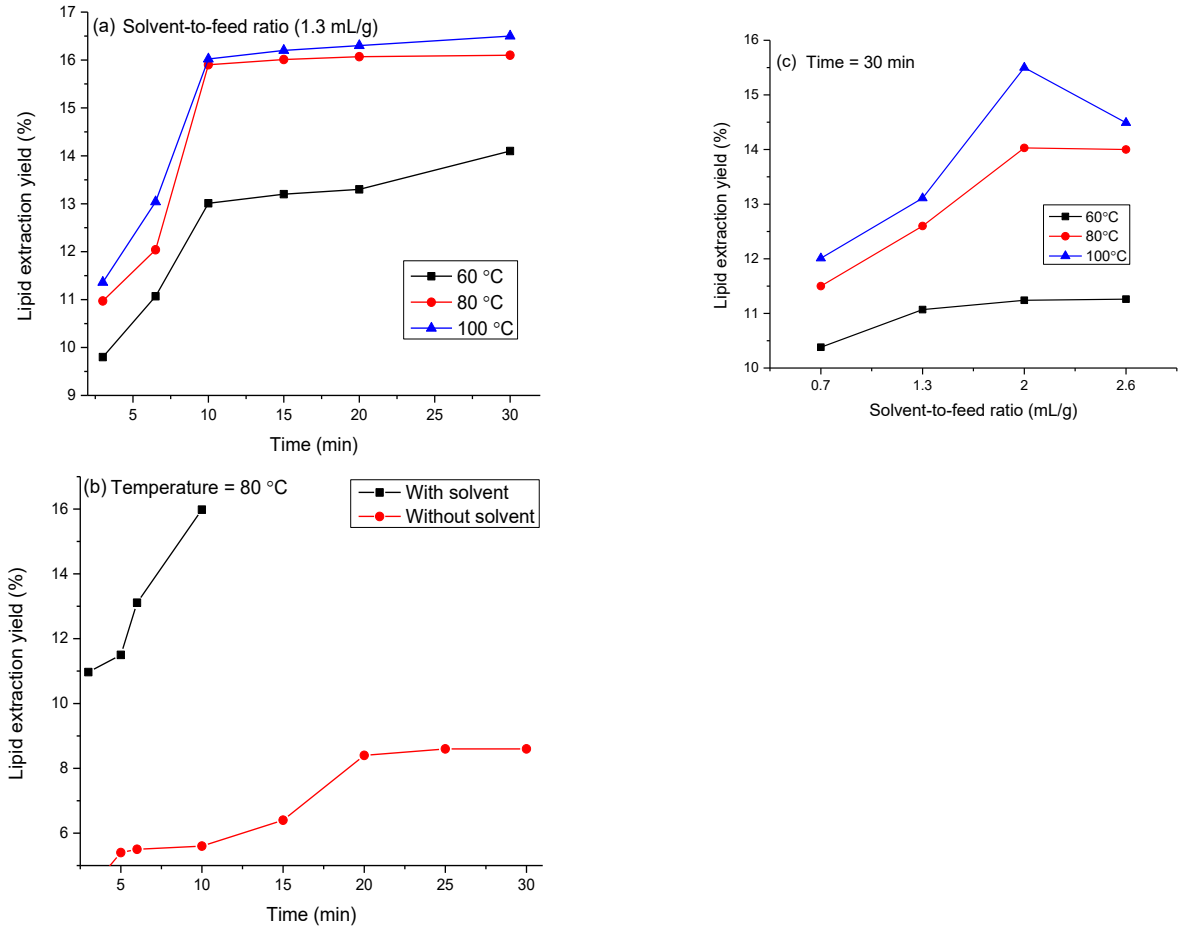

Figure 3.1: Effect of (a) temperature, (b) solvent addition and (c) solvent-to-feed ratio (v/wt) on the lipid extraction yield of spent hen, all the values are average of duplicates.

3.3.2. Optimization of extraction variables by RSM

Solid-liquid extraction involves the mass transfer of solute molecules from the solid phase to the liquid phase. The phenomena behind mass transfer are capillary flow, which has a direct relation to the viscosity of the solvents. Use of microwave irradiation produces heat inside the sample, and as a result, a rapid increase in temperature develops inside the matrix, which could

create pressure on the cell structure. Hence, during microwave-assisted extraction heat and mass transfers are in the same direction, which enhances the extraction rate (Luque de Castro and Castillo-Peinado, 2016). In this study, the relationship of lipid extraction yield and three input variables, i.e., extraction temperature, time and the solvent-to-feed ratio (v/wt) were assessed by RSM. Statistical software was used to evaluate the full regression model, including linear, quadratic, and interaction terms. The results of ANOVA showed that the quadratic and interaction terms were not significant, and the model was simplified to a linear model. To observe the fitness of an empirical model with the generated responses, a regression analysis was conducted. A linear equation was generated to calculate the predicted lipid extraction yield based on the actual parameters (Eq. (3.1))

$$Y = +4.04327 + 0.041750A + 0.46536B + 0.090625C \quad (3.1)$$

where Y is the lipid extraction yield (%), A is temperature (°C), B is time (min), and C is the solvent-to-feed ratio (v/wt). At a certain level of each parameter, the equation regarding actual parameters can be used to predict the response.

To find out the significance and fitness of the linear model, the ANOVA results were analyzed, including the main effects of selected variables, which are compiled in Table 3.3 for the linear model. The model F-value of 17.77 suggested the model was significant ($p < 0.0001$). With $p < 0.05$, A, B, and C were found to be significant model terms. Among these terms, time (B) had the most significant effect ($p < 0.0001$). The low value of the coefficient of variation (C.V. = 6.47%) and a non-significant lack of fit showed that the linear model results were reliable. The effects of the operating parameters on lipid extraction yield were shown in Figure 3.2, where the extraction yield increased linearly with temperature, time and solvent-to-feed ratio within the ranges tested.

The maximum extraction yield of 15.98% was obtained experimentally at a temperature of 80 °C, with 10 min extraction time and the solvent-to-feed ratio of 2 mL/g, showing good consistency with the predicted value of 15.6%. The lipid recovery was 98% by the microwave-assisted method under these optimized conditions.

3.3.3. Bootstrapping of data

To bootstrap the data, all of the 13 combinations of individual input variables, i.e., temperature, time and solvent-to-feed ratio were conducted in triplicates experimentally (Table 3.4). In RSM analysis, the interaction effects were not significant. In addition to individual parameters, their interactions also significantly affected the yield of lipid at $p < 0.00001$ after bootstrapping (Table 3.5). As the sample size increased the standard deviation decreased, which showed the successful bootstrapping of data. The p-value decreased as the sample size increased (Halsey et al., 2015).

3.3.4. Two-fold scale up extractions

The extraction parameters were optimized by RSM studies at laboratory scale, and those were used for two-fold scale up, to assess the feasibility of microwave-assisted lipid extraction from spent hens. In the scaled-up extraction process, the yield of extracted lipid was slightly less than that obtained at the laboratory scale, with 96.5+0.2% crude lipid recovery. The findings showed that comparable results could be obtained when the amount of starting material was doubled, indicating the future applicability of microwave-assisted lipid extractions at larger scales.

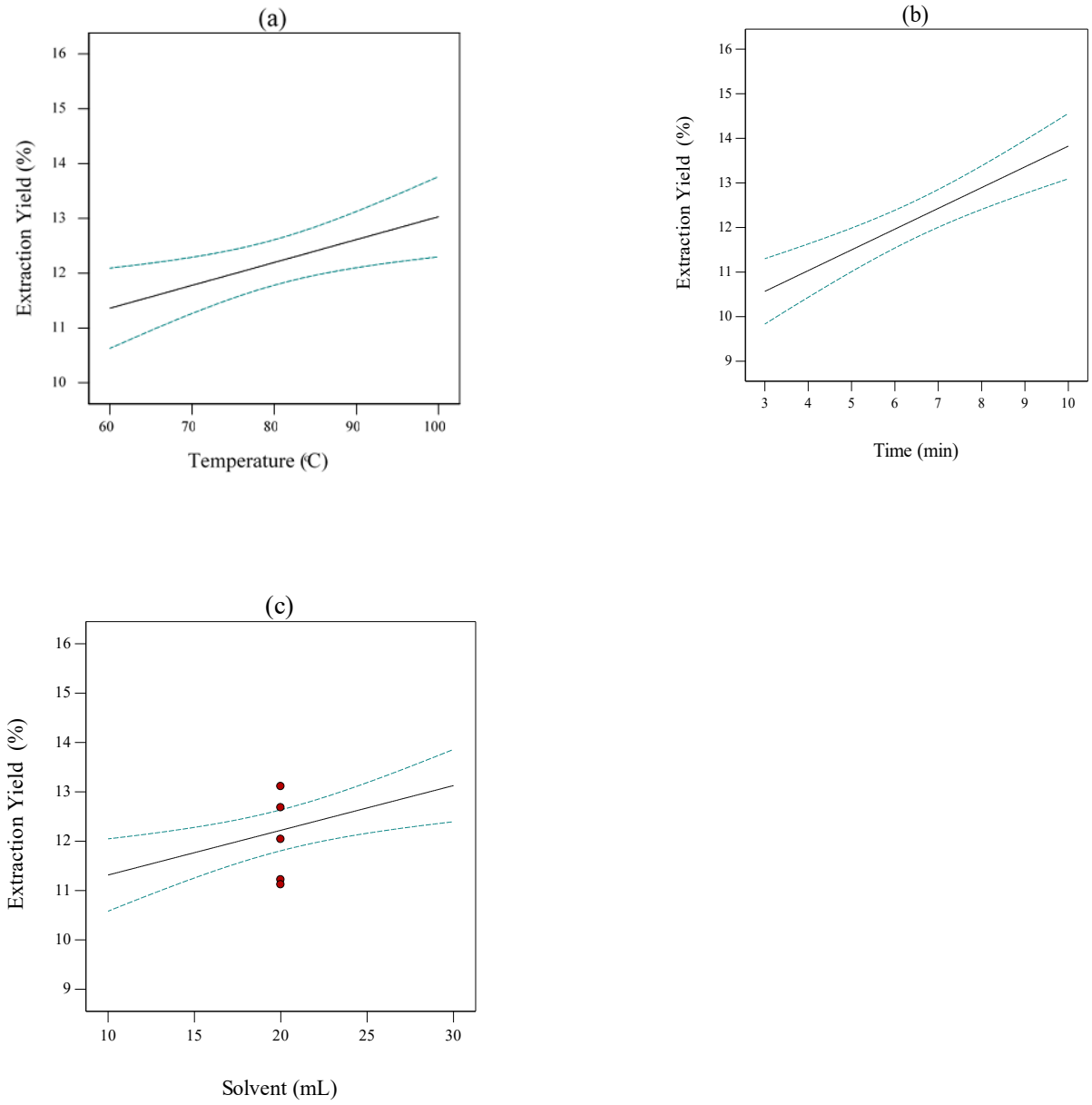

Figure 3.2: Response Surface Methodology plots for optimizing different parameters, showing extraction yield as a function of (a) temperature, (b) time, and (c) total amount of solvent used for 15 g feed.

Table 3.3: ANOVA results for the RSM experiments listed in Table 3.2 described by Eq. (3.1)

Source	Sum of squares	Degree of freedom	Mean square	F-Value	P-Value
Model	33.37	3	11.12	17.77	< 0.0001
A-Temperature	5.58	1	5.58	8.91	*0.0105*
B-Time	21.22	1	21.22	33.90	*< 0.0001*
C-Solvent	6.57	1	6.57	10.50	*0.0065*
Residual	8.14	13	-	-	-
Lack of Fit	5.06	9	0.56	0.73	*0.6805*
Pure Error	3.07	4	-	-	-
Cor Total	41.51	16	-	-	-

3.3.5. Characterization of extracted lipids

The characterization of extracted lipids was done using GC-MS, GC-FID, ^{1}H NMR, ATR-FTIR, and TGA as discussed below.

3.3.5.1. Fatty acid compositional analysis by GC-MS and GC-FID

The GC-MS spectrum of the transesterified crude lipid extract is shown in Figure 3.3, where methyl heptadecanoate (C17:0) was used as a standard. Five peaks were observed in the mass chromatogram, in which three predominant peaks were identified as palmitic (C16:0), oleic (C18:1) and linoleic (C18:2) methyl esters depending on their mass-to-charge ratio, while palmitoleic (C16:1) and stearic (C18:0) acids were also observed but in lower concentrations as it was evident from their peak intensities (Figure 3.3).

Table 3.4: The Bootstrap results for the process parameters of time (3, 6.5, 10 min), temperature (60, 80, 100 °C), and the solvent-to-feed ratio (0.7, 1.3, 2.0 mL/g).

Entry	Combinations			Mean	SDE	SDB	sem
1	H	H	M	14.36	0.76	0.36	0.0036
2	H	L	M	14.36	0.6	0.36	0.0036
3	H	M	H	14.03	0.25	0.12	0.0012
4	H	M	L	11.79	0.2	0.09	0.0009
5	L	H	M	12.27	0.64	0.30	0.0030
6	L	L	M	10.67	0.42	0.19	0.0019
7	L	M	H	11.37	0.4	0.19	0.0019
8	L	M	L	10.20	0.2	0.09	0.0009
9	M	H	H	15.80	0.27	0.12	0.0012
10	M	H	L	12.00	0.5	0.23	0.0023
11	M	L	H	11.73	0.64	0.30	0.0030
12	M	L	L	10.03	0.4	0.19	0.0019
13	M	M	M	12.02	0.95	0.35	0.0035

The abbreviations SDE, SDB, sem stand for standard deviation experimentally, standard deviation bootstrap and standard error of the mean, respectively, and L, M and H stand for low, medium and high, respectively.

Table 3.5: Three way ANOVA results for the Bootstrap experiments listed in Table 3.4

Source	Sum of squares	Degree of freedom	Mean square	F-Value	P-Value
Temperature	1302.32	2	651.16	10416.73	< 0.00001
Time	1055.28	3	351.76	5627.17	< 0.00001
Solvent	1042.35	2	521.17	8337.28	< 0.00001
Temp : Time	228.83	2	114.42	1830.35	< 0.00001
Temp : Solvent	87.19	2	43.60	697.41	< 0.00001
Time : Solvent	107.33	1	107.33	1716.97	< 0.00001
Residual	80.45	1287	0.06	-	-

To determine the composition of fatty acid components in the extracted lipids, the GC-FID analysis was performed. Table 3.6 showed the fatty acid compositions of extracted lipids under the different extraction conditions, and the results are reported as peak area percentage (normalized to 100%). The most abundant fatty acids were myristic (0.9-1.3%), palmitic (21.1-23.1%), palmitoleic (5.2-6.2%), stearic (4.8-5.4%), oleic (43.9-46.4%), and linoleic (20.1-22.5%) acids. On a two-fold scale up level, only slight variation was observed in the fatty acid compositions of the extracts. Fatty acid compositional analysis of all lipid extracts obtained at different extraction conditions showed that the temperature, time and solvent-to-feed ratios had no substantial effect on their fatty acid composition.

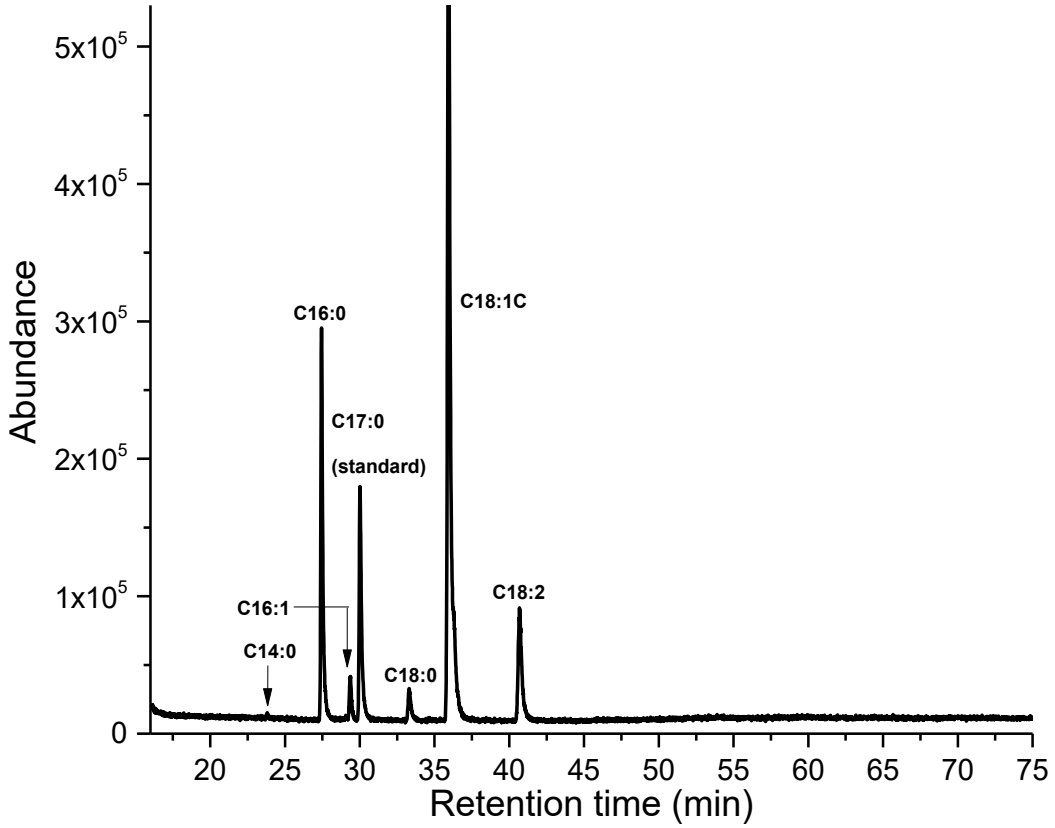

Figure 3.3: GC-MS spectrum of transesterified crude lipid extract.

3.3.5.2. ^{1}H NMR analysis of extracted lipids

Figure 3.4 represents ^{1}H NMR spectra of crude lipids extracted from the spent hen, where the peaks labeled as "*b*" and "*c*" correspond to the methylene and methine protons of glycerol part (O-C*H*$_2$-C*H*-C*H*$_2$-*O*). Unsaturated protons of hydrophobic fatty acid chains were observed in the chemical shift range of 5.3 - 5.5 ppm marked as “a”. The signals in the up field region (0.5-3.0 ppm) of NMR spectra correspond to saturated hydrocarbon (-CH$_2$-) protons. The triplet at δ 0.7 ppm represents the terminal methyl protons ("j") of fatty acid chains, while the internal methylene protons were observed at 1.3 ppm marked as “i”. The signals at chemical shift values of 2.05 and 2.75 ppm labeled as “h” and “e” are associated with methylene protons adjacent to olefinic groups. The rest of the signals marked as “f” at δ 2.4 ppm, and “h” at δ 1.6 ppm indicate those methylene

protons present adjacent to the carbonyl functionality (O=C-CH_2-CH_2-). All of these peaks in the spectrum are characteristic for triglyceride molecules and are consistent with the reported literature (Arshad et al., 2014).

3.3.5.3. ATR-FTIR analysis

Figure 3.5 represents an ATR-FTIR spectrum of the extracted lipids under the optimal extraction conditions. The strong absorbance at 2850 and 2926 cm^{-1} linked to the saturated C-H stretching, indicating large amount of methyl and methylene functionalities. Furthermore, the presence of small stretching bands at 3008 cm^{-1} is characteristic for alkene protons, confirming the presence of unsaturation in extracted lipids. The strong absorption peak at 1742 cm^{-1} represents the carbonyl functionality stretching associated with an ester group, showing a high content of carbonyl in the lipids. The absorption bands in between 1420 cm^{-1} and 1485 cm^{-1} belong to bending vibrations of alkanes, while the wavenumber region from 1080-1260 cm^{-1} represents the stretching vibrations of ester group (=C-O-C-). The strong peaks in the fingerprint region at around 730 cm^{-1} were attributed to rocking vibrations of methylene group and out of plane vibrations of *cis*-disubstituted alkenes. These results confirm the presence of triglyceride functional groups as was reported for the lipid extract of black soldier fly (Wang et al., 2017) and are consistent with the proton NMR results given in Figure 3.4.

Table 3.6: Effect of operation conditions on the fatty acid composition of lipids extracted from the spent hen.

Entry [a]	C14:0 (%)	C16:0 (%)	C16:1 (%)	C18:0 (%)	C18:1 (%)	C18:2 (%)
1	1.3	23.1	5.8	5.1	43.9	20.7
2	0.9	22.4	5.7	5.0	45.1	20.7
3	0.9	22.2	5.7	5.0	45.6	20.5
4	0.9	21.9	6.4	5.1	44.8	20.8
5	0.9	22.9	5.3	5.4	44.4	21.0
6	1.0	22.5	5.5	5.1	45.8	20.1
7	1.1	22.6	5.4	5.1	45.3	20.6
8	1.1	21.1	6.2	4.8	44.2	22.5
9	1.1	21.9	5.5	5.1	44.3	22.3
10	1.0	23.1	5.2	5.1	44.5	21.1
11	0.9	21.1	5.4	5.4	44.9	22.3
12	1.0	21.7	5.5	4.9	45.3	21.5
13	1.0	21.9	5.2	5.1	44.7	21.9
14	1.0	21.9	5.5	5.0	44.2	22.3
15	1.0	21.8	5.6	5.1	44.5	22.0
16	1.0	22.2	5.6	5.0	45.3	20.9
17	1.1	22.5	5.7	4.9	46.4	19.3
18 [b]	1.2	22.3	5.5	5.2	45.0	20.8
19 [c]	1.0	22.4	5.7	5.2	45.0	20.7
20 [d]	1.0	22.0	6.1	4.8	47.7	18.1

[a] Operation conditions of all entries are provided in Table 3.2
[b] Extraction of lipids by Soxhlet method
[c] Extraction of lipids by Folch method
[d] Extraction of lipids on a two fold scale-up process

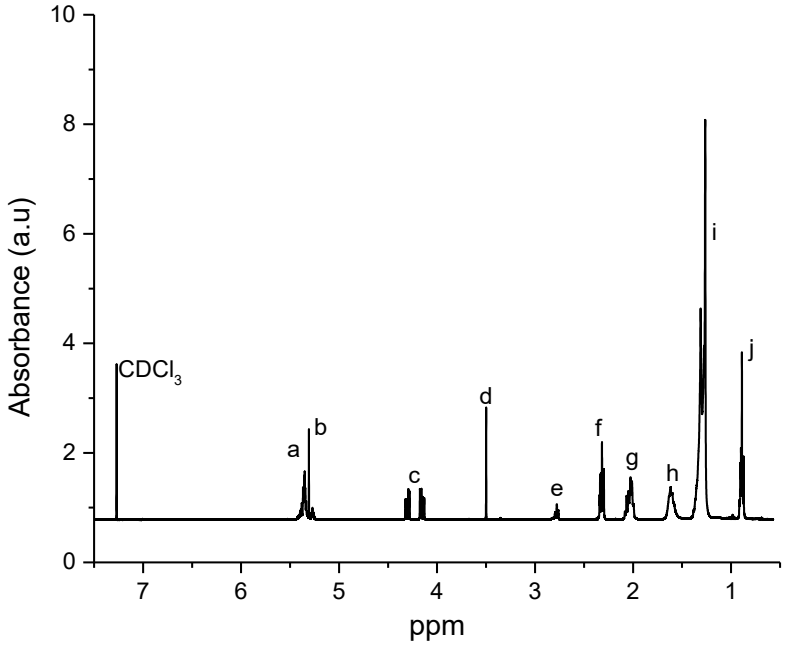

Figure 3.4: ^{1}H NMR spectrum of crude lipid extract.

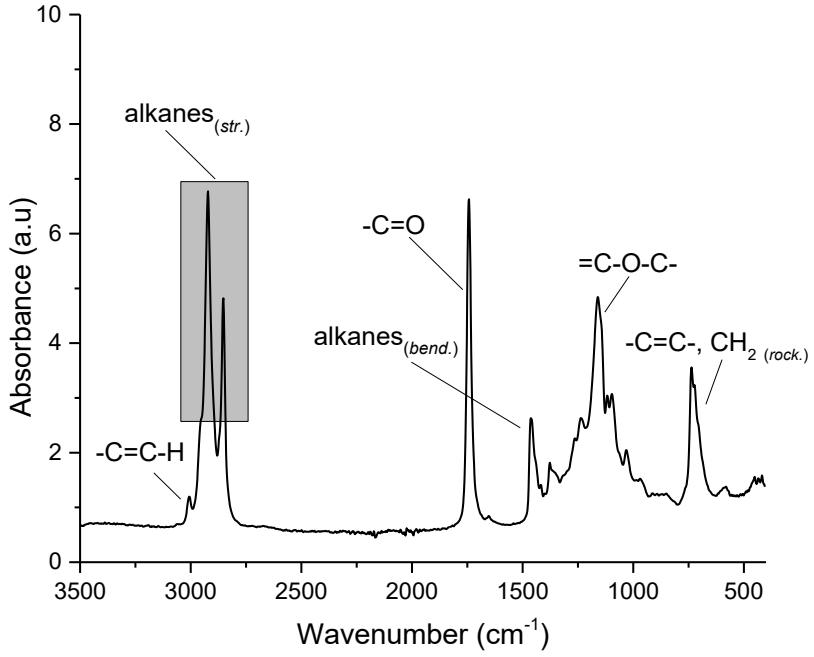

Figure 3.5: ATR-FTIR spectra of a crude lipid extract from spent hen.

3.3.5.4. DSC profile of extracted lipids

To investigate the phase transition behavior of crude extracted lipids, DSC analysis was performed as shown in Figure 3.6. Two broad exothermic peaks were observed in the cooling profile of the DSC thermogram, which represented the transition from liquid phase to solid. These two peaks indicate the presence of saturated and unsaturated lipids, while their broadness can be attributed to the different chain lengths of fatty acids present. The lower solidification temperatures (-0.2 and -8.4 °C) indicate the presence of a larger amount of unsaturated fatty acids, as this result is consistent with the fatty acid compositional data (27.6% saturated and 71.8% unsaturated fatty acids) determined by GC-FID (Table 3.6). The thermal data of lipids shown in Figure 3.6 are also consistent with the data reported previously for vegetable oils (Teles dos Santos et al., 2012).

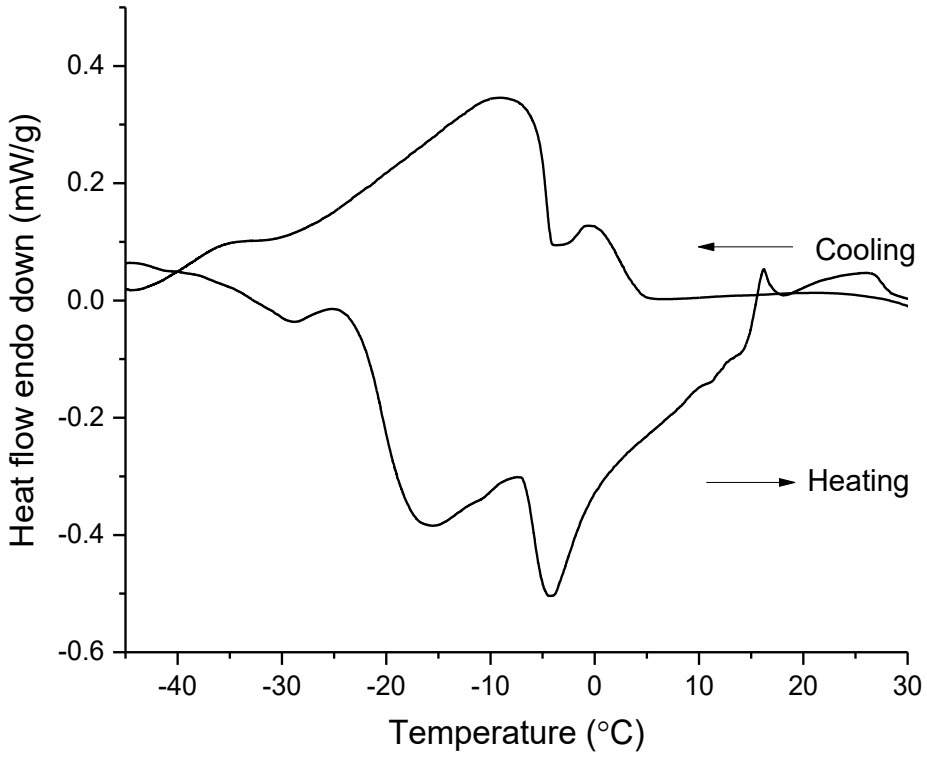

Figure 3.6: DSC thermogram of crude lipids extracted from spent hen.

3.3.5.5. Thermogravimetric analysis of the lipids

The thermal decomposition behavior of the extracted lipids was analyzed using the TGA. The weight loss profile attained by TGA and its derivatives (d-TGA) are shown in Figure 3.7. The curves showed that the entire thermal decomposition could be divided into two stages: the first stage of weight loss in between 30 and 125 °C is attributed to the loss of moisture (less than 10%), while the second stage represents the volatilization/decomposition of lipid molecules between 330 to 485 °C. The sudden increase in weight loss at 350 °C can be attributed to the breakdown of large molecules into lower molecular weight hydrocarbons, CO_2 and CO (Loo et al., 2015). The maximum weight loss of crude lipids was observed at 415 °C as obvious in the d-TGA curve with no residue left after the complete degradation of lipids. Similar thermal decomposition behavior of triglycerides extracted from black soldier fly was reported previously (Wang et al., 2017).

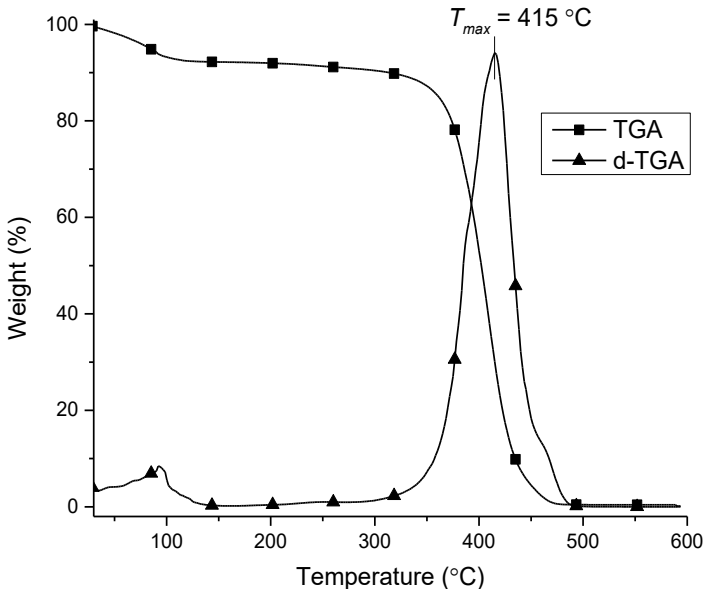

Figure 3.7: TGA and d-TGA curves of crude lipids extracted from spent hen.

3.3.6. Industrial applicability of microwave technology

The use of microwave technology is not only confined to lab scale experiments. Recently, industrial microwave units have been used in several areas, including chemical synthesis, food processing, sterilization, pasteurization and extraction of oils. For example, Radient Technology Inc. (Edmonton, AB, Canada) is using microwave systems on a pilot scale consuming up to 800 kg of biomass from different sources for the extraction of oils (Radient, 2018, January 12). In this study, the lipid extraction yield was 98% in 10 min. The two-fold extraction also gave a similar yield. The bootstrapping of data also supported its feasibility on industrial scale extraction of lipids from spent hens, as the p-value and standard deviation decreased with the increase in sample size.

3.4. Conclusions

The spent hen is an untapped biomass source for producing a variety of lipid-derived materials. The spent hen lipids were rapidly extracted using microwaves. The effects of extraction parameters such as the solvent-to-feed ratio, extraction time, and temperature on lipid extraction yield were studied and observed to be significant. The optimal yield was obtained using 2 mL/g solvent-to-feed ratio for 10 min at 80 °C. To account for the low sample size, parametric bootstrapping was used with a replacement approach, and data in all combinations were bootstrapped up to 10,000 times, which showed a decrease in standard deviation and p-value with an increase in sample size. The lipids predominantly had oleic, linoleic, and palmitic acids. The physicochemical characteristics of the lipids revealed their suitability for biomaterial production. The rapid extraction of lipids from spent hen provides a unique and promising opportunity for the production of lipid-based materials in subsequent stages of production.

3.5. References

Álvarez-Díaz, P.D., Ruiz, J., Arbib, Z., Barragán, J., Garrido-Pérez, M.C., Perales, J.A. 2017. Freshwater microalgae selection for simultaneous wastewater nutrient removal and lipid production. *Algal Research*, **24**(Part B), 477-485.

Amarni, F., Kadi, H. 2010. Kinetics study of microwave-assisted solvent extraction of oil from olive cake using hexane: Comparison with the conventional extraction. *Innovative Food Science & Emerging Technologies*, **11**(2), 322-327.

Arshad, M., Saied, S., Ullah, A. 2014. PEG-lipid telechelics incorporating fatty acids from canola oil: synthesis, characterization and solution self-assembly. *RSC Advances*, **4**(50), 26439-26446.

Bernhart, M., Fasina, O.O. 2009. Moisture effect on the storage, handling and flow properties of poultry litter. *Waste Management*, **29**(4), 1392-1398.

Binnington, D.S. 1932. Improved soxhlet extraction apparatus. *Industrial & Engineering Chemistry Analytical Edition*, **4**(1), 125-126.

Bryant, J., Clausen, T., Reichardt, P., McCarthy, M., Werner, R. 1987. Effect of nitrogen fertilization upon the secondary chemistry and nutritional value of quaking aspen (Populus tremuloides Michx.) leaves for the large aspen tortrix (Choristoneura conflictana (Walker)). *Oecologia*, **73**(4), 513-517.

Chen, L., Wang, C., Wang, W., Wei, J. 2013. Optimal conditions of different flocculation methods for harvesting Scenedesmus sp. cultivated in an open-pond system. *Bioresource Technology*, **133**(Supplement C), 9-15.

Cravotto, G., Boffa, L., Mantegna, S., Perego, P., Avogadro, M., Cintas, P. 2008. Improved extraction of vegetable oils under high-intensity ultrasound and/or microwaves. *Ultrasonics Sonochemistry*, **15**(5), 898-902.

da Silva, T.L., Gouveia, L., Reis, A. 2014. Integrated microbial processes for biofuels and high value-added products: the way to improve the cost effectiveness of biofuel production. *Applied Microbiology and Biotechnology*, **98**(3), 1043-1053.

Fang, H., Zhao, C., Kong, Q., Zou, Z., Chen, N. 2016. Comprehensive utilization and conversion of lignocellulosic biomass for the production of long chain α,ω-dicarboxylic acids. *Energy*, **116**(Part 1), 177-189.

Folch, J., Lees, M., Stanley, G.H.S. 1957. A simple method for the isolation and purification of total lipides from animal tissues. *Journal of Biological Chemistry*, **226**, 497-509.

Halsey, L.G., Curran-Everett, D., Vowler, S.L., Drummond, G.B. 2015. The fickle P value generates irreproducible results. *Nature Methods*, **12**, 179.

Hong, H., Roy, B.C., Chalamaiah, M., Bruce, H.L., Wu, J. 2018. Pretreatment with formic acid enhances the production of small peptides from highly cross-linked collagen of spent hens. *Food Chemistry*, **258**, 174-180.

Horwitz, W., Latimer, G.W. 2005. *Official methods of analysis of AOAC International*. AOAC International, Gaithersburg, Md.

Jin, L., Zeng, H., Ullah, A. 2017. Rapid copolymerization of canola oil derived epoxide monomers with anhydrides and carbon dioxide (CO_2). *Polymer Chemistry*, **8**(41), 6431-6442.

Karlovic, D., Sovilj, M., Turkulov, J. 1992. Kinetics of oil extraction from corn germ. *Journal of the American Oil Chemists' Society*, **69**(5), 471-476.

Katouzian, I., Faridi Esfanjani, A., Jafari, S.M., Akhavan, S. 2017. Formulation and application of a new generation of lipid nano-carriers for the food bioactive ingredients. *Trends in Food Science & Technology*, **68**(Supplement C), 14-25.

Kondaiah, N., Panda, B. 1992. Processing and utilization of spent hens. *World's Poultry Science Journal*, **48**(3), 255-268.

Kumar, M., Ghosh, P., Khosla, K., Thakur, I.S. 2016. Biodiesel production from municipal secondary sludge. *Bioresource Technology*, **216**(Supplement C), 165-171.

Loo, L., Maaten, B., Siirde, A., Pihu, T., Konist, A. 2015. Experimental analysis of the combustion characteristics of Estonian oil shale in air and oxy-fuel atmospheres. *Fuel Processing Technology*, **134**(Supplement C), 317-324.

Luque de Castro, M.D., Castillo-Peinado, L.S. 2016. 3 - Microwave-Assisted Extraction of Food Components. in: *Innovative Food Processing Technologies*, Woodhead Publishing, pp. 57-110.

McMillan, J.R., Watson, I.A., Ali, M., Jaafar, W. 2013. Evaluation and comparison of algal cell disruption methods: Microwave, waterbath, blender, ultrasonic and laser treatment. *Applied Energy*, **103**(Supplement C), 128-134.

Meullemiestre, A., Breil, C., Abert-Vian, M., Chemat, F. 2016. Microwave, ultrasound, thermal treatments, and bead milling as intensification techniques for extraction of lipids from oleaginous Yarrowia lipolytica yeast for a biojetfuel application. *Bioresource Technology*, **211**(Supplement C), 190-199.

Olkiewicz, M., Caporgno, M.P., Fortuny, A., Stüber, F., Fabregat, A., Font, J., Bengoa, C. 2014. Direct liquid–liquid extraction of lipid from municipal sewage sludge for biodiesel production. *Fuel Processing Technology*, **128**, 331-338.

Orr, V.C.A., Plechkova, N.V., Seddon, K.R., Rehmann, L. 2016. Disruption and wet extraction of the microalgae *Chlorella vulgaris* using room-temperature ionic liquids. *ACS Sustainable Chemistry & Engineering*, **4**(2), 591-600.

Osen, R., Toelstede, S., Wild, F., Eisner, P., Schweiggert-Weisz, U. 2014. High moisture extrusion cooking of pea protein isolates: Raw material characteristics, extruder responses, and texture properties. *Journal of Food Engineering*, **127**(Supplement C), 67-74.

Pane, L., Franceschi, E., De Nuccio, L., Carli, A. 2001. Applications of thermal analysis on the marine phytoplankton, Tetraselmis Suecica. *Journal of Thermal Analysis and Calorimetry*, **66**(1), 145-154.

Papanikolaou, S., Dimou, A., Fakas, S., Diamantopoulou, P., Philippoussis, A., Galiotou-Panayotou, M., Aggelis, G. 2011. Biotechnological conversion of waste cooking olive oil into lipid-rich biomass using Aspergillus and Penicillium strains. *Journal of Applied Microbiology*, **110**(5), 1138-1150.

Piker, A., Tabah, B., Perkas, N., Gedanken, A. 2016. A green and low-cost room temperature biodiesel production method from waste oil using egg shells as catalyst. *Fuel*, **182**(Supplement C), 34-41.

Qadeer, S., Khalid, A., Mahmood, S., Anjum, M., Ahmad, Z. 2017. Utilizing oleaginous bacteria and fungi for cleaner energy production. *Journal of Cleaner Production*, **168**, 917-928.

Radient. 2018. Radient technology (https://www.radientinc.com/) [Accessed on January 12, 2018].

Tactacan, G.B., Guenter, W., Lewis, N.J., Rodriguez-Lecompte, J.C., House, J.D. 2009. Performance and welfare of laying hens in conventional and enriched cages. *Poultry Science*, **88**(4), 698-707.

Tao, B.Y. 2007. Chapter 24 - Industrial Applications for Plant Oils and Lipids A2 - Yang, Shang-Tian. in: *Bioprocessing for Value-Added Products from Renewable Resources*, Elsevier. Amsterdam, pp. 611-627.

Teles dos Santos, M., Gerbaud, V., Le Roux, G.A.C. 2012. Comparison of predicted and experimental DSC curves for vegetable oils. *Thermochimica Acta*, **545**(Supplement C), 96-102.

Wahidin, S., Idris, A., Shaleh, S.R.M. 2014. Rapid biodiesel production using wet microalgae via microwave irradiation. *Energy Conversion and Management*, **84**(Supplement C), 227-233.

Wang, C., Qian, L., Wang, W., Wang, T., Deng, Z., Yang, F., Xiong, J., Feng, W. 2017. Exploring the potential of lipids from black soldier fly: New paradigm for biodiesel production (I). *Renewable Energy*, **111**(Supplement C), 749-756.

Wang, H., Wu, J., Betti, M. 2013. Chemical, rheological and surface morphologic characterisation of spent hen proteins extracted by pH-shift processing with or without the presence of cryoprotectants. *Food Chemistry*, **139**(1), 710-719.

Xiao, W., Han, L., Shi, B. 2008. Microwave-assisted extraction of flavonoids from Radix Astragali. *Separation and Purification Technology*, **62**(3), 614-618.

Yanık, D.K. 2017. Alternative to traditional olive pomace oil extraction systems: Microwave-assisted solvent extraction of oil from wet olive pomace. *LWT - Food Science and Technology*, **77**(Supplement C), 45-51.

Yu, W., Field, C.J., Wu, J. 2018. Purification and identification of anti-inflammatory peptides from spent hen muscle proteins hydrolysate. *Food Chemistry*, **253**, 101-107.

Zhao, L., Temelli, F., Curtis, J.M., Chen, L. 2015. Preparation of liposomes using supercritical carbon dioxide technology: Effects of phospholipids and sterols. *Food Research International*, **77**(Part 1), 63-72.

CHAPTER 4 - SUPERCRITICAL CO_2 EXTRACTION AND SOLVENT-FREE RAPID ALTERNATIVE BIOEPOXY PRODUCTION FROM SPENT HENS[2]

4.1. Introduction

Currently, one of the main foci of industry and academia is to find sustainable raw materials for the chemical manufacturing industries due to concerns related to the environment and decreasing fossil fuel reservoirs (Loh, 2017; Zubair and Ullah, 2019). To address these concerns and fulfill the industry requirements, utilization of industrial wastes or by-products has been evaluated (Arshad et al., 2016b; Kaur et al., 2018; Stephen and Periyasamy, 2018). One such potential, inexpensive and renewable bioresource, which has not been explored previously, is spent hens as described in Chapter 2 (Section 2.1). The current study aims to harvest this bioresource for the recovery of lipids with the ultimate goal of developing epoxidized lipids to be used as plasticizers.

In conventional lipid extraction, large volumes of organic solvents are used i.e., *n*-hexane, which has several drawbacks including lengthy extraction times (García-Ayuso and Luque de Castro, 2001). To overcome these limitations of solvent extraction, supercritical carbon dioxide (SC-CO_2) is considered to be an alternative to organic solvents, which is abundant, nontoxic, non-flammable, cheap, sustainable and also has tunable physico-chemical properties (Brennecke, 1997; Leitner, 2000; Temelli, 2009). The inherent properties of CO_2, i.e., density, viscosity and diffusivity can be adjusted by altering temperature and pressure (Brunner, 2013; Soh and Zimmerman, 2011). Because of the solvent properties of CO_2, it is not only used for extractions but also as a reaction medium. This modern extraction technology has been used for the extraction of lipids from a variety of sources, including meat and poultry feed with over 96% lipid recovery

[2] A version of this chapter has been published: Safder, M., Temelli, F., Ullah, A. 2019b. Supercritical CO_2 extraction and solvent-free rapid alternative bioepoxy production from spent hens. Journal of CO_2 Utilization, 34, 335-342.

(King et al., 1989; Orellana et al., 2013).

Epoxides are chemical compounds commonly produced from fossil resources and extensively used in several industrial applications, including automobile, aerospace, electronics, adhesives, and coatings (Aris et al., 2015; Goodman and Hanna, 2014; Parameswaranpillai et al., 2016). However, due to their non-renewable and hazardous nature, development of sustainable epoxides from renewables has attracted considerable research interest to synthesize them from vegetable oils (Auvergne et al., 2013; Kamarudin et al., 2018; Xia et al., 2016; Xia and Larock, 2010). These oil-derived epoxides, being bio-renewable, have numerous applications including lubricants, thermosetting polymers (Galià et al., 2010; Yan et al., 2016) and plasticizers (Mungroo et al., 2008; Sharma et al., 2006). The major use of these plasticizers is in polyvinyl chloride (PVC) materials, which are one of the most widely consumed thermoplastics (Arrieta et al., 2017) with numerous applications (Suzuki et al., 2018). Nevertheless, the edible oil based bio-plasticizers are competing with the food chain, and therefore, negatively affecting the price of edible oils, which have a major use in human consumption (Fernandes et al., 2017; Greco et al., 2016). Therefore, environmentally benign extraction of fats/oils from alternative low cost, renewable and sustainable feedstock, which does not compete with the food chain is highly desirable.

The literature lacks information on the extraction of lipids from spent hens using SC-CO_2 and subsequent conversion of the lipid extract into epoxides. Consequently, the overall objective of this study was to evaluate SC-CO_2 extraction of lipids from spent hen and their oxidation for the development of a bio-plasticizer. The specific objectives were first to investigate the effects of pressure and temperature on the extraction of lipids using SC-CO_2 and then perform epoxidation of the extracted lipids for the preparation of a bio-plasticizer with and without the use of an organic solvent.

4.2. Materials and Methods

4.2.1. Materials

The spent hens were obtained from Alberta Hatching Egg Producers (AHEP). Toluene (≥99%), n-hexane (95%, Caledon), dichloromethane (DCM, 99.5%), anhydrous sodium sulphate (Na_2SO_4, 99%), formic acid (≥95%), Amberlite IR-120 resin, hydrogen peroxide (35%) and all other chemicals were purchased from Sigma-Aldrich (St. Louis, MO, USA) and used as received.

4.2.2. Sample preparation

The grinding of the spent hen was carried out as previously described in Chapter 3 (Section 3.2.1). Moisture was removed by freeze drying using Virtis Ultra 35L Freeze Dryer (SP Scientific, Stone Ridge, NY, USA) and the moisture content was calculated after gravimetric measurement of the sample before and after drying. The ground samples were stored in a freezer at -20 °C until further use for lipid extraction. Crude lipid content was determined by Soxhlet extraction in triplicate using *n*-hexane for 5 h followed by solvent removal under vacuum at 40 °C. The moisture content of ground spent hen was 60.1 ± 0.1% (w/w). The lipid content of the spent hen was 40.5±0.4% as determined by Soxhlet extraction (Mello et al., 2017), which was in agreement with the previous study on the extraction of lipids from spent hens using microwaves (Chapter 3).

The density of the spent hen before and after the SC-CO_2 extraction was measured by a nitrogen pycnometer (AccuPyc 1330, micrometrics, Norcross GA, USA) using standard sample holder (10 cm^3) according to ASTM D2856-94 (ASTM, 1994). The density of the ground spent hen before and after the SC-CO_2 extraction was 1.2165±0.0016 and 1.4573±0.0052 g/cm^3 with the porosities of 65.5±1% and 86.1±1%, respectively.

4.2.3. Supercritical extraction unit

SC-CO_2 extractions were performed using a laboratory-scale supercritical fluid extraction unit (Newport Scientific, Inc., Jessup, MD, USA) as described previously (Bozan and Temelli, 2002) with some modifications. Briefly, the system was operated in a semi-continuous mode by pumping SC-CO_2 through a fixed bed of ground spent hen, depressurizing the CO_2 to precipitate the lipid extract after the extraction cell, and releasing the expanded CO_2 to the atmosphere. For each run, approximately 2 g of ground sample was loaded into a basket (20 mL), and the basket was placed in the 300 mL extraction cell. To prevent bed compaction glass beads were used in between the sample and glass wool at both ends of the basket. Two o-rings placed around the basket ensured that CO_2 would flow through the sample. CO_2 in gaseous state was compressed to the desired pressure by using a diaphragm compressor with a maximum rating of 70 MPa. Pressure was controlled (±1 MPa) by a back-pressure regulator located at the compressor exit and monitored by a pressure gauge. The extraction vessel was heated with an electrical heating jacket. The temperature inside the vessel was monitored by a type K thermocouple and controlled by a temperature controller with an accuracy of ±1 °C (United Electric Control Co., model D921, Watertown, MA, USA). CO_2 was preheated to the targeted extraction temperature prior to entry into the vessel, using a heating tape wrapped around the tubing, which was connected to a temperature controller. The flow rate of the CO_2 was maintained manually by adjusting a micrometering valve, which was placed at the exit of the extraction vessel and heated to avoid freezing due to the Joule-Thomson effect upon CO_2 expansion. The flow rate and total volume of CO_2 used in each run were measured at ambient conditions by a flow meter and a dry gas meter (±0.05 L), respectively.

4.2.4. Experimental design

To maximize the recovery of lipids from ground spent hens, a range of temperatures and pressures were employed. Extractions were performed at temperatures of 40, 55, and 70 °C and pressures of 30, 40, and 50 MPa at a constant CO_2 flow rate of 1 L/min (measured at ambient conditions). The extracted lipid fractions were collected with a short time interval of 10 min for the first 30 min of extraction due to the larger extraction rate of lipids initially followed by 15 min intervals for 30 min, and 30 min intervals for 120 min for a total extraction time of 180 min. Extracted fractions were collected in scintillation glass vials held in a cold trap at −20 °C after the depressurization valve. The amount of each fraction was determined gravimetrically, and the lipid extraction yield was expressed as a percentage of the mass of ground sample used as feed. Extracted lipid samples were stored at −20 °C until further use. All experiments were conducted in duplicates.

A 10-fold scale up of the extraction was performed using the optimized SC-CO_2 extraction conditions obtained (50 MPa, 70 °C) and keeping the flow rate of CO_2 as 1 L/min. The extraction time was extended up to 240 min because of the larger amount of sample loaded and the extractions were conducted in duplicate. For each run, approximately 20 g of ground sample was loaded into a larger basket (100 mL), and the basket was placed in the 300 mL extraction cell, while the rest of the conditions were kept the same. The amount of extracted lipid was reported as percentage yield on dry basis using the freeze-dried feed material, according to Eq. (1). In addition, the recovery of extracted lipids was determined by considering Soxhlet extracted lipids using dichloromethane-methanol (2:1, v/v) as 100 percent, according to Eq. (2).

$$Lipid\ extraction\ yield\ (\%) = \frac{Amount\ of\ lipid\ extracted\ by\ CO2}{Amount\ of\ feed\ used}\ X100 \quad (4.1)$$

$$Lipid\ recovery\ (\%) = \frac{Amount\ of\ lipid\ extracted\ by\ CO2}{Amount\ of\ lipid\ extracted\ by\ Soxhlet}\ X100 \quad (4.2)$$

4.2.5. Characterization of extracts

To assess the effect of pressure and temperature on the fatty acid composition of the extracts, the gas chromatography-mass spectrometry (GC-MS) and gas chromatography-flame ionization detector (GC-FID) analyses of the transesterified crude lipid was conducted using methyl heptadecanoate (C17:0) as an internal standard (Arshad et al., 2014). GC-MS analysis was performed using Agilent 6890N gas chromatograph (Ramsey, MN, USA), equipped with a fused silica SP2560 capillary column (100 m length × 0.25 mm diameter × 0.2 mm film thickness) and detector (5975B inert XL MSD) as described in Chapter 3 (Section 3.2.4.1.). The fatty acids were identified by the comparison of retention time and mass from the GC library. GC-FID analysis was performed using a Perkin Elmer GC-FID Clarus 500 instrument (Alexandria, VA, USA) fitted with a flame ionization detector as described in Chapter 3 (Section 3.2.4.1).

The morphological changes of the ground spent hen matrix before and after SC-CO_2 and Soxhlet extractions were examined using a Zeiss Orion nanoFab Helium Ion Microscope (HIM) (Carl Zeiss AG, Oberkochen, Germany) located at the nanoFab facility of the University of Alberta. To neutralize the positive charges concentrated on the surface of sample, an electron flood gun was used, which helps to get the images of insulating samples. Unlike scanning electron microscopy (SEM), the HIM uses a beam of He^+ ions and due to the defined gas ionized source with a smaller probe size, high resolution images with larger field depth can be obtained (Burch et al., 2017; Byrne et al., 2018). Therefore, HIM was deliberately selected for the analysis of ground samples before and after SC-CO_2 extraction because it offers the advantage of using low-energy ion beams, minimizes sample surface damage, and provides high surface contrast in direct imaging of biological samples to prevent charging caused by the insulating properties of most biological

materials (Bazou et al., 2011). It also maintains subtle surface features by eliminating any metal coating requirements for sample preparation generally used in SEM (Joens et al., 2013).

4.2.6. Epoxidation without solvent use

Lipids extracted from spent hens (3 g) using SC-CO_2 at optimized conditions (50 MPa and 70 °C) were placed into a 25 mL round bottom flask with a magnetic stir bar and the mixture was stirred at room temperature (24 °C) in a paraffin oil bath for 2 min. Then, 1 g of Amberlite IR-120 resin and 0.5 g of formic acid were added, and the reaction mixture was kept on stirring for 2 min. Hydrogen peroxide (3 mL) was added drop wise to the reaction mixture. Then, the temperature of the oil bath was raised to 50 °C, which was taken as t=0 min (Aerts and Jacobs, 2004). Samples were collected during the reaction at the time intervals of 0, 15, 30, 60, and 120 min and the completion of reaction was monitored by attenuated total reflectance-Fourier transform infrared spectroscopy (ATR-FTIR) and proton nuclear magnetic spectroscopy (^{1}H NMR). After the completion of reaction, a yellow epoxidized product (2.5 g) was obtained. The reactions were performed in duplicate.

4.2.7. Epoxidation with solvent use

The epoxidation procedure was kept the same as described above except the lipid extract was first dissolved in an equal amount of toluene as solvent. The samples were collected through a capillary tube at relatively shorter intervals of 0, 5, 10, 20, 30 and 60 min during the reaction to analyse the progress of reaction more precisely using ATR-FTIR and ^{1}H NMR spectroscopy. The epoxidized spent hen lipids were extracted from the reaction mixture using *n*-hexane and distilled water (20 mL each). The emulsion formed during the extraction of product was broken by the addition of saturated sodium chloride solution (10 mL). Then, the hexane layer was passed through

anhydrous Na_2SO_4 to remove residual moisture. A yellow epoxidized lipid product (2.4 g) was obtained after the completion of the reaction. The experiments were conducted in duplicates.

4.2.8. Characterization of reaction products

ATR-FTIR spectra of the reaction mixture were recorded during the epoxidation using a Bruker Optics (Esslingen, Germany) unit equipped with a single bounce diamond ATR crystal. All samples were scanned in the wavelength range of 410-4000 cm^{-1}. Spectra were obtained using OPUS software version 6.5 from Bruker and a total of 16 scans at a resolution of 4 cm^{-1} were recorded for each sample.

The progress of epoxidation reaction was also investigated with the help of ^1H NMR spectroscopy. The ^1H NMR spectra of samples obtained at different time intervals were taken with and without solvent using deuterated chloroform at 400 MHz using a Varian instrument (Varian Inova, Palo Alto, CA, USA).

4.3. Results and Discussion

4.3.1. SC-CO_2 extraction of lipids; extraction yield and apparent solubility

Experimental extraction curves of total lipids obtained at different operating conditions are presented in Figure 4.1. As expected, the extraction curves present the three typical regions: solubility-controlled region, transition region and the diffusion-controlled region. The apparent solubility of lipids from spent hen in SC-CO_2 at each combination of pressure and temperature was determined from the slopes of the initial linear portion of extraction curves, representing the solubility-controlled region. Keeping the CO_2 flow rate low enough to allow sufficient contact time is essential for the determination of apparent solubility. The CO_2 flow rate was maintained constant at 1 L/min in this study based on a previous study, which evaluated the effect of flow rate on extract loading in CO_2 using the same extraction unit (Sun and Temelli, 2006).

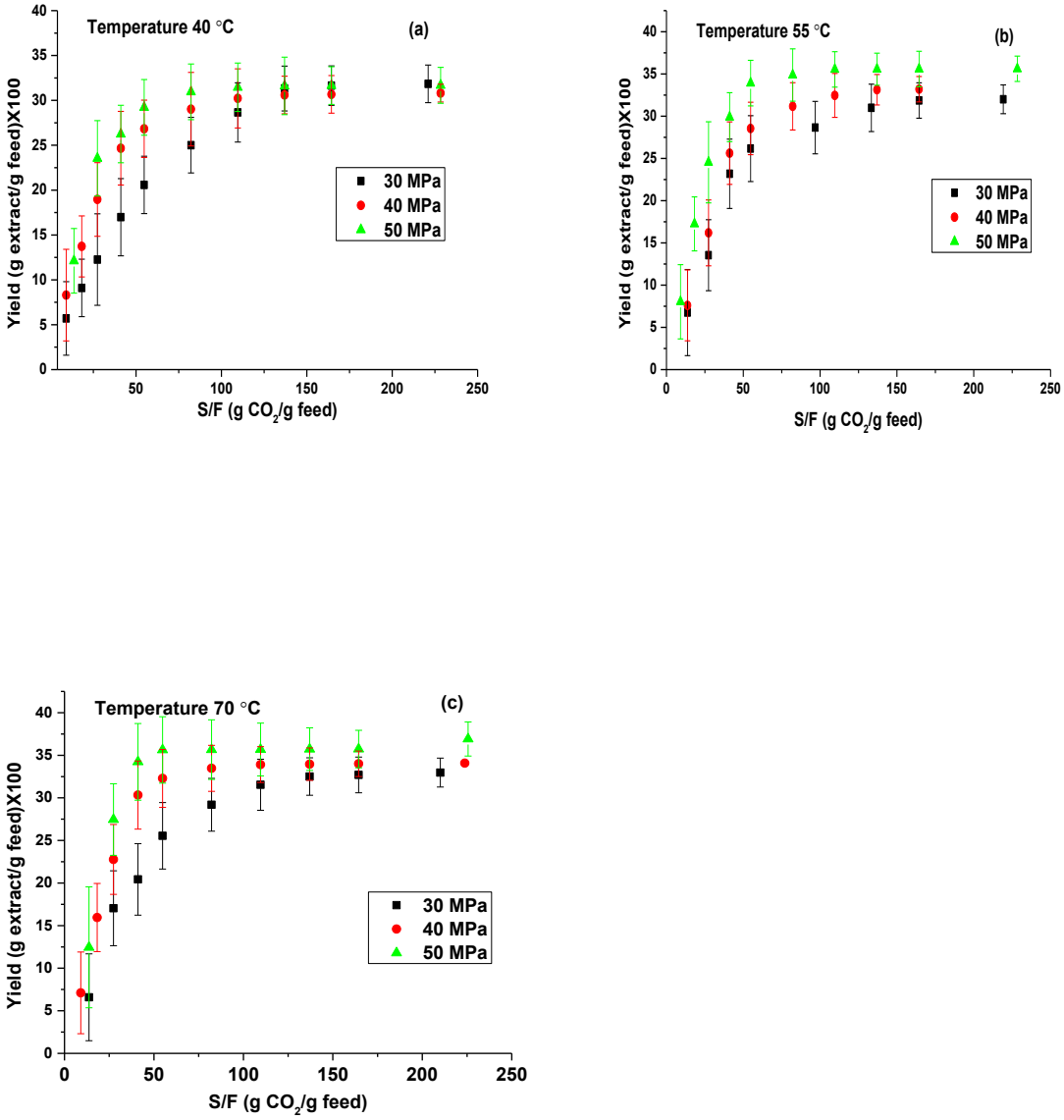

Figure 4.1: SC-CO_2 extraction yield as a function of solvent-to-feed ratio at pressures of 30, 40, and 50 MPa at (a) 40 °C (b) 55 °C and (c) 70 °C.

The apparent solubility of spent hen lipids is given in Table 4.1. As expected, higher solubility of total lipids was obtained at higher pressures at all temperatures and the results were in agreement with the already reported study on extracted lipids from shrimp waste (Sánchez-Camargo et al., 2011). The extraction results showed that the apparent solubility varied from

4.4±0.5 to 7.5±0.5 mg/g CO_2 at 40 °C, 5.4±0.4 to 9.0±0.3 mg/g CO_2 at 55 °C and 4.9±0.95 to 8.7±0.3 mg/g CO_2 at 70 °C within the pressure range of 30, 40, and 50 MPa. Similar solubility behavior has been reported in the literature for lipids from different biological sources, for example, flaxseed oil solubility was reported as 11.3 mg oil/g CO_2 at 70 ^oC and 55 MPa (Bozan and Temelli, 2002) while the fat solubility from poultry meal was 6.3 mg/g CO_2 at 50 ^oC and 34.5 MPa (Orellana et al., 2013). The increase in apparent solubility with pressure was due to an increase in the density of CO_2 at higher pressures, which in turn increased its dissolving power (Wu et al., 2016). As presented in Table 4.1, apparent solubility increased with temperature at higher pressures. Increasing temperature also has an impact on physicochemical properties with reduced viscosity and enhanced diffusivity, which is beneficial for mass transfer. A higher amount of CO_2 is needed at lower temperatures and pressures for the extraction of total lipids of ground spent hen (Figure 4.1) (Güçlü-Üstündağ and Temelli, 2006; Viner et al., 2018). The lowest SC-CO_2 consumption for the extraction of the maximum amount of total lipids was observed at 40 MPa and 70 °C from the initial linear portion of extraction curves. The maximum yield of 37 g/g feed at an S/F of ~60 to 125 g/g feed (Figure 4.1) was obtained at 50 MPa and 70 °C, corresponding to a recovery of 92%. The plateau was reached at S/F of 59.7 without much change with further increase of S/F. The lower lipid extraction recovery compared to Soxhlet extraction could be mainly due to the differences in the lower solubility of polar lipids in SC-CO_2. On a ten-fold scale up level, the observed extraction yield was 17.5% at S/F of 16.6 g/g feed. While in comparison to the small scale, 19.4% yield was obtained at a similar S/F of 16.6, so S/F of ~60 should be tested at larger scale.

Table 4.1: Apparent solubility of spent hen lipids in SC-CO_2 at different temperatures and pressures.

P (MPa)	T (°C)	CO_2 density[a] (kg/m^3)	Apparent solubility[b] (mg lipid/g CO_2)
30	40	910	4.4±0.5
40	40	950	8.9±0.95
50	40	990	7.5±0.5
30	55	850	5.4±0.4
40	55	910	5.7±1.05
50	55	950	9.0±0.3
30	70	790	4.9±0.95
40	70	860	9.1±0.9
50	70	910	8.7±0.3

[a]CO_2 density values were obtained from NIST Chemistry Webbook.
[b]Values are reported as mean ± standard deviation based on duplicate runs.

4.3.2. Morphological analysis of spent hen before and after SC-CO_2 extraction

Figure 4.2 shows the visual appearance of ground spent hen before and after SC-CO_2 extraction, where the brown and coarse feed material became light brown and fine after extraction because of the removal of lipids.

Figure 4.2: Physical appearance of ground spent hen (a) before and (b) after SC-CO_2 extraction.

The ground spent hen was investigated by HIM to examine the effect of high-pressure CO_2 treatment on morphological changes. The HIM images of the ground spent hen matrix showed smooth surfaces, no cavities and droplets in the matrix before extraction (Figure 4.3a), while there were remarkable changes on its surface morphology after the SC-CO_2 extraction (Figure 4.3b) in the form of ruptured surfaces with some visible pores in the matrix and rough texture compared to the native sample before extraction. However, the surface morphology of the sample after the Soxhlet extraction showed less disrupted surface compared to SC-CO_2 extraction as can be seen in Figure 4.3c. The release of high-pressure SC-CO_2 following extraction has been previously reported to cause cell rupture in pollen, soybeans, leather industry waste and *Mortierella alpina* biomass (Devaraj et al., 2018; Li et al., 2004; Nisha et al., 2012; Xu et al., 2009).

4.3.3. Fatty acid composition of lipid extracts

Five peaks were observed in the mass chromatogram, in which three predominant peaks were identified as palmitic (C16:0), oleic (C18:1) and linoleic (C18:2) methyl esters depending on their mass-to-charge ratio, while palmitoleic (C16:1) and stearic (C18:0) acids were also present but at lower concentrations.

Table 4.2 shows the fatty acid composition of the lipids obtained under the different extraction conditions and the results are reported as peak area percentage (normalized to 100%) based on GC-FID analysis. The most abundant fatty acids were myristic (0.8-1.4$\pm$0.2%), palmitic (19.5-24.8$\pm$2.5%), palmitoleic (4.1-5.9$\pm$0.5%), stearic (4.7-6.8$\pm$0.8%), oleic (52.1-59.9$\pm$2.7%), and linoleic (5.6-15.9$\pm$5.2%) acids, and the results are in agreement with the literature (Rocha Garcia et al., 2003). Fatty acid compositional analysis of all lipid extracts obtained at different extraction conditions showed that the pressure and temperature had no substantial effect on their

fatty acid composition. In addition, the fatty acid composition of the lipid extract obtained after ten-fold scale up was similar with only a slight variation.

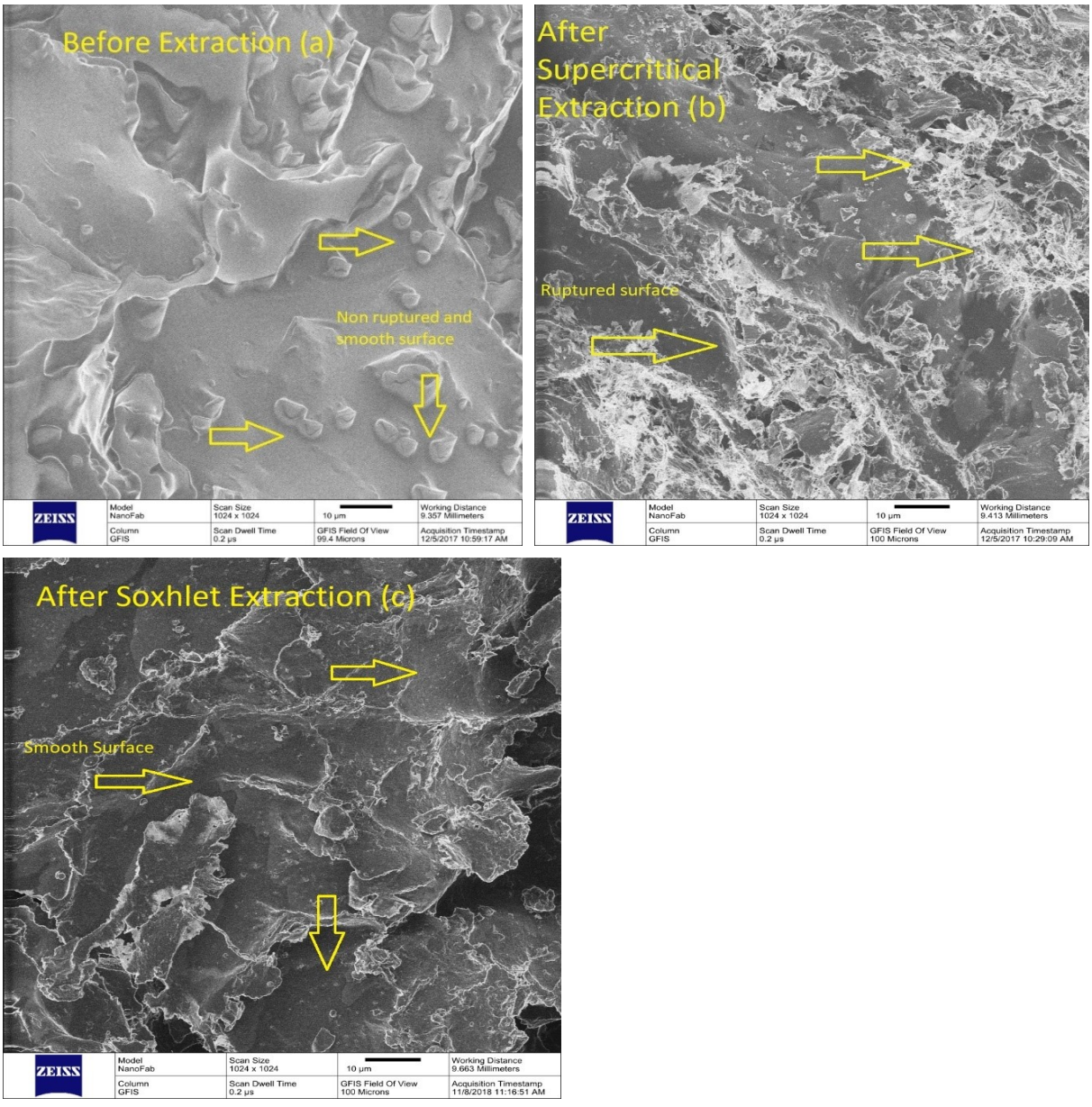

Figure 4.3: HIM images of ground spent hen sample: a) untreated ground sample, b) solid residue after SC-CO_2 extraction performed at 50 MPa and 70 °C, and c) residue after Soxhlet extraction.

4.3.4. Epoxidation and characterization of reaction products

The SC-CO_2 extracted lipids from ground spent hen were epoxidized using Amberlite IR-120 as ion exchange resin (Aguilera et al., 2018; Fernandes et al., 2017) and the proposed reaction scheme is shown in Figure 4.4. The reactions using Amberlite-120 resin is a rapid and green method because there is no use of metals, ligands, and basic conditions, and also the Amberlite is recyclable by simple filtration and could be reused at least four times without any significant change in its activity (Mulakayala et al., 2012).

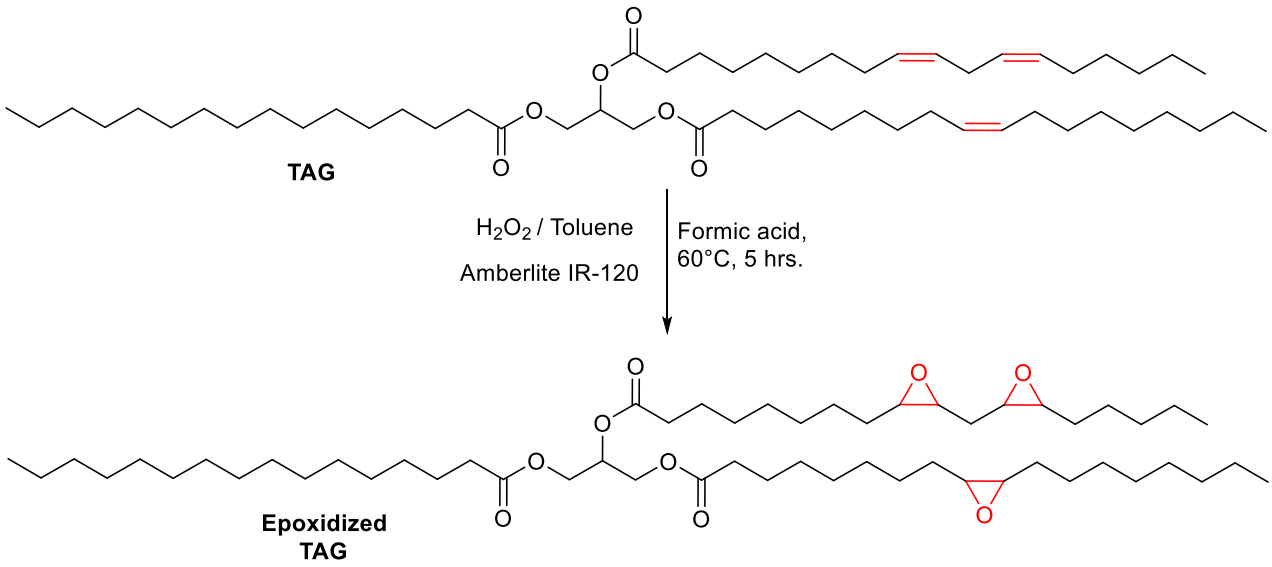

Figure 4.4: Schematic representation of the epoxidation reaction for spent hen lipids.

4.3.5. Epoxidation without solvent use

The epoxidation of spent hen lipids under solvent-free conditions was monitored by ATR-FTIR spectroscopy to assess the presence of double bonds and their transformation to epoxides (Figure 4.5). As the reaction proceeded with time, the band intensity of double bonds decreased and that of epoxide ring increased. The band at 827 cm^{-1} is the most important band on the ATR-

FTIR spectra, which is associated to epoxide group, while the band present at 3007 cm^{-1} is related to the unsaturated oils (Mashhadi et al., 2018) as shown in Figure 4.5.

Table 4.2: Fatty acid composition of lipid extracts (GC peak area %)

Pressure (MPa)	Temperature (°C)	C14:0	C16:0	C16:1	C18:0	C18:1	C18:2
30	40	1.12	23.66	4.49	6.79	58.24	5.68
40	40	1.23	24.82	5.39	5.71	56.51	6.31
50	40	1.11	24.58	4.86	6.77	59.96	2.71
30	55	1.03	20.95	4.61	5.09	53.68	14.63
40	55	1.47	23.30	5.99	4.86	53.91	10.45
50	55	0.90	20.73	4.70	5.18	53.62	14.86
30	70	1.04	21.12	4.99	4.69	52.18	15.97
40	70	0.97	19.50	4.53	4.94	52.19	12.91
50	70	0.78	21.03	4.13	6.29	55.85	11.92
1[a]		1.45	17.59	5.74	5.41	50.07	19.73
2[b]		1.23	26.63	4.98	6.97	56.10	4.04

[a] Extraction of lipids by Soxhlet method

[b] Extraction of lipids on a ten-fold scale up process using SC-CO_2 at 50 MPa and 70 °C.

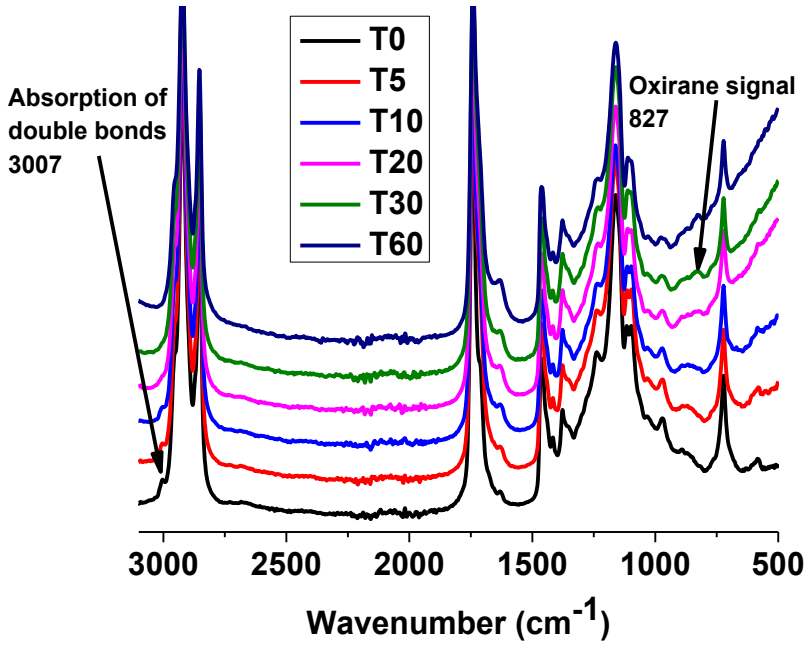

Figure 4.5: Epoxidation ATR-FTIR spectra at different time intervals i.e., T_0- T_{60} under solvent free conditions.

The peak present at wave number 3007 cm^{-1} was prominent at the start of experiment, i.e., 0 min while there was no peak at 827 cm^{-1} at the start of reaction. Band frequency of the characteristic peaks was almost the same after 5 min of reaction time. However, the intensity of double bond peak started decreasing at 3007 cm^{-1} while the peak of epoxide was found at 827 cm^{-1} after 10 min of reaction time. After 20 min reaction time, the double bond peak almost disappeared, and a prominent peak of epoxide was found at 827 cm^{-1}. These results indicated that the reaction was completed in 20 min with conversion of all unsaturated molecules present in the sample into corresponding epoxides.

The monitoring and confirmation of the epoxidation of spent hen lipids under solvent-free conditions was also elucidated by ^{1}H NMR spectroscopy (Figure 4.6). During the first 10 min, the two distinct peaks resonating at 5.35 and 2.02 ppm associated to double bond and -CH_2- adjacent

to double bond started disappearing and new peaks were observed at 2.94 and 1.50 ppm, which were characteristic of oxirane and -CH_2- neighboring oxirane ring (Fernandes et al., 2017; Xia et al., 2016) as shown in Figure 4.6. As the reaction proceeded, the peaks associated to unsaturation completely vanished and the epoxidized ring peaks were found after 20 min. The epoxidation reaction was continued up to 60 min to make sure that all the double bonds were converted into epoxides. By examining the ^{1}H NMR spectra of spent hen lipid epoxides at different time intervals, epoxidation conversion rates were calculated using glycerol protons as internal standard as their peak integration were the same before and after the epoxidation (Xia et al., 2016). The conversion rates were found to be 59.8, 84.2 and 100% at 5, 10, and 20 min, respectively. It was concluded that all the double bonds were consumed, and the epoxidation was completed in 20 min of reaction time.

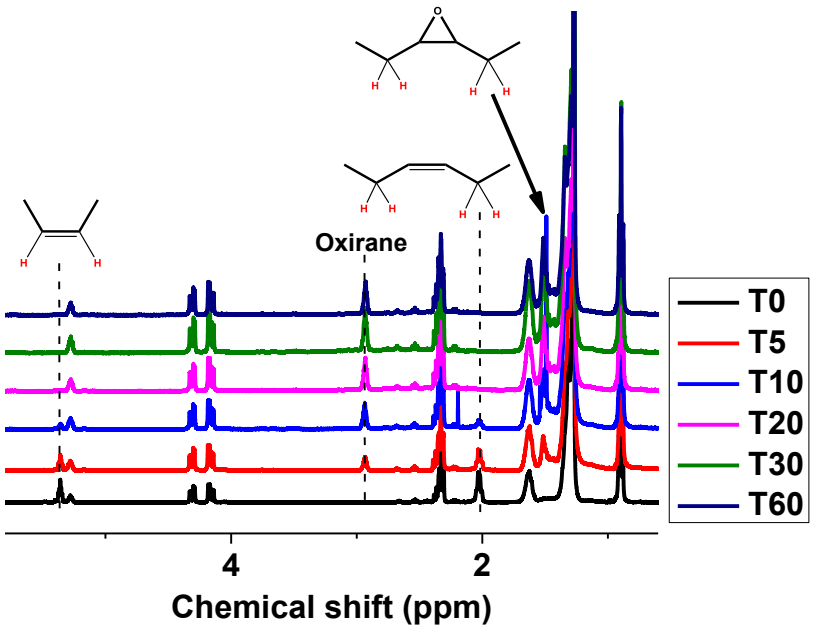

Figure 4.6: Epoxidation ^{1}H NMR spectra at different time intervals i.e., T_0- T_{60} under solvent free conditions.

4.3.6. Epoxidation with solvent use

The ATR-FTIR analysis of spent hen epoxidized lipid samples obtained at different time intervals using toluene as the solvent was performed to evaluate the presence of double bonds and their subsequent transformation to epoxide. An olefinic signal was observed at 3005 cm^{-1} but there was no oxirane peak in the range of 824-840 cm^{-1} (Mashhadi et al., 2018) at 0 min reaction time as presented in Figure 4.7.

A similar pattern of deflection was observed at both wavelengths at 15 min. As the reaction time proceeded, unsaturated bonds started transforming into epoxide groups. At 30 min, the absorptions associated to double bonds disappeared and a signal of epoxy ring was observed at 837 cm^{-1}, which indicated the formation of epoxides. The reaction was further continued until 360 min but no further change in the ATR-FTIR spectra was observed after 30 min. These results showed that initially, there were signals of double bonds while the epoxide group was absent in the sample; however, with reaction time, double bonds started converting into epoxide groups. Transition from double bond to epoxide group is expressed in the spectra. All unsaturated molecules present in the sample were converted into corresponding epoxides.

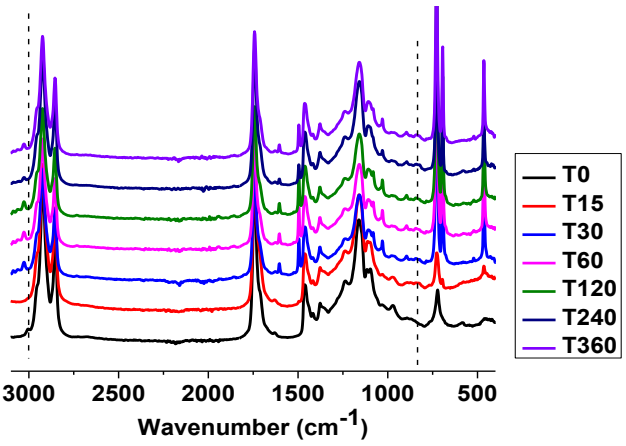

Figure 4.7: ATR-FTIR spectra of epoxidation reaction samples obtained at different time intervals i.e., T_0- T_{360} in the presence of toluene.

4.4. Conclusions

The spent hen is an unexplored sustainable source of lipids for the production of lipid-based materials. An environmentally friendly method of lipid extraction, the SC-CO_2 method was used to extract the lipids. A range of pressures and temperatures were investigated for the maximum extraction of lipids from spent hen. Over 92% of lipids were recovered at 50 MPa and 70 °C. Furthermore, the extracted lipids were epoxidized. The epoxidation of lipids was completed in less than 20 min under solvent-free conditions and epoxidation conversion rates were calculated, which indicated the conversion rates of 59.8, 84.2 and 100% at 5, 10, and 20 min, respectively. The environmentally friendly extraction of lipids and their subsequent conversion into epoxides under solvent-free conditions provide a promising green approach for the production of lipid-derived bio-epoxy materials from an unutilized sustainable resource.

4.5. References

Aerts, H.A., Jacobs, P.A. 2004. Epoxide yield determination of oils and fatty acid methyl esters using 1H NMR. *Journal of the American Oil Chemists' Society*, **81**(9), 841-846.

Aguilera, A.F., Tolvanen, P., Heredia, S., Muñoz, M.G.l., Samson, T., Oger, A., Verove, A., Eränen, K., Leveneur, S., Mikkola, J.-P. 2018. Epoxidation of fatty acids and vegetable oils assisted by microwaves catalyzed by a cation exchange resin. *Industrial & Engineering Chemistry Research*, **57**(11), 3876-3886.

Aris, A., Shojaei, A., Bagheri, R. 2015. Cure kinetics of nanodiamond-filled epoxy resin: influence of nanodiamond surface functionality. *Industrial & Engineering Chemistry Research*, **54**(36), 8954-8962.

Arrieta, M.P., Samper, M., Jiménez-López, M., Aldas, M., López, J. 2017. Combined effect of linseed oil and gum rosin as natural additives for PVC. *Industrial Crops and Products*, **99**, 196-204.

Arshad, M., Kaur, M., Ullah, A. 2016. Green biocomposites from nanoengineered hybrid natural fiber and biopolymer. *ACS Sustainable Chemistry & Engineering*, **4**(3), 1785-1793.

Arshad, M., Saied, S., Ullah, A. 2014. PEG-lipid telechelics incorporating fatty acids from canola oil: synthesis, characterization and solution self-assembly. *RSC Advances*, **4**(50), 26439-26446.

Auvergne, R., Caillol, S., David, G., Boutevin, B., Pascault, J.-P. 2013. Biobased thermosetting epoxy: present and future. *Chemical Reviews*, **114**(2), 1082-1115.

Bazou, D., Behan, G., Reid, C., Boland, J., Zhang, H. 2011. Imaging of human colon cancer cells using He-Ion scanning microscopy. *Journal of Microscopy*, **242**(3), 290-294.

Bernhart, M., Fasina, O.O. 2009. Moisture effect on the storage, handling and flow properties of poultry litter. *Waste Management*, **29**(4), 1392-1398.

Bozan, B., Temelli, F. 2002. Supercritical CO_2 extraction of flaxseed. *Journal of the American Oil Chemists' Society*, **79**(3), 231-235.

Brennecke, J.F. 1997. Molecular trees for green chemistry. *Nature*, **389**, 333.

Brunner, G. 2013. *Gas extraction: an introduction to fundamentals of supercritical fluids and the application to separation processes*. Springer Science & Business Media.

Burch, M.J., Ievlev, A.V., Mahady, K., Hysmith, H., Rack, P.D., Belianinov, A., Ovchinnikova, O.S. 2017. Helium ion microscopy for imaging and quantifying porosity at the nanoscale. *Analytical Chemistry*, **90**(2), 1370-1375.

Byrne, J.M., Schmidt, M., Gauger, T., Bryce, C., Kappler, A. 2018. Imaging organic–mneral aggregates formed by Fe (II)-oxidizing bacteria using helium ion microscopy. *Environmental Science & Technology Letters*, **5**(4), 209-213.

Devaraj, K., Aathika, S., Mani, Y., Thanarasu, A., Periyasamy, K., Periyaraman, P., Velayutham, K., Subramanian, S. 2018. Experimental investigation on cleaner process of enhanced fat-oil extraction from alkaline leather fleshing waste. *Journal of Cleaner Production*, **175**, 1-7.

Fernandes, F.C., Kirwan, K., Lehane, D., Coles, S.R. 2017. Epoxy resin blends and composites from waste vegetable oil. *European Polymer Journal*, **89**, 449-460.

Galià, M., de Espinosa, L.M., Ronda, J.C., Lligadas, G., Cádiz, V. 2010. Vegetable oil-based thermosetting polymers. *European Journal of Lipid Science and Technology*, **112**(1), 87-96.

García-Ayuso, L.E., Luque de Castro, M.D. 2001. Employing focused microwaves to counteract conventional Soxhlet extraction drawbacks. *TrAC Trends in Analytical Chemistry*, **20**(1), 28-34.

Goodman, S.H., Hanna, D. 2014. Handbook of thermoset plastics, Elsevier, San Diego, CA

, USA

Greco, A., Ferrari, F., Maffezzoli, A. 2016. Effect of the epoxidation yield of a cardanol derivative on the plasticization and durability of soft PVC. *Polymer Degradation and Stability*, **134**, 220-226.

Güçlü-Üstündağ, Ö., Temelli, F. 2006. Solubility behavior of ternary systems of lipids in supercritical carbon dioxide. *The Journal of Supercritical Fluids*, **38**(3), 275-288.

Joens, M.S., Huynh, C., Kasuboski, J.M., Ferranti, D., Sigal, Y.J., Zeitvogel, F., Obst, M., Burkhardt, C.J., Curran, K.P., Chalasani, S.H. 2013. Helium Ion Microscopy (HIM) for the imaging of biological samples at sub-nanometer resolution. *Scientific reports*, **3**, 3514.

Kamarudin, S.H., Abdullah, L.C., Aung, M.M., Ratnam, C.T., Jusoh, E.R. 2018. A study of mechanical and morphological properties of PLA based biocomposites prepared with EJO vegetable oil based plasticiser and kenaf fibres. *Materials Research Express*, **368**, 12011.

Kaur, M., Arshad, M., Ullah, A. 2018. In-situ Nanoreinforced green bionanomaterials from natural keratin and montmorillonite (MMT)/cellulose nanocrystals (CNC). *ACS Sustainable Chemistry & Engineering*, **6**(2), 1977-1987.

Kersey, J.H., Waldroup, P.W. 1998. Utilization of spent hen meal in diets for broiler chickens. *Poultry Science*, **77**(9), 1377-1387.

King, J.W., Johnson, J.H., Friedrich, J.P. 1989. Extraction of fat tissue from meat products with supercritical carbon dioxide. *Journal of Agricultural and Food Chemistry*, **37**(4), 951-954.

Kondaiah, N., Panda, B. 2007. Processing and utilization of spent hens. *World's Poultry Science Journal*, **48**(3), 255-268.

Leitner, W. 2000. Designed to dissolve. *Nature*, **405**, 129.

Li, H., Pordesimo, L., Weiss, J. 2004. High intensity ultrasound-assisted extraction of oil from soybeans. *Food Research International*, **37**(7), 731-738.

Loh, S.K. 2017. The potential of the Malaysian oil palm biomass as a renewable energy source. *Energy Conversion and Management*, **141**, 285-298.

Mashhadi, F., Habibi, A., Varmira, K. 2018. Enzymatic production of green epoxides from fatty acids present in soapstock in a microchannel bioreactor. *Industrial Crops and Products*, **113**, 324-334.

Mello, J.L.M., Souza, R.A., Paschoalin, G.C., Ferrari, F.B., Berton, M.P., Giampietro-Ganeco, A., Souza, P.A., Borba, H. 2017. Physical and chemical characteristics of spent hen breast meat aged for 7 days. *Animal Production Science*, **57**(10), 2133-2140.

Mulakayala, N., Kumar, K.M., Rapolu, R.K., Kandagatla, B., Rao, P., Oruganti, S., Pal, M. 2012. Catalysis by Amberlite IR-120 resin: a rapid and green method for the synthesis of phenols from arylboronic acids under metal, ligand, and base-free conditions. *Tetrahedron Letters*, **53**(45), 6004-6007.

Mungroo, R., Pradhan, N.C., Goud, V.V., Dalai, A.K. 2008. Epoxidation of canola oil with hydrogen peroxide catalyzed by acidic ion exchange resin. *Journal of the American Oil Chemists' Society*, **85**(9), 887-896.

Nisha, A., Sankar, K.U., Venkateswaran, G. 2012. Supercritical CO_2 extraction of Mortierella alpina single cell oil: Comparison with organic solvent extraction. *Food Chemistry*, **133**(1), 220-226.

Orellana, J.L., Smith, T.D., Kitchens, C.L. 2013. Liquid and supercritical CO_2 extraction of fat from rendered materials. *The Journal of Supercritical Fluids*, **79**, 55-61.

Parameswaranpillai, J., Sidhardhan, S.K., Jose, S., Hameed, N., Salim, N.V., Siengchin, S., Pionteck, J.r., Magueresse, A., Grohens, Y. 2016. Miscibility, phase morphology, thermomechanical, viscoelastic and surface properties of poly (ε-caprolactone) modified epoxy systems: effect of curing agents. *Industrial & Engineering Chemistry Research*, **55**(38), 10055-10064.

Rocha Garcia, C., Youssef, E., Souza, N., Matsushita, M., Figueiredo, E., Shimokomaki, M. 2003. Preservation of spent leghorn hen meat by a drying and salting process. *Journal of Applied Poultry Research*, **12**(3), 335-340.

Sánchez-Camargo, A.P., Martinez-Correa, H.A., Paviani, L.C., Cabral, F.A. 2011. Supercritical CO_2 extraction of lipids and astaxanthin from Brazilian redspotted shrimp waste (*Farfantepenaeus paulensis*). *The Journal of Supercritical Fluids*, **56**(2), 164-173.

Sharma, B.K., Adhvaryu, A., Liu, Z., Erhan, S.Z. 2006. Chemical modification of vegetable oils for lubricant applications. *Journal of the American Oil Chemists' Society*, **83**(2), 129-136.

Soh, L., Zimmerman, J. 2011. Biodiesel production: the potential of algal lipids extracted with supercritical carbon dioxide. *Green Chemistry*, **13**(6), 1422-1429.

Stephen, J.L., Periyasamy, B. 2018. Innovative developments in biofuels production from organic waste materials: A review. *Fuel*, **214**, 623-633.

Sun, M., Temelli, F. 2006. Supercritical carbon dioxide extraction of carotenoids from carrot using canola oil as a continuous co-solvent. *The Journal of Supercritical Fluids*, **37**(3), 397-408.

Suzuki, A.H., Botelho, B.G., Oliveira, L.S., Franca, A.S. 2018. Sustainable synthesis of epoxidized waste cooking oil and its application as a plasticizer for polyvinyl chloride films. *European Polymer Journal*, **99**, 142-149.

Tactacan, G.B., Guenter, W., Lewis, N.J., Rodriguez-Lecompte, J.C., House, J.D. 2009. Performance and welfare of laying hens in conventional and enriched cages. *Poultry Science*, **88**(4), 698-707.

Temelli, F. 2009. Perspectives on supercritical fluid processing of fats and oils. *The Journal of Supercritical Fluids*, **47**(3), 583-590.

Viner, K., Champagne, P., Jessop, P.G. 2018. Comparison of cell disruption techniques prior to lipid extraction from Scenedesmus sp. slurries for biodiesel production using liquid CO_2. *Green Chemistry*, **20**(18), 4330-4338.

Wang, H., Wu, J., Betti, M. 2013. Chemical, rheological and surface morphologic characterisation of spent hen proteins extracted by pH-shift processing with or without the presence of cryoprotectants. *Food Chemistry*, **139**(1), 710-719.

Wu, T., Xue, Q., Li, X., Tao, Y., Jin, Y., Ling, C., Lu, S. 2016. Extraction of kerogen from oil shale with supercritical carbon dioxide: Molecular dynamics simulations. *The Journal of Supercritical Fluids*, **107**, 499-506.

Xia, W., Budge, S.M., Lumsden, M.D. 2016. ^{1}H-NMR Characterization of epoxides derived from polyunsaturated fatty acids. *Journal of the American Oil Chemists' Society*, **93**(4), 467-478.

Xia, Y., Larock, R.C. 2010. Vegetable oil-based polymeric materials: synthesis, properties, and applications. *Green Chemistry*, **12**(11), 1893-1909.

Xu, X., Sun, L., Dong, J., Zhang, H. 2009. Breaking the cells of rape bee pollen and consecutive extraction of functional oil with supercritical carbon dioxide. *Innovative Food Science & Emerging Technologies*, **10**(1), 42-46.

Yan, M., Huang, Y., Lu, M., Lin, F.-Y., Hernández, N.B., Cochran, E.W. 2016. Gel point suppression in RAFT polymerization of pure acrylic cross-linker derived from soybean oil. *Biomacromolecules*, **17**(8), 2701-2709.

Zubair, M., Ullah, A. 2019. Recent advances in protein derived bionanocomposites for food packaging applications. *Critical Reviews in Food Science and Nutrition*, 1-29.

CHAPTER 5 - LIPID-DERIVED HYBRID BIONANOCOMPOSITES FROM SPENT HENS[3]

5.1. Introduction

In the last few decades, the use of fossil fuel-derived chemicals and polymers has tremendously increased in various applications, including packaging, automotive, aerospace, construction, adhesives, cosmetics, medical, and other industrial fields. In fact, the largest application for plastics today is packaging, and food packaging is the largest sector within the packaging market (Fauziah et al., 2015; Passos and Ribeiro, 2016). Packaging, on the one hand, is needed as it helps to preserve food and hence reduces organic waste but the use of plastics in huge amounts for this purpose is directly linked with alarming environmental issues. Plastics as a threat to environment arose mainly out of their use as packaging materials. The majority of petroleum-derived plastic packaging items can last for several hundred years in the landfills and do not degrade (Philp et al., 2013). As a result, there has been a strong research interest both in academia and industry on the development and use of biodegradable and/or biobased materials. "Biobased" sustainable materials, the so-called bioplastics, are currently considered as the way to go and may be the only alternative in the future as fossil fuel resources become exhausted (Ullah et al., 2011; Zhang and Wang, 2012).

The biobased polymers may be classified into three main categories: (1) biopolymers directly extracted from biomass such as cellulose, starch and protein etc. (2) biopolymers produced by microorganisms or genetically modified bacteria such as poly (hydroxy alkanoates) (PHAs); and (3) biopolymers synthesized using biobased monomers such as polylactide (PLA) etc (Andreeßen and Steinbüchel, 2019). The control of the structure and improvement in some

[3] A version of this chapter has been submitted for consideration for publication: Safder, M., Temelli, F., Ullah, A. 2019. Lipid-derived hybrid bionanocomposites from spent hens.

properties can be achieved by using biopolymers synthesized from biobased monomers. However, compared to proteins and carbohydrates, lipid-derived monomers and biopolymers, being hydrophobic in nature, have the potential to provide renewable alternatives to petroleum-based raw materials and can be produced in large scale to meet the current and growing industrial demand (Arshad et al., 2016a; Cohen-Karni et al., 2017; Jiang et al., 2018).

Although the development and applications of biopolymers can overcome some of the environmental challenges, it is highly desirable for them to be cost competitive and have material properties comparable to existing fossil-based materials, including thermal stability, mechanical strength, flame retardancy, and processability to increase their utilization in many applications (Khanra et al., 2018). An emerging approach, to improve such properties, is the incorporation of nanostructures. A complete transformation of the material properties can be achieved by the proper addition of nanoparticles. As the size is reduced to the nanoscale, the properties differ remarkably from their bulk counterparts, owing to increased surface area and nano effects (Paul and Robeson, 2008). Therefore, reinforcement of bio-polymer matrices with organic or inorganic fillers (e.g., particles and fibers) from either synthetic or natural sources can lead to high-performance composite materials (Bertolino et al., 2016; Souza and Fernando, 2016). These composites can be designed with multifunctional properties, such as dielectric properties or antibacterial properties, making them suitable materials for a variety of applications (Makaremi et al., 2017; Mousa et al., 2016).

In the recent years, extensive amount of work is being done on the use of triglycerides for monomer and subsequent polymer production to achieve materials with improved mechanical and thermal properties comparable to their plastic competitor (Garrison et al., 2016; Mauck et al., 2016). The use of oils from industrial wastes and by-products is necessary because it will not only

provide a sustainable solution to produce materials but also address the waste management problem. Large amounts of non-edible lipids are wasted on a daily basis such as restaurant waste, which contains up to 30% lipids and can be used as lipid feedstock (Olkiewicz et al., 2014; Papanikolaou et al., 2011). This study targeted to harvest lipids from spent hens, which is a huge bioresource, as discussed in more detail in Chapter 2 (Section 2.1) with an ultimate goal of developing nanocomposites for different potential applications.

Recently, some work has been done to extract and use proteins for the preparation of hybrid bionanocomposite films to be used in the packaging industry and other applications from spent hens (Hong et al., 2018; Wang et al., 2013; Yu et al., 2018; Zubair et al., 2019), but to the best of my knowledge no work has been reported on the lipid-derived nano-reinforced biocomposites from spent hens. Therefore, the objectives of the present study were to investigate the use of spent hen lipids for monomer preparation and subsequent polymerization to evaluate the effect of time and temperature on the molecular weight of the polymer obtained, and to investigate the effect of different proportions of nanoclay addition during polymerization on the properties of the nanocomposites obtained.

5.2. Materials and Methods

5.2.1 Materials

Thin layer chromatography (TLC, Merck, Darmstadt, Germany) was performed on silica gel 60 F254 Aluminum plates. 4-(Dimethylamino) pyridine (DMAP≥99%), dicyclohexylcarbodiimide (DCC, 99%), 2-hydroxyethyl acrylate (96%), sodium chloride (99.9%), anhydrous sodium sulfate (≥99%), dichloromethane (DCM, 99.9%), Montmorillonite nanoclay modified with 35-45 wt% dimethyl dialkyl (-C14 and -C18) amine, azobisisobutyronitrile (AIBN,

98%, recrystallized in methanol), tetrahydrofuran (THF, ≥99%) were purchased from Sigma-Aldrich (St. Louis, MO, USA) and used as received.

5.2.2. Microwave-assisted lipid extraction

Lipids were extracted from whole ground spent hens using microwave-assisted extraction as described previously in Chapter 3 (Section 3.2.3) at 80 ºC for 10 min using a CEM-Discover unit (120 V, CEM Corporation, Matthews, NC, USA).

5.2.3. Monomer and polymer synthesis

Hydrolysis of triacylglycerols (TAGs) was performed using a standard procedure with slight modifications (Salimon et al., 2011). To the oil (24.7 g) dissolved in a mixture of 230 mL DCM and 23 mL methanol was added 112 mL of 2N KOH solution in MeOH in a 500 mL flask and stirred for 2 h at 35 ºC. The completion of the reaction was monitored by TLC and ^{1}H NMR spectroscopy. After that, the organic layer was separated using a separatory funnel, and another 200 mL of DCM was added into the mixture to make sure that all of the nonpolar compounds were removed. The aqueous layer was acidified to pH 1-2 using concentrated HCl, the pH was estimated by Litmus paper and the free fatty acids were extracted with DCM. The extraction was repeated three times using the same amount 200 mL of DCM every time and the DCM was removed by rotary evaporator. All the experiments were performed in duplicates.

Figure 5.1 shows the synthesis of spent hen derived fatty acid monomer (SFAM) and the subsequent nanocomposites. The monomer was prepared using the previously reported method (Arshad et al., 2016a) with some minor changes. Briefly, hydrolyzed free fatty acids (8 g) and DMAP (0.353 g) were dissolved in DCM (30 mL) in a 250 mL flask. The reaction mixture was stirred followed by purging with nitrogen gas for 10 min in an ice bath. In a separate beaker, DCC (6.43 g) was dissolved in a minimum amount (~10 mL) of DCM and added into the reaction

mixture dropwise. Then, 2-hydroxyethyl acrylate (3.13 mL) was added dropwise over 30 min. The ice bath was removed after 20 min and the resulting mixture was stirred overnight at room temperature (25 ˚C). The reaction was monitored by TLC until the complete utilization of starting material. The reaction mixture was filtered to remove the white precipitate followed by 60 mL distilled water addition to the filtrate. Then, the organic phase was washed with a saturated solution of $NaHCO_3$ (4 x 80 mL) and brine solution (2 x 80 mL) and dried using anhydrous Na_2SO_4 for 18 h. The organic solvent was removed by rotary evaporator and the extracted monomer was purified by column chromatography using silica gel and hexane/ethyl acetate (95:5 v/v) as the mobile phase. The lipid hydrolysis yield and the monomer yield were calculated using the Eqs. (5.1) and (5.2), respectively.

$$Lipid\ hydrolysis\ yield\ (\%) = \frac{Amount\ of\ hydrolysed\ lipid}{Amount\ of\ lipid}\ X100 \quad (5.1)$$

$$Monomer\ yield\ (\%) = \frac{Amount\ of\ monomer}{Amount\ of\ hydrolysed\ lipid}\ X100 \quad (5.2)$$

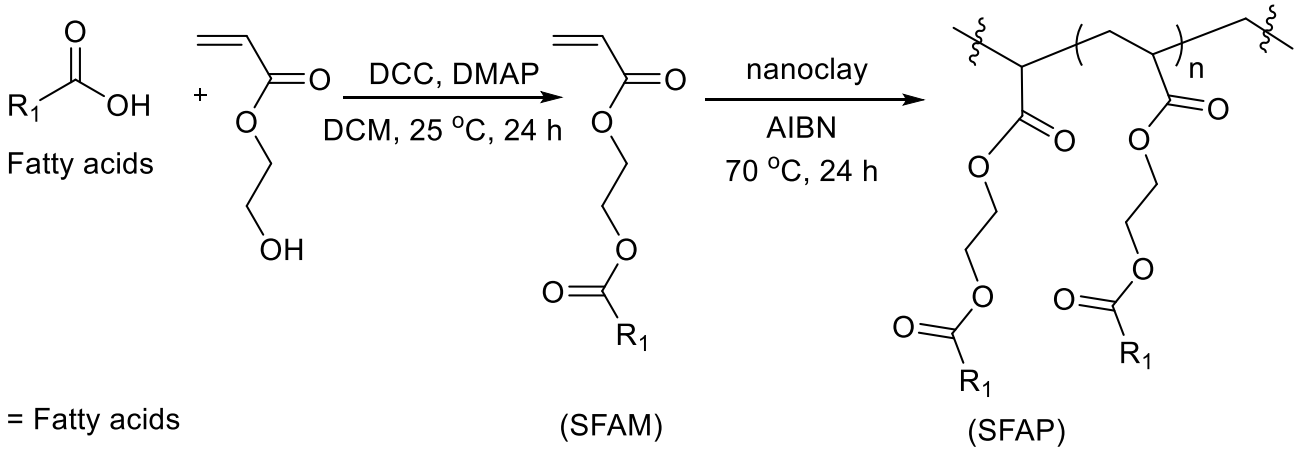

Figure 5.1: Schematic representation of SFAM and SFAP synthesis from spent hen derived fatty acids.

To synthesize the polymer, the SFAM monomer (1.5 g) was placed in a 25 mL flask, together with a stirrer. The septum was used to seal the top with parafilm. The reaction mixture was purged with nitrogen for 15 min. Then, 20 mg of initiator AIBN was added when the temperature reached 70 ˚C and the reaction was allowed to proceed for 24 h. To optimize the reaction conditions to get a high molecular weight polymer, temperatures of 70, 90 and 110 ºC and reaction times of 2, 4, 8, 12, 15 and 24 h were tested.

5.2.4. *In situ* nanoclay dispersion and synthesis of nanocomposites

SFAM monomer (1.5 g) and nanoclay modified (3, 5 and 10% by weight) were placed in a flask separately and the temperature was raised to 50 ºC to liquefy the reaction mixture components. Then, the mixture was stirred mechanically for 10 min followed by sonication for 10 min for complete dispersion of nanoclay into the reaction mixture. The stirring and sonication steps of 10 min each were repeated three times for maximum dispersion of nanoclay. The reaction mixture was then purged with nitrogen gas to remove entrapped air before adding the initiator AIBN (20 mg) and raising the temperature up to 65 ºC to initiate the polymerization. After the completion of reaction, THF was used to remove any unreacted monomer.

5.2.5. Preparation of nanocomposite films

Films of nanocomposite materials for thermal and flammability testing were prepared by compression molding of the powder for 10 min at 150 ºC and 3.45 – 4.83 MPa pressure, using a Carver press (Carver Inc. hydraulic unit model no. 3912, Wabash, IN, USA). The films were then cut into a standard size (approximately 30 mm length, 10 mm width and 1 mm thickness) to be used for thermal and flammability tests.

5.2.6. Characterization tests

5.2.6.1. Attenuated total reflectance-Fourier transform infrared (ATR-FTIR) spectroscopy

ATR-FTIR spectra of reaction mixtures were recorded using a Bruker Optics (Esslingen, Germany) system equipped with a single bounce diamond ATR crystal. All samples were scanned in the wavelength range of 410-4000 cm^{-1}. In total, 16 scans at a resolution of 4 cm^{-1} were recorded. Spectra were obtained using OPUS software 6.5 version from Bruker.

5.2.6.2. Proton nuclear magnetic resonance spectroscopy (^{1}H NMR)

^{1}H NMR analyses of reaction components were performed using a Varian INOVA instrument (Palo Alto, CA, USA) at 400 MHz frequency at room temperature where deuterated chloroform ($CDCl_3$) and methanol (MeOD) were used as solvent. The extent of conversion of double bonds was determined by taking one of the internal peaks as a standard, which remained the same throughout the reaction. Specifically, the signal at 0.90 ppm (-CH_3, *t*) was used for this purpose because it remained unchanged throughout the reaction (Aerts and Jacobs, 2004).

5.2.6.3. Thermogravimetric analysis (TGA)

The thermal degradation behavior was investigated using thermal gravimetric analysis technique on Q50 TGA instrument (New Castle, DE, USA) in the presence of inert nitrogen gas. TGA measurements were conducted by heating the samples up to 600 °C with the ramp rate of 10 $^{\circ}$C/min.

5.2.6.4. Differential scanning calorimetry (DSC)

To investigate thermal transitions, DSC analyses were performed using a TA Instrument (2920 Modulated DSC, New Castle, DE, USA), where a purge of nitrogen gas was used. Samples with a quantity of 2.0–5.0 mg were weighed in a pan, which was sealed and placed into a DSC cell. The thermograms were recorded over the 25-250 °C temperature range, where the heating rate was set at 3 °C/min. DSC profiles of the 2nd heating cycle of samples were selected to eliminate material thermal history.

5.2.6.5. Gel permeation chromatography (GPC)

Gel permeation chromatography (GPC) was performed using an Agilent 1200 series system (LabX, Midland, ON, Canada) equipped with a Waters Styragel HR 4E THF 4.6 × 300 mm column. A series of polystyrene standards with peak molecular range of 770-113,300 g/mol was used for calibration of the instrument.

5.2.6.6. Dynamic mechanical analysis (DMA)

The viscoelastic properties of the films were measured using a TA Instrument (DMA Q800, New Castle, DE, USA) device at an oscillatory frequency of 1 Hz with applied deformation of 0.2% during heating. The measurement was carried out in a tensile mode where the temperature was programmed from −80 to 150 °C at a rate of 2 °C/min.

5.2.6.7. Transmission electron microscopy (TEM)

A standard method for the preparation of the sample for TEM analysis was followed with slight modification (Spurr, 1969; Wu, S. et al., 2012). Briefly, the composites were cut into small pieces (~1 mm^3) and rinsed twice with 100% ethanol for 1 h. Infiltration was done in Spur's resin at room temperature in four steps using 25, 50, 75 and 100% Spurr's resin (in 100% ethanol) for 24 h each, except the 100% resin was repeated twice first for 24 h and then for 5 h. The polymerization was performed at 75 ˚C in an oven for 16 h. The sectioning was completed from top to bottom in the range of 70-100 nm. The blocks were cut using a Leica EM UC6 ultramicrotome equipped with a diamond knife (Leica Microsystems Inc., Concord, ON, Canada). The TEM analysis of different nanoclay reinforced composites was conducted using a JEM-2100 Electron Microscope (JEOL Ltd., Akishima, Tokyo, Japan).

5.2.6.8. X-ray diffraction (XRD)

XRD analyses were performed using a Rigaku Ultima IV XRD unit with Co radiation operated at 38 kV and 38 mA. The samples were scanned from 5° to 80° (2θ) in a continuous scanning mode at a rate of 2°/min with a 0.02 step size.

5.2.6.9. Atomic force microscopy (AFM)

The nanoclay dispersion in the prepared bionanocomposites was studied using a atomic force microscope (Dimension Edge) (Bruker, Santa Barbara, CA, USA).

5.2.6.10. Film thickness

A digital caliper (Digi-Max Caliper, Sigma-Aldrich, Monticello, MN, USA) was used to measure the thickness and width of the films at three different places, and the values were averaged. The average film thickness was used for mechanical, flammability and DMA testing.

5.2.6.11. Flammability test

Flammability of the nanocomposite films was evaluated by a vertical hanging burning test using the ASTM based UL94V standard method with slight modifications (Paul, D. and Robeson, L.M., 2008). Rectangular films with dimensions of around 30 mm length, 10 mm width and 1 mm thickness were prepared. The films were clamped vertically in hanging position and a laboratory scale burner with a supply of methane gas (99.9%) was used with a flame height of 25 mm. The top 10 mm part of the flame was applied to the lower end of the films for 1 s and then the total time for the films to burn completely was recorded by a stopwatch.

5.3. Results and discussion

5.3.1. Monomer and polymer production from spent hen lipids

To synthesize the monomer from spent hen lipids, the extracted lipids were first hydrolyzed, and the amount of free fatty acids was reported as percentage yield (Eq. (5.1)), where 35.1±1% yield was obtained. Infrared spectroscopy is widely used for molecular structure analysis of biomolecules, including lipids where the mid-infrared region (4000–400 cm^{-1} wavenumbers) is used the most commonly. FTIR is mainly used for qualitative characterization of TAGs and free fatty acids by assigning the peak at 1744-1754 cm^{-1} to the carbonyl of TAG esters and the peak at 1700-1711 cm^{-1} to the carbonyl of free fatty acids (Forfang et al., 2017; Vlachos et al., 2006). As can be seen from Figure 5.2, the carbonyl band of spent hen lipids at 1744 cm^{-1} due to TAGs was clearly differentiated from the carbonyl band at 1707 cm^{-1} due to free fatty acids of hydrolyzed spent hen lipids.

The free fatty acids were converted to acrylate monomer by the reaction of free fatty acids with acryl alcohol in the presence of DCC and DMAP in DCM at room temperature for 24 h (Figure 5.3) and the monomer (SFAM) was obtained as a colorless liquid with a yield of 74±0.5% according to Eq. (5.2). The reaction products were characterized by ATR-FTIR and ^{1}H NMR spectroscopies. The reason for the introduction of the acryl group in the monomer was to introduce a terminal double bond, which would then be used for polymerization. In addition, this approach allowed the utilization of both saturated and unsaturated fatty acids from the spent hen lipids.

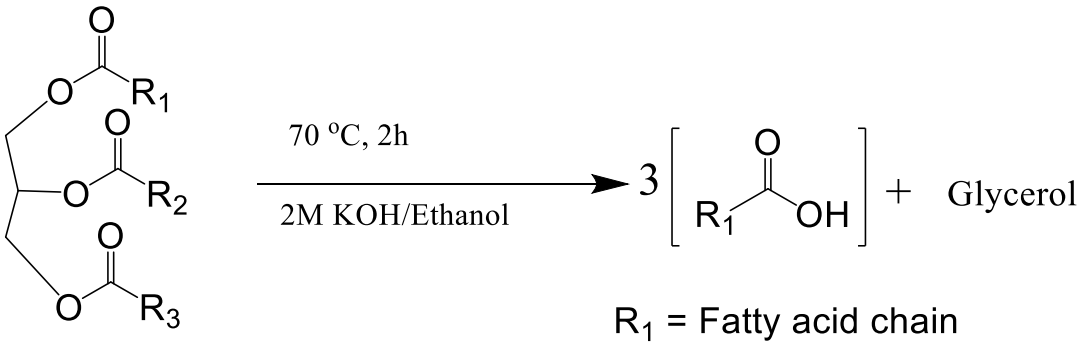

Hydrolysis of extracted lipids (TAGs)

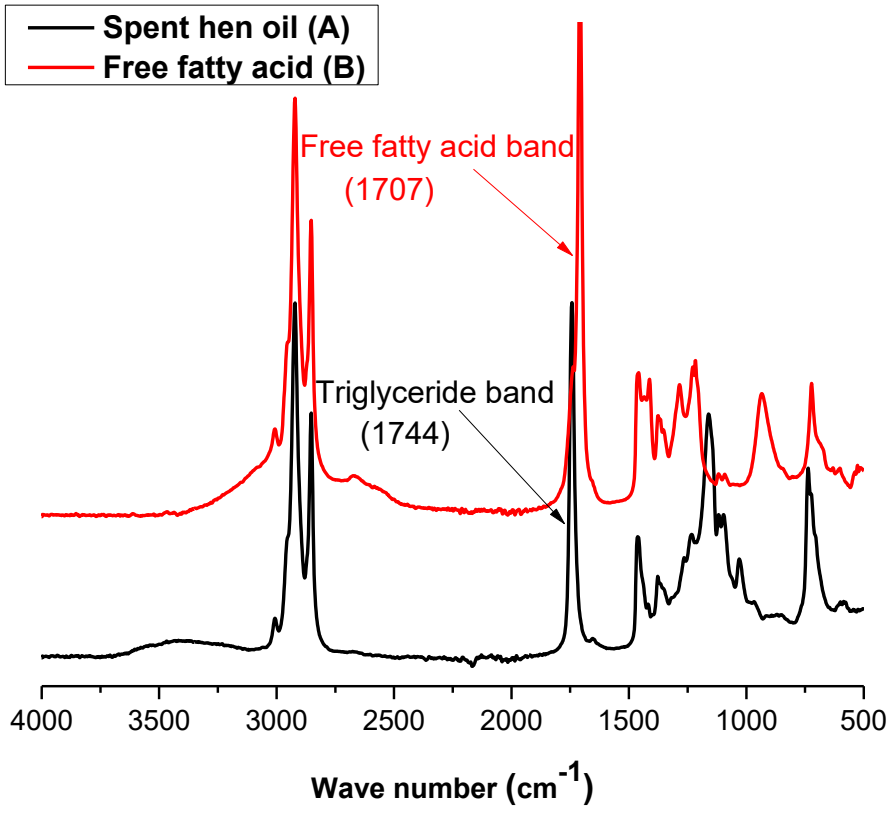

Figure 5.2: ATR-FTIR spectra of (A) spent hen oil, and (B) hydrolyzed spent hen oil.

To optimize the polymerization reaction conditions in order to get a higher molecular weight polymer, temperatures of 70, 90 and 110 ^{o}C and reaction times of 2, 4, 8, 12, 15 and 24 h were tested. ^{1}H NMR spectra of acrylated lipid monomer and polymers at these conditions are shown in Figure 5.3. The spectra clearly indicated the synthesis of polymer as the characteristic peaks associated with the double bond protons disappeared, i.e., a doublet of doublet at 6.43 ppm, 6.17 ppm and 5.89 ppm and a multiplet at 4.37 ppm.

Proton nuclear magnetic spectroscopy can also be used to measure the conversion of double bonds to polymers using a standard, i.e., 1,3,5-trioxane (Bharti and Roy, 2012). The percentage conversions were calculated by comparing the peak intensity of double bonds before and after the polymerization with respect to the peak intensity of standard using Eq. (5.3).

$$Conversion\ (\%) = \frac{Io-I}{Io} X100 \tag{5.3}$$

where 'Io' denotes peak area of double bonds before the polymerization and 'I' represents the peak area of double bonds after the polymerization. The calculated conversion percentages are shown in Table 5.1. For the optimization of maximum molecular mass homopolymer, different temperatures and times were used for homopolymer synthesis. Gel permeation chromatography (GPC) was used to determine the average molecular weights (Mn) of the homopolymers synthesized under different temperature and time periods. The molecular weights were determined by GPC as shown in Table 5.1. A temperature of 70 $^{\circ}$C and 24 h reaction time resulted in the highest molecular weight of biopolymer ($2.858x10^{5}$).

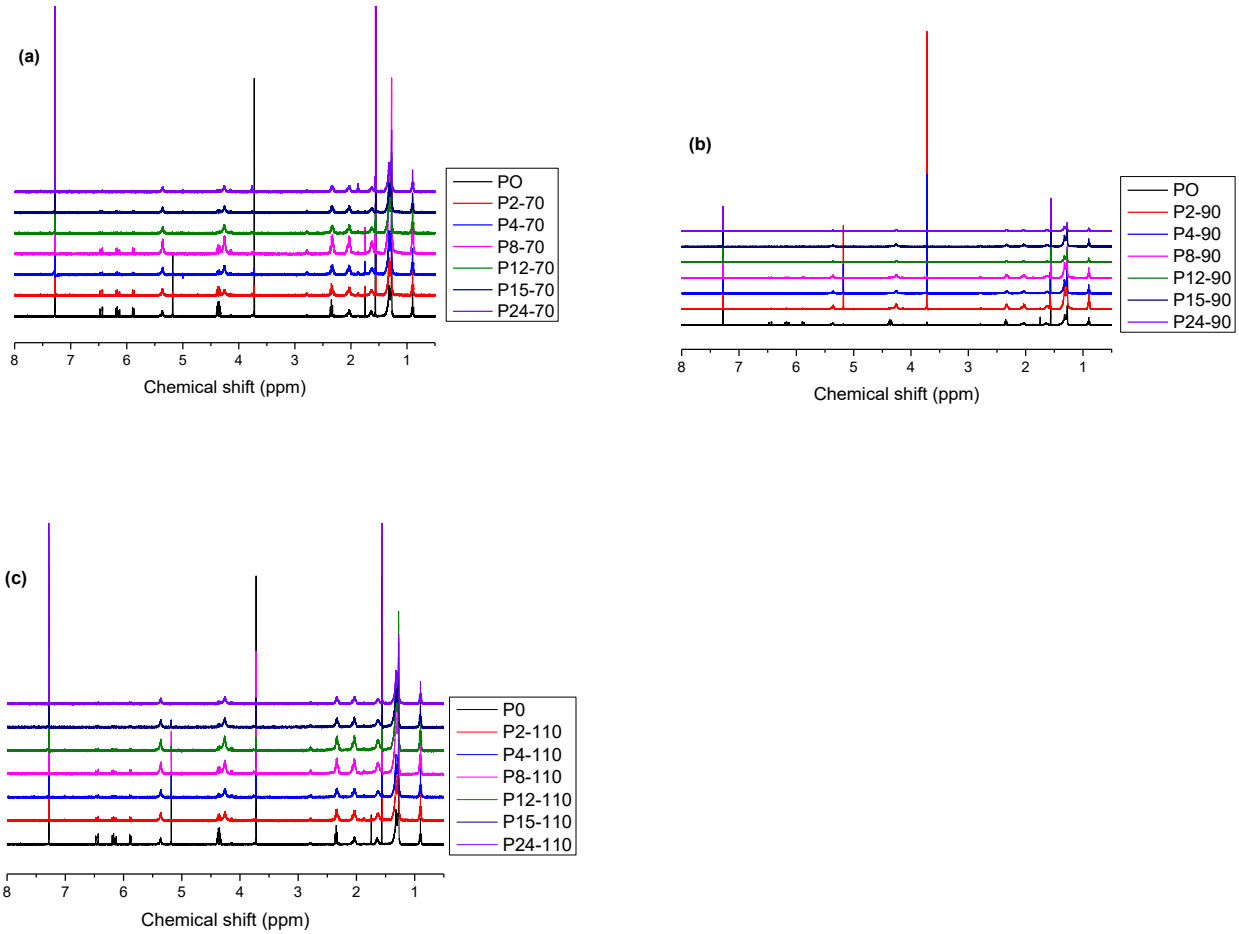

Figure 5.3: ^{1}H NMR spectra of polymerization at (a) 70 ˚C, (b) 90 ˚C and (c) 110 ˚C for 0, 2, 4, 8, 12, 15 and 24 h.

Monomer and subsequent polymer synthesis from spent hen lipids were confirmed by FTIR. A peak of a double bond at 3013 cm^{-1} was observed in the starting lipid as well as in the monomer, whereas the peak of double bond disappeared in the homopolymer, which showed the successful preparation of the polymer (Figure 5.4).

^{1}H NMR spectra of extracted lipids from spent hens, acrylated monomer and polymer are shown in Figure 5.5. The spectra clearly indicate the synthesis of monomer, as three new

characteristic peaks were observed as a doublet of doublet at 6.43 ppm, 6.17 ppm and 5.89 ppm, which were assigned to acrylic part and a multiplet at 4.37 ppm was associated to two methylene groups of conjugated alcohol. All those acrylic peaks disappeared in the spectrum of polymer (Figure 5.5), which indicated the successful synthesis of the polymer.

Table 5.1: Optimization of reaction conditions for polymerization of the monomer

Sr. No.	Temperature (°C)	Time (h)	Conversion (%) using ^{1}H NMR	Molecular weight (M_w) using GPC
$P_{2\text{-}70}$		2	75	$4.5276X10^4$
$P_{4\text{-}70}$		4	98	$2.1194\ X10^5$
$P_{8\text{-}70}$	70	8	99	$1.8781\ X10^5$
$P_{12\text{-}70}$		12	100	$1.4092\ X10^5$
$P_{15\text{-}70}$		15	100	$1.4231\ X10^5$
$P_{24\text{-}70}$		24	100	$2.8582\ X10^5$
$P_{2\text{-}90}$		2	85	$1.1655\ X10^5$
$P_{4\text{-}90}$		4	100	$9.5443\ X10^4$
$P_{8\text{-}90}$	90	8	100	$1.9722\ X10^5$
$P_{12\text{-}90}$		12	100	$7.7443\ X10^4$
$P_{15\text{-}90}$		15	100	$2.4407\ X10^5$
$P_{24\text{-}90}$		24	100	$1.0829\ X10^5$
$P_{2\text{-}110}$		2	92	$3.6004\ X10^4$
$P_{4\text{-}110}$		4	100	$4.8851\ X10^4$
$P_{8\text{-}110}$	110	8	100	$2.9859\ X10^4$
$P_{12\text{-}110}$		12	100	$2.3213\ X10^4$
$P_{15\text{-}110}$		15	100	$5.7803\ X10^4$
$P_{24\text{-}110}$		24	100	$4.2382\ X10^4$

5.3.2. Characterization of nanocomposites

The nanocomposites synthesized from monomer (SFAM) and modified with the addition of nanoclay at different levels (3, 5 and 10% by weight) were characterized with different techniques. Figure 5.6 shows the ATR-FTIR spectra of the nanoclay reinforced composites, where the characteristic peaks were observed at 1050, 1748 and 3647 assigned to (Si-O) silicate groups of nanoclay, the carbonyl group of the fatty ester and structural groups of nanoclay (Al-OH), respectively.

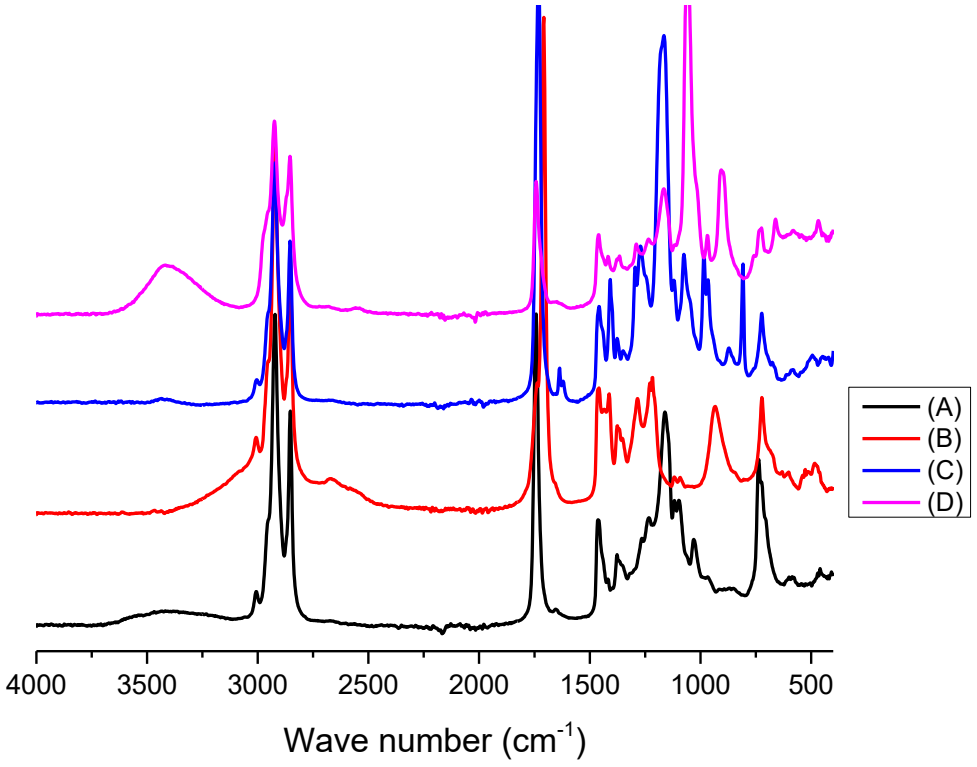

Figure 5.4: ATR-FTIR spectra of (A) spent hen oil, (B) hydrolyzed spent hen oil, (C) monomer, and (D) polymer.

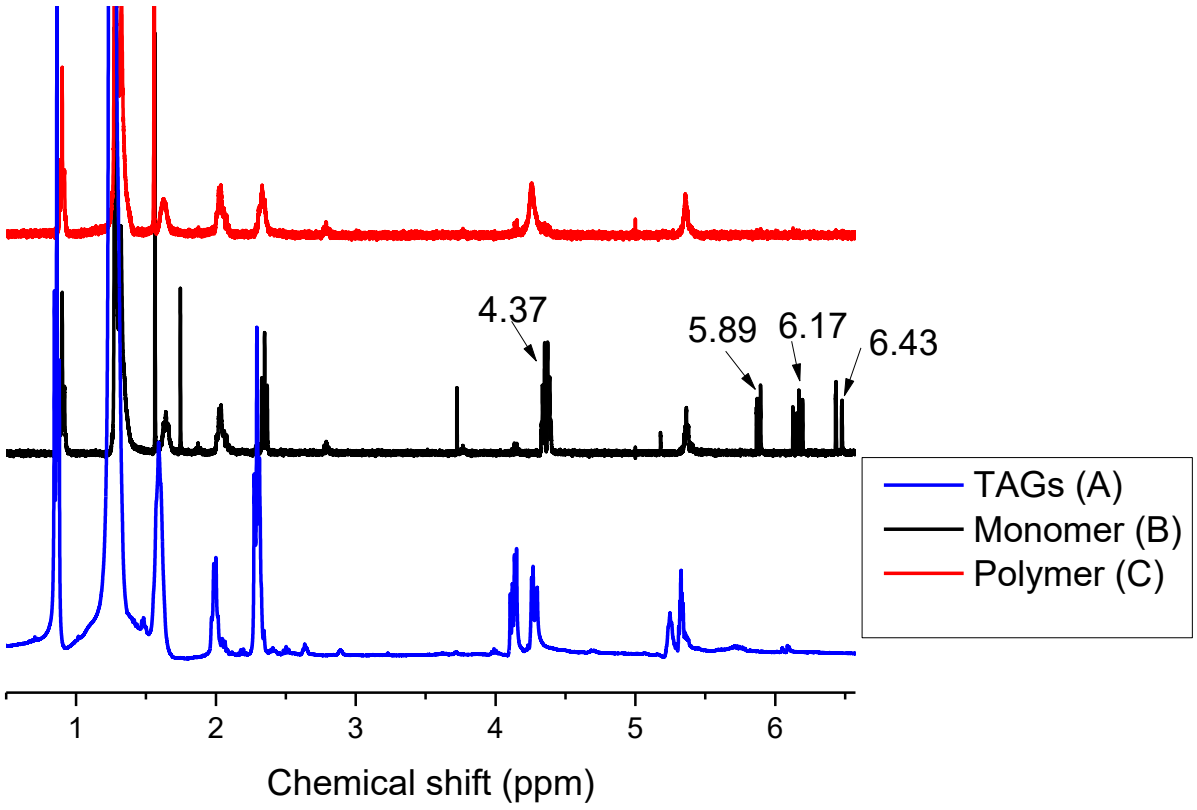

Figure 5.5: ^{1}H NMR spectra of (A) lipids extracted from the spent hen, (B) acrylated monomer, and (C) polymer.

The thermal stability and degradation behavior of nanoclay composites was studied by thermogravimetric analysis (TGA) and its derivative (DTG). Figure 5.7 shows the thermogravimetric analysis (Figure 5.7 (X)) and derivative thermogravimetric curves (Figure 5.7 (Y)) of the homopolymer and nanocomposites. As shown in Figures 5.7 (X) and (Y), the first stage of weight loss occurred from 130 °C to 220 °C, which could be due to the evaporation of some bound moisture from the homopolymer and nanocomposites. The second stage of major weight loss started at about 350 °C because of the thermal degradation of the homopolymer in nanocomposites. As can be seen from DTG curves, there are two weight loss zones in nanoclay reinforced biopolymers compared to a neat homopolymer, which could be due to the presence of

low molecular mass polymer chains. (Ray and Bousmina, 2005) previously reported that the incorporation of silicate layers increased the degradation onset temperature and also widened the degradation process. The added clay acts as a superior insulator and barrier to the volatile products generated during decomposition and therefore enhances the performance of the char formed (Qi et al., 2018). A prominent improvement in thermal stability was observed by the addition of nanoclay, and the char left as a residue after complete combustion up to 600 ˚C could be due to the presence of silica and alumina (Figure 5.7). Overall, the composites with 3, 5 and 10% nanoclay showed less weight loss compared to the neat homopolymer (Figure 5.7). The 50% weight loss was observed around 400 ºC for all the composites (Figure 5.7 B, C, and D). The homopolymer showed 100% weight loss at 600 ºC while the composites with 3, 5 and 10% nanoclay showed 92, 91 and 90% weight loss, respectively, as shown in Table 5.2.

The thermal transitions of the biopolymer and its nanocomposites were studied by DSC and are shown in Figure 5.8. The neat biopolymer exhibited a melting peak at around 160 °C and among the nanocomposites, the 5% clay containing bionanocomposite displayed a melting peak at around 180 °C and the nanocomposites containing 3 and 10% clay melted at lower temperatures. The nanocomposite with 10% nanoclay clearly displayed 2 melting peaks, one at lower temperature around 109 °C and a second peak at around 150 °C. This could be due to less homogeneous distribution of nanoclay, leading to a nanoclay-rich phase and partially intercalated regions with different crystallization behaviors. A sharp endothermic peak can clearly be seen for the 5% nanoclay reinforced biopolymer, which demonstrates improved dispersion and more exfoliation compared to the other nanocomposites.

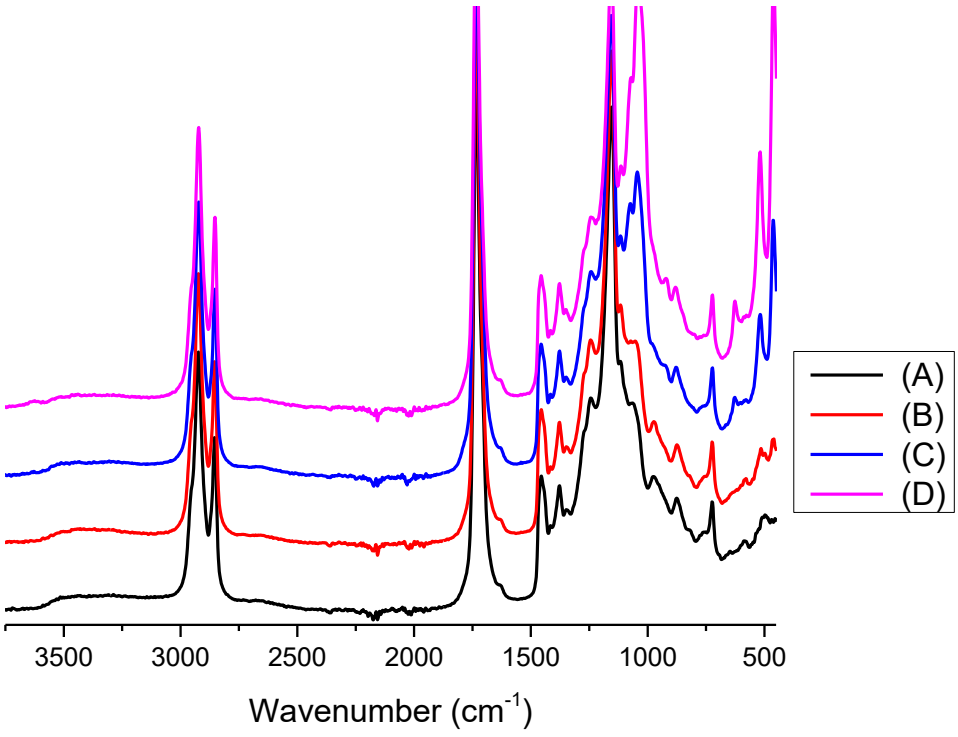

Figure 5.6: ATR-FTIR spectra of (A) homopolymer, (B) 3% nanoclay composite, (C) 5% nanoclay composite, and (D) 10% nanoclay composite.

Dynamic mechanical analysis (DMA) is used to measure the changes in the viscoelastic properties of the polymers with changing temperature. Thermal transitions are generally associated with chain mobility and the glass transition (T_g) is useful in determining the occurrence of molecular mobility transition. A typical DMA plot of storage modulus and tan δ (ratio of loss modulus/storage modulus) for bionanocomposites is presented in Figure 5.9 The neat biopolymer films were very soft and therefore DMA analysis could not be performed for the neat biopolymer. For bionanocomposites, the highest storage modulus below zero degrees was seen in the case of 5% nanoclay addition compared to biopolymers with 3 and 10 % nanoclay. This is due to the fact that 5% nanoclay based nanocomposites are more exfoliated and/or intercalated compared to 3 and

10% nanoclay as seen in TEM investigations. The T_g of 5% nanoclay was also slightly higher than that for the other two nanocomposites. At high temperatures, above T_g, the reinforcement effect weakens in all nanocomposites, indicating weakening of the thermal-mechanical stability of these materials at high temperature.

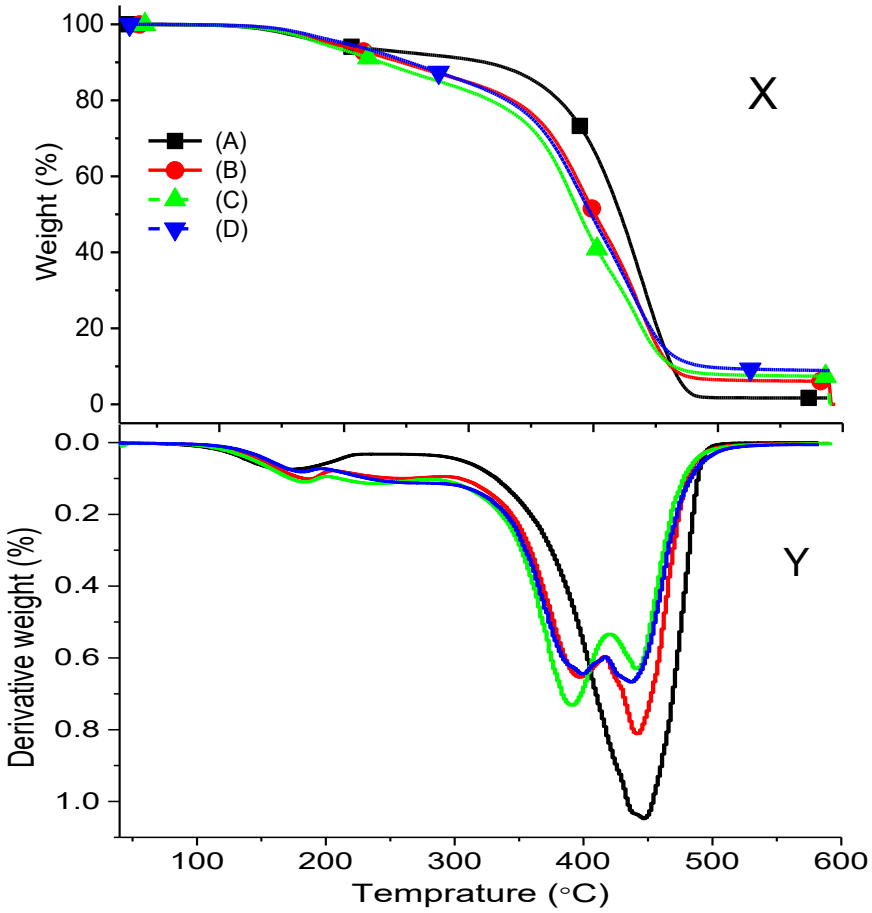

Figure 5.7: (X) TGA curves and (Y) DTG curves of (A) homopolymer, and (B) 3%, (C) 5%, and (D) 10% nanoclay composites.

Table 5.2: Thermal stability of nanoclay reinforced lipid-derived composites

Sample (% nanoclay)	Weight loss temperatures (˚C)				Char at 600 ˚C (%)
	5%	10%	50%	90%	
A (0%)	189.3	312.6	419.6	460.6	1.76
B (3%)	190.6	245.6	402.2	460.5	6.03
C (5%)	181.4	229.7	387.9	464.6	7.47
D (10%)	200.9	250.9	397.5	489.2	8.91

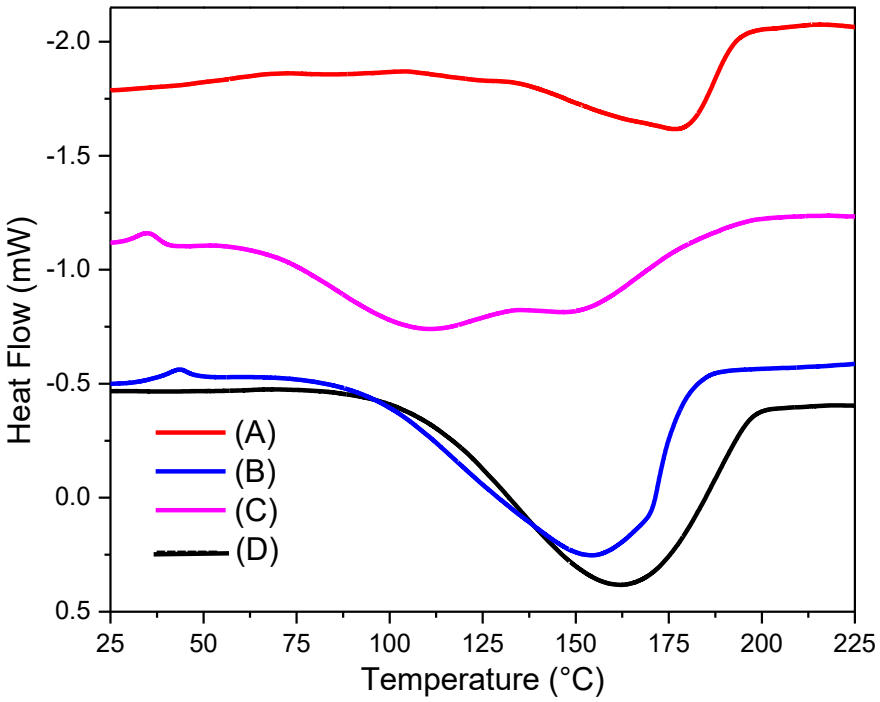

Figure 5.8: DSC curves of (A) 3%, (B) 5%, and (C) 10% of nanoclay composites and (D) homopolymer.

X-ray diffraction (XRD) pattern is a characteristic method to evaluate the crystal structure and to study the changes in the crystallinity patterns of nanoreinforced lipid-derived composites. Figure 5.10 shows the XRD patterns of the nanocomposites prepared with the addition of different

levels of nanoclay. The clay showed XRD peaks at a 2θ angle of 5.85°, 19.78°, 26.70°, 29.01°, 35.07°, 53.99°, 61.82°, and 73.09°, while the homopolymer showed a broad peak at 22.84°. All the characteristic peaks, assigned to modified nanoclay (Jose et al., 2014), completely disappeared in the nanocomposites, which showed that the homopolymer developed interactions with the clay particles, and as a result, clay crystallinity was disrupted. The differences in XRD patterns are prominent with the appearance of some small new distinct peaks in samples containing 5% (D) and 10% (E) nanoclay at 31.06°, 44.42°, and 51.92°, which may be attributed to a new crystalline region created during *in situ* polymerization (Sahmani et al., 2018). These new peaks could be related to the formation of a new crystal pattern, which may be created during the dispersion, indicating that the nanoclay sheets were intercalated or exfoliated into the polymers or complete nanoclay dispersion/exfoliation was achieved, leading to greater inter layer spacing, as further confirmed by TEM analysis.

TEM analysis was conducted to analyse and confirm the dispersion of clay in the composite matrix either by exfoliation or intercalation. Figure 5.11 showed TEM micrographs of composites containing 3, 5 and 10% of nanoclay and homopolymer The dark stripes in the micrographs showed the nanoclay sheets and the light color gap between the lines is the distance (*d*-spacing), which is formed due to polymer development in between the nanoclay layers. Figures 5.11 (A), (B) and (C) show clear exfoliation and intercalation of nanoclay sheets with greater values of *d*-spacing in between these sheets. In the intercalated region, the *d*-spacing was similar in Figures 5.11 (A) and (C) in the range of 2.14-16.57 nm and 2.12-15.05 nm, respectively, whereas in Figure 5.11 (B) it was 2.01-9.05 nm. In conclusion, the range of *d*-spacing in all the composites was between 2 – 16 nm, while in the exfoliated region as the layers have dispersed randomly the *d*-spacing was about 20 – 60 nm or more (Giannakas and Leontiou, 2018). In these nanocomposite

micrographs, intercalated assemblies were present with stacked sheets and some individual clay sheets were also found in Figures 5.11 (A), (B) and (C). The silicate layers were nearly homogeneously dispersed either intercalated or exfoliated in the composite matrices as was further confirmed by the XRD analysis (Figure 5.10) and AFM images (Figure 5.12).

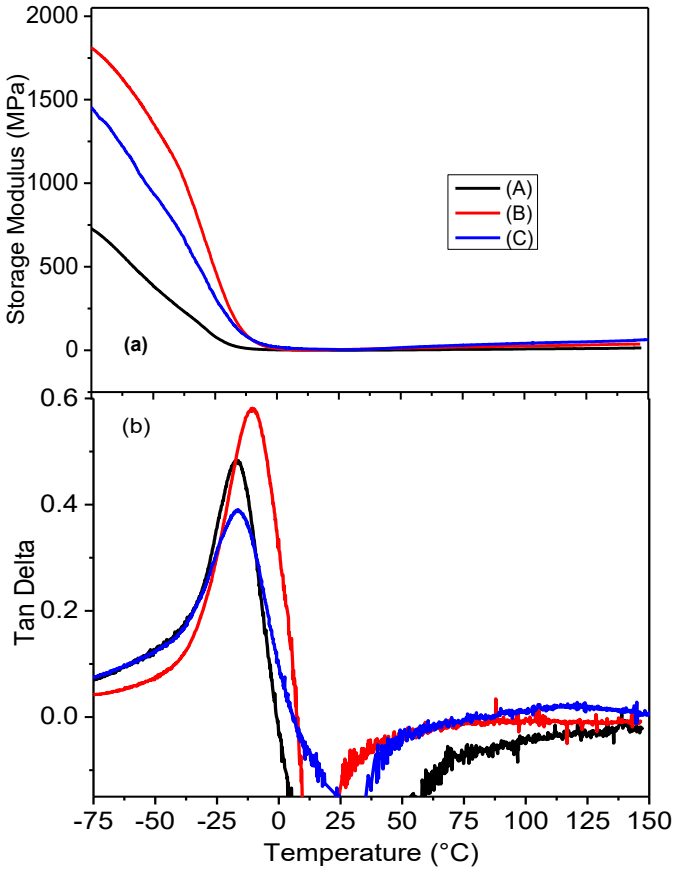

Figure 5.9: DMA thermograms of (A) 3%, (B) 5% and (C) 10 % nanoclay composites (a) plot of storage modulus vs temperature and (b) tan delta vs temperature.

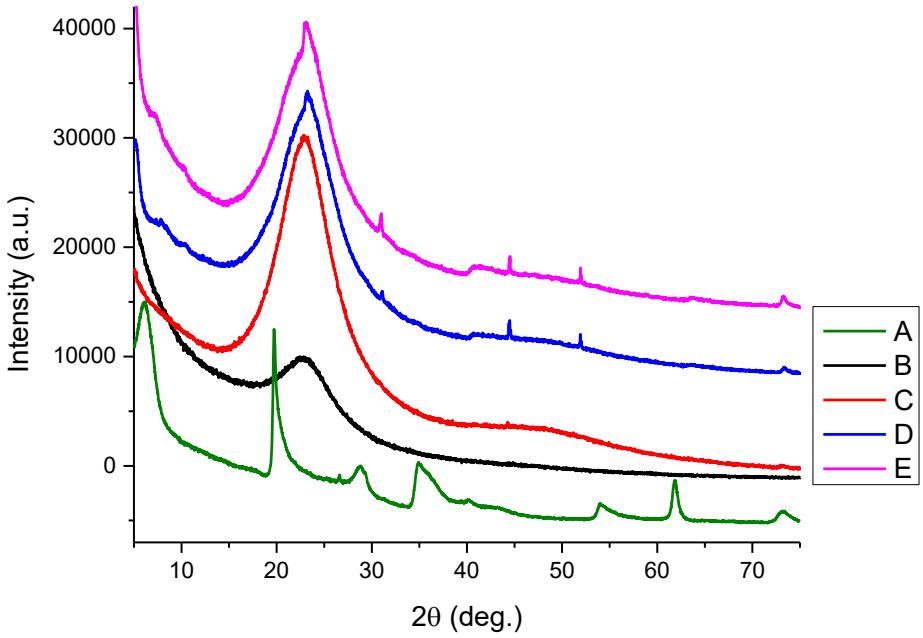

Figure 5.10: XRD patterns of (A) nanoclay, (B) homopolymer, (C) 3% nanoclay composite, (D) 5% nanoclay composite, and (E) 10% nanoclay composite.

Atomic force microscopy (AFM) can be used to measure surface topology of samples to angstroms level resolution measuring forces existing between atoms (Binnig et al., 1986) and can be used to probe nanoscale interaction forces between various kinds of materials including polymers (Xu et al., 2019). The orientation and distribution of nanoclay in polymer nanocomposites is substantially influenced by the percentage of nanoclay added and therefore high percentage and non-uniform distribution of nanoclay causes surface defects (Pacheco-Torgal et al., 2018). The 3D phase images of the neat biopolymer and the nanoclay-loaded samples are illustrated in Figure 5.12. In the nanoclay bionanocomposites, the nanoclay appears as white bright features in the reddish biopolymer matrix.

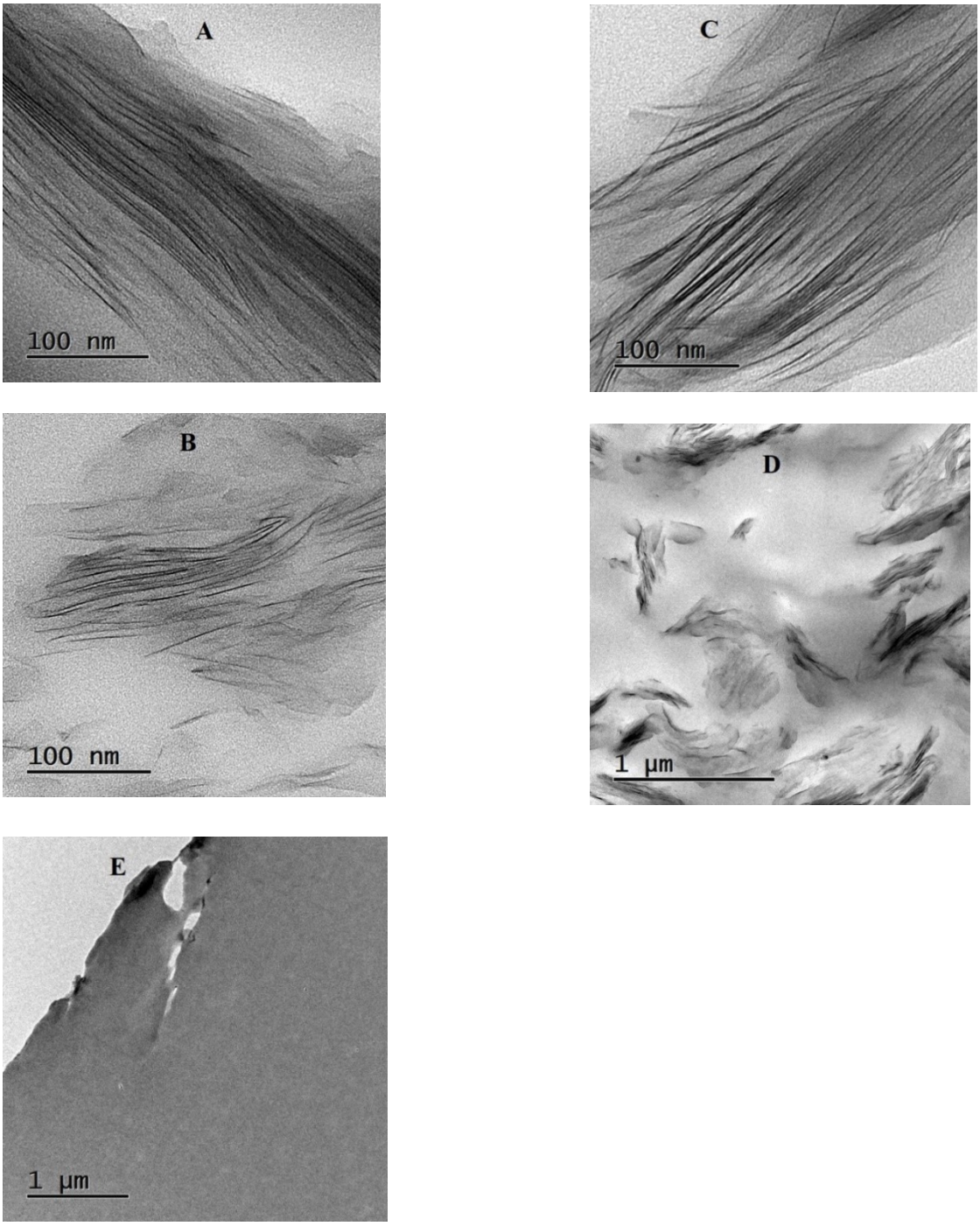

Figure 5.11. TEM micrographs of composites with (A) 3%, (B) 5% and (C) 10% nanoclay with scale bar at 100 nm, (D) 5% nanoclay with scale bar at 1 µm and (E) neat polymer with scale bar at 1 µm.

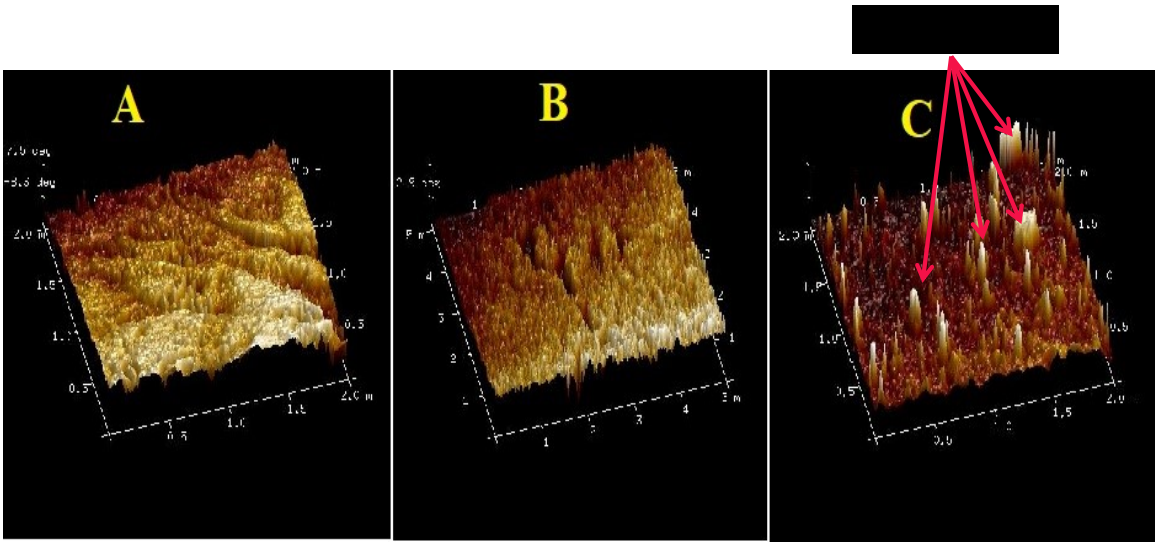

Figure 5.12: Three-dimensional (3D) morphology of phase images of nanocomposite films containing varying amounts of nanoclay: (A) 3%, (B) 5%, and (C) 10%.

It can be clearly seen in Figure 5.12 that the clay particles are well distributed all over the matrix in the case of 3% and 5% nanoclay reinforced biopolymers, while in the case of 10% nanoclay reinforced samples the clay particles are more confined in particular regions and not homogeneously distributed all over the matrix. The non-uniform dispersion of nanoclay has a significant influence on the nanoscale surface topology of the bionanocomposites.

5.3.3. Nanocomposite films

The physical appearance of bionanocomposite films containing 3, 5, and 10 wt% nanoclay prepared by compression molding is shown in Figure 5.13, demonstrating the level of transparency where the film with 3% nanoclay is more transparent compared to 5 and 10% nanoclay composite films.

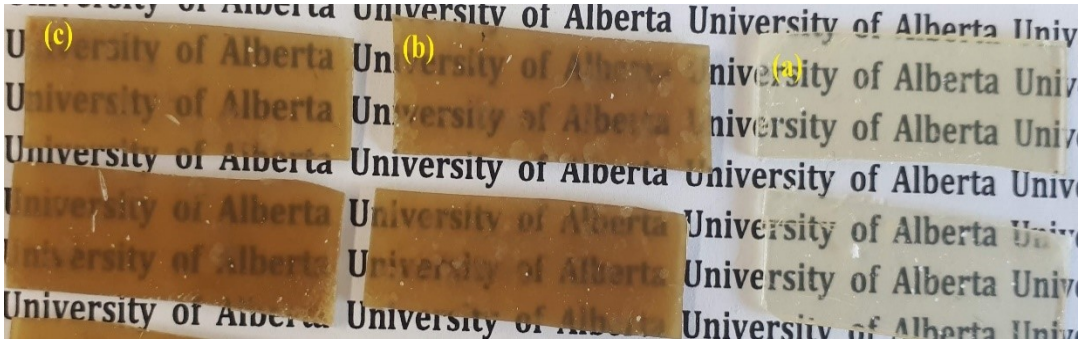

Figure 5.13: Physical appearance of nanoclay reinforced films prepared using compression molding containing (a) 3%, (b) 5%, and (c) 10 wt% nanoclay.

After the dispersion of nanoclay in the polymer nanocomposites, flammability test was performed on the films to study the effect of nanoclay dispersion on flame retardancy. The uniform dispersion of nanoclay in the composites normally decreases the flammability. Figure 5.14 shows images of the flammability test of neat homopolymer and the nanocomposites. It was found that the neat polymer caught fire rapidly when exposed to the flame for one second and the films burnt completely within 30 sec without leaving any residue. On the other hand, it took 52, 60 and 53 sec for the nanocomposites containing 3, 5 and 10% nanoclay, respectively, to burn completely after exposure to a flame (Figure 5.14). Overall, all the nanoclay reinforced composites delayed complete burning of the films by about 22 - 30 sec in comparison to the neat polymer. It was also found that the composites with higher nanoclay concentration deposited more residue after complete burning. This trend showed that the presence of nanoclay in the composites facilitated fire retardancy. Similarly, the composites with 5% and 10% nanoclay did not catch fire on the first exposure to a flame, but these caught fire on the second time exposure to flame. The nanocomposites containing 5% and 10% nanoclay took 60 and 53 sec, respectively, for complete burning, which is almost two folds the time compared to the neat polymer that could be due to better dispersion of the nanoclay particles in the polymer matrix, which enhanced the fire

retardancy. Ultimately, the nanoclay reinforced composites displayed very good resistance against flammability compared to the homopolymer.

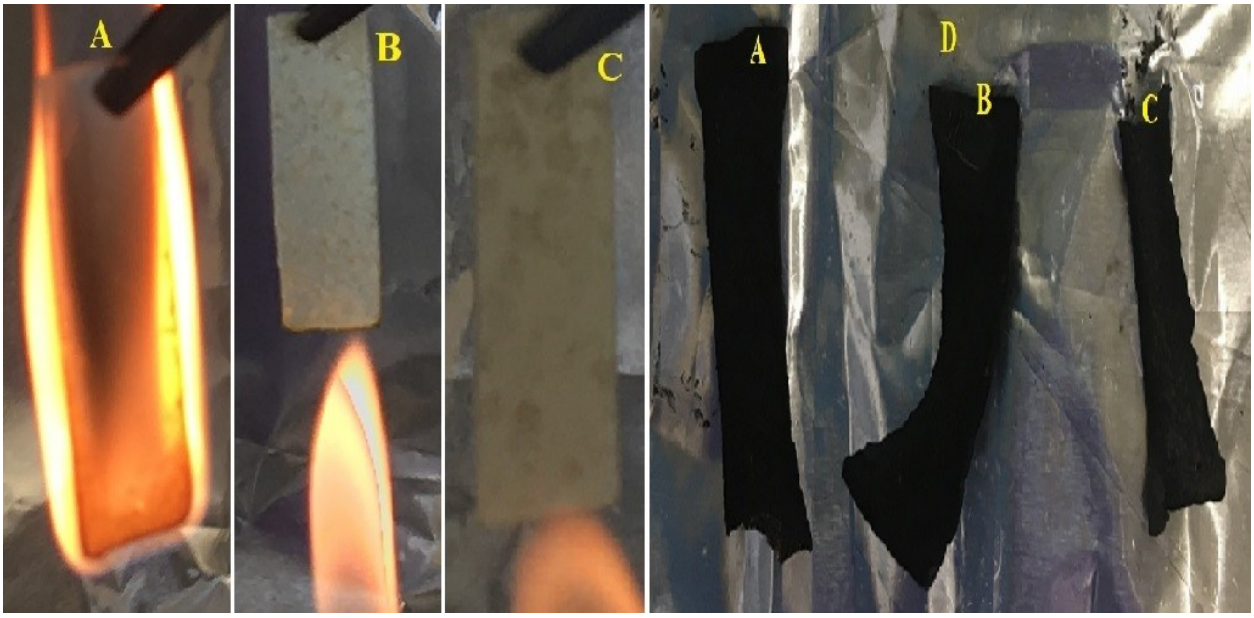

Figure 5.14: Flammability tests of composite films: (A) 3% nanoclay, (B) 5% nanoclay, (C) 10% nanoclay, and (D) residues.

5.4. Conclusions

The saturated and unsaturated fatty acids from a sustainable source, the poultry byproduct spent hens have been successfully used in monomer synthesis. The bulk polymerization of the spent hen derived monomer at different temperatures and times showed that the highest molecular weight polymer was obtained at 70 ˚C for 24 h. The *in situ* addition of different proportions of nanoclay during the polymer formation resulted in significant improvement in the thermal properties. Specifically, the fire retardancy of the nanoclay reinforced films was substantially improved to double as compared to the homopolymer without the addition of nanoclay. In conclusion, the spent hen lipids were successfully modified to nanoclay composites, which show great potential for further development targeting different applications.

5.5. References

Aerts, H.A., Jacobs, P.A. 2004. Epoxide yield determination of oils and fatty acid methyl esters using 1H NMR. *Journal of the American Oil Chemists' Society*, **81**(9), 841-846.

Andreeßen, C., Steinbüchel, A. 2019. Recent developments in non-biodegradable biopolymers: Precursors, production processes, and future perspectives. *Applied Microbiology and Biotechnology*, **103**(1), 143-157.

Arshad, M., Huang, L., Ullah, A. 2016. Lipid-derived monomer and corresponding bio-based nanocomposites. *Polymer International*, **65**(6), 653-660.

Bernhart, M., Fasina, O.O. 2009. Moisture effect on the storage, handling and flow properties of poultry litter. *Waste Management*, **29**(4), 1392-1398.

Bertolino, V., Cavallaro, G., Lazzara, G., Merli, M., Milioto, S., Parisi, F., Sciascia, L. 2016. Effect of the biopolymer charge and the nanoclay morphology on nanocomposite materials. *Industrial & Engineering Chemistry Research*, **55**(27), 7373-7380.

Brockhaus, S., Petersen, M., Kersten, W. 2016. A crossroads for bioplastics: exploring product developers' challenges to move beyond petroleum-based plastics. *Journal of Cleaner Production*, **127**, 84-95.

Cohen-Karni, D., Kovaliov, M., Ramelot, T., Konkolewicz, D., Graner, S., Averick, S. 2017. Grafting challenging monomers from proteins using aqueous ICAR ATRP under bio-relevant conditions. *Polymer Chemistry*, **8**(27), 3992-3998.

Dietrich, K., Dumont, M.-J., Del Rio, L.F., Orsat, V. 2017. Producing PHAs in the bioeconomy—Towards a sustainable bioplastic. *Sustainable Production and Consumption*, **9**, 58-70.

Forfang, K., Zimmermann, B., Kosa, G., Kohler, A., Shapaval, V. 2017. FTIR spectroscopy for evaluation and monitoring of lipid extraction efficiency for oleaginous fungi. *PloS One*, **12**(1), e0170611.

Garrison, T., Murawski, A., Quirino, R. 2016. Bio-based polymers with potential for biodegradability. *Polymers*, **8**(7), 262.

Giannakas, A.E., Leontiou, A.A. 2018. Montmorillonite composite materials and food packaging. *Composites Materials for Food Packaging*, 1-71.

He, M., Wang, X., Wang, Z., Chen, L., Lu, Y., Zhang, X., Li, M., Liu, Z., Zhang, Y., Xia, H. 2017. Biocompatible and biodegradable bioplastics constructed from chitin via a "green" pathway for bone repair. *ACS Sustainable Chemistry & Engineering*, **5**(10), 9126-9135.

Hong, H., Roy, B.C., Chalamaiah, M., Bruce, H.L., Wu, J. 2018. Pretreatment with formic acid enhances the production of small peptides from highly cross-linked collagen of spent hens. *Food Chemistry*, **258**, 174-180.

Jambeck, J.R., Geyer, R., Wilcox, C., Siegler, T.R., Perryman, M., Andrady, A., Narayan, R., Law, K.L. 2015. Plastic waste inputs from land into the ocean. *Science*, **347**(6223), 768-771.

Jiang, Y., Ding, D., Zhao, S., Zhu, H., Kenttämaa, H.I., Abu-Omar, M.M. 2018. Renewable thermoset polymers based on lignin and carbohydrate derived monomers. *Green Chemistry*, **20**(5), 1131-1138.

Jose, T., George, S.C., Maria, H.J., Wilson, R., Thomas, S. 2014. Effect of bentonite clay on the mechanical, thermal, and pervaporation performance of the poly (vinyl alcohol) nanocomposite membranes. *Industrial & Engineering Chemistry Research*, **53**(43), 16820-16831.

Khanra, S., Mondal, M., Halder, G., Tiwari, O., Gayen, K., Bhowmick, T.K. 2018. Downstream processing of microalgae for pigments, protein and carbohydrate in industrial application: A review. *Food and Bioproducts Processing*, **110**, 60-84.

Kondaiah, N., Panda, B. 1992. Processing and utilization of spent hens. *World's Poultry Science Journal*, **48**(3), 255-268.

Lambert, S., Wagner, M. 2017. Environmental performance of bio-based and biodegradable plastics: the road ahead. *Chemical Society Reviews*, **46**(22), 6855-6871.

Makaremi, M., Pasbakhsh, P., Cavallaro, G., Lazzara, G., Aw, Y.K., Lee, S.M., Milioto, S. 2017. Effect of morphology and size of halloysite nanotubes on functional pectin bionanocomposites for food packaging applications. *ACS Applied Materials & Interfaces*, **9**(20), 17476-17488.

Malinconico, M. 2017. *Soil degradable bioplastics for a sustainable modern agriculture*. Springer, Verlag GmbH Germany.

Mauck, S.C., Wang, S., Ding, W., Rohde, B.J., Fortune, C.K., Yang, G., Ahn, S.-K., Robertson, M.L. 2016. Biorenewable tough blends of polylactide and acrylated epoxidized soybean oil compatibilized by a polylactide star polymer. *Macromolecules*, **49**(5), 1605-1615.

Miller, S.A. 2013. Sustainable polymers: opportunities for the next decade, *ACS Macro Lett.*, **2**(6), 550-554.

Mohanty, A.K., Vivekanandhan, S., Pin, J.-M., Misra, M. 2018. Composites from renewable and sustainable resources: Challenges and innovations. *Science*, **362**(6414), 536-542.

Mousa, M.H., Dong, Y., Davies, I.J. 2016. Recent advances in bionanocomposites: Preparation, properties, and applications. *International Journal of Polymeric Materials and Polymeric Biomaterials*, **65**(5), 225-254.

Olkiewicz, M., Caporgno, M.P., Fortuny, A., Stüber, F., Fabregat, A., Font, J., Bengoa, C. 2014. Direct liquid–liquid extraction of lipid from municipal sewage sludge for biodiesel production. *Fuel Processing Technology*, **128**, 331-338.

Papanikolaou, S., Dimou, A., Fakas, S., Diamantopoulou, P., Philippoussis, A., Galiotou-Panayotou, M., Aggelis, G. 2011. Biotechnological conversion of waste cooking olive oil into lipid-rich biomass using Aspergillus and Penicillium strains. *Journal of Applied Microbiology*, **110**(5), 1138-1150.

Paul, D., Robeson, L.M. 2008a. Polymer nanotechnology: nanocomposites. *Polymer*, **49**(15), 3187-3204.

Qi, X., Zhang, Y., Chang, C., Luo, X., Li, Y. 2018. Thermal, Mechanical, and Morphological Properties of Rigid Crude Glycerol-Based Polyurethane Foams Reinforced With Nanoclay and Microcrystalline Cellulose. *European Journal of Lipid Science and Technology*, **120**(5), 1700413.

Ray, S.S., Bousmina, M. 2005. Biodegradable polymers and their layered silicate nanocomposites: in greening the 21st century materials world. *Progress in Materials Science*, **50**(8), 962-1079.

Sahmani, S., Shahali, M., Khandan, A., Saber-Samandari, S., Aghdam, M. 2018. Analytical and experimental analyses for mechanical and biological characteristics of novel nanoclay bio-nanocomposite scaffolds fabricated via space holder technique. *Applied Clay Science*, **165**, 112-123.

Salimon, J., Abdullah, B.M., Salih, N. 2011. Hydrolysis optimization and characterization study of preparing fatty acids from Jatropha curcas seed oil. *Chemistry Central Journal*, **5**(1), 67.

Schneiderman, D.K., Hillmyer, M.A. 2017. 50th anniversary perspective: There is a great future in sustainable polymers. *Macromolecules*, **50**(10), 3733-3749.

Souza, V.G.L., Fernando, A.L. 2016. Nanoparticles in food packaging: Biodegradability and potential migration to food—A review. *Food Packaging and Shelf Life*, **8**, 63-70.

Spurr, A.R. 1969. A low-viscosity epoxy resin embedding medium for electron microscopy. *Journal of Ultrastructure Research*, **26**(1-2), 31-43.

Tactacan, G.B., Guenter, W., Lewis, N.J., Rodriguez-Lecompte, J.C., House, J.D. 2009. Performance and welfare of laying hens in conventional and enriched cages. *Poultry Science*, **88**(4), 698-707.

Tuck, C.O., Pérez, E., Horváth, I.T., Sheldon, R.A., Poliakoff, M. 2012. Valorization of biomass: deriving more value from waste. *Science*, **337**(6095), 695-699.

Vlachos, N., Skopelitis, Y., Psaroudaki, M., Konstantinidou, V., Chatzilazarou, A., Tegou, E. 2006. Applications of Fourier transform-infrared spectroscopy to edible oils. *Analytica Chimica Acta*, **573**, 459-465.

Wang, H., Wu, J., Betti, M. 2013. Chemical, rheological and surface morphologic characterisation of spent hen proteins extracted by pH-shift processing with or without the presence of cryoprotectants. *Food Chemistry*, **139**(1), 710-719.

Wróblewska-Krepsztul, J., Rydzkowski, T., Borowski, G., Szczypiński, M., Klepka, T., Thakur, V.K. 2018. Recent progress in biodegradable polymers and nanocomposite-based packaging materials for sustainable environment. *International Journal of Polymer Analysis and Characterization*, **23**(4), 383-395.

Wu, S., Baskin, T.I., Gallagher, K.L. 2012. Mechanical fixation techniques for processing and orienting delicate samples, such as the root of Arabidopsis thaliana, for light or electron microscopy. *Nature Protocols*, **7**(6), 1113.

Yu, W., Field, C.J., Wu, J. 2018. Purification and identification of anti-inflammatory peptides from spent hen muscle proteins hydrolysate. *Food Chemistry*, **253**, 101-107.

Zhang, C., Garrison, T.F., Madbouly, S.A., Kessler, M.R. 2017. Recent advances in vegetable oil-based polymers and their composites. *Progress in Polymer Science*, **71**, 91-143.

Zhu, Y., Romain, C., Williams, C.K. 2016. Sustainable polymers from renewable resources. *Nature*, **540**(7633), 354.

Zubair, M., Wu, J., Ullah, A. 2019. Hybrid bionanocomposites from spent hen proteins. *ACS Omega*, **4**(2), 3772-3781.

CHAPTER 6 - CNC GRAFTED NANOCLAY REINFORCED BIONANOCOMPOSITES FROM SPENT HENS[4]

6.1. Introduction

In recent times, polyesters are extensively being used in different areas, i.e., automobiles (Beardmore, 1986), health (Migneco et al., 2009), personal care products (Ammala, 2013), fibres, ropes, belts (Deopura and Padaki, 2015) and others, and when reinforced with a small amount of nanoparticles their thermal and mechanical properties are substantially improved (Haq et al., 2008). Alternative polyesters can be prepared from sustainable feedstocks, i.e., plant oils, waste oils, animal oils because the petroleum resources are not only depleting but also causing severe environmental threats (Meier et al., 2007). Industrial wastes and byproducts are a great source of renewable lipids, which are cheap and with chemical modification the undesirable materials can be used as alternative polymer composites (Miao et al., 2014; Tharanathan, 2003). One such important sustainable resource of lipids is the spent hens as discussed in more detail in Chapter 2 (Section 2.1).

Normally, the lipids are converted to introduce polymerizable unsaturated moieties (Xia and Larock, 2010), e.g., introducing reactive hydroxyl groups first followed by reacting with acrylic (Cho et al., 2010), maleic (Espana et al., 2012) or isocynate (John et al., 2002) precursors to obtain the required macromonomer (Zhang and Zhang, 2013). Hydroxyl groups can be introduced in different ways, e.g., transesterification of oils and polyols or oxidation of double bonds to epoxide first and then reduction to hydroxyl groups (Campanella et al., 2010; Petrović, 2008). Acrylated vegetable oils are prepared when epoxidized oils are reacted with acrylic acid, acrylic anhydride or methacrylic anhydride (Meier et al., 2007).

[4] A version of this chapter is to be submitted for consideration for publication: Safder, M., Temelli, F., Ullah, A. 2019. CNC grafted nanoclay reinforced bionanocomposites from spent hens.

In the previous study reported in Chapter 4, spent hen epoxy resin macromonomer was synthesized by the epoxidation reaction of spent hen oil in the presence of an ion exchange resin, i.e., Amberlite IR-120. In this study, a novel approach is targeted to introduce hydroxyl groups by grafting cellulose nanocrystals (CNC) on epoxidized spent hen lipids followed by acrylation to synthesize the macromonomer. This study aims to harvest this massive bioresource for the value addition of lipids with the ultimate goal of developing nanocomposites for different potential applications. To the best of my knowledge, this is the first report on the synthesis of spent hen oil-based monomers by introducing first the epoxy groups, then grafting CNC and subsequently the acrylic groups onto spent hen oils and production of composites with nanoclay reinforcements.

6.2. Materials and methods

6.2.1. Materials

Thin layer chromatography (TLC, Merck, Darmstadt, Germany) was performed on silica gel 60 F254 aluminium plates. 4-(Dimethylamino) pyridine (DMAP≥99%), dicyclohexylcarbodiimide (DCC, 99%), 2-hydroxyethyl acrylate (96%), sodium chloride (99.9%), anhydrous sodium sulfate (≥99%), dichloromethane (DCM, 99.9%), montmorillonite nanoclay modified with 35 - 45 wt% dimethyl dialkyl (-C14 and --C18) amine, azobisisobutyronitrile (AIBN, 98%, recrystallized in methanol), tetrahydrofuran (THF, ≥99%), $ZnCl_2$, ion exchange resin Amberlie IR-120, cellulose nanocrystals (CNC), toluene, ethylacetate, n-hexane, buffers (pH 4, 7 and 10), methacrylic anhydride, 1-methylimidazole were purchased from Sigma-Aldrich (St. Louis, MO, USA) and used as received.

6.2.2. Extraction of lipids from spent hens

Lipids were extracted from spent hens using microwave-assisted technology according to the protocol described in Chapter 3 (Section 3.2.3.)

6.2.3. Epoxidation of extracted lipids from spent hens

Epoxidation of extracted lipids was performed according to the previous study on the solvent free rapid epoxidation using recyclable resin Aberlite IR-120 as described in Chapter 4 (Section 4.2.6).

6.2.4. Grafting of cellulose nanocrystals (CNC) on epoxidized lipid

Epoxidized spent hen oil (ESHO, 100 g) in toluene (150 mL) was mixed with CNC (0.2 g) in the presence of $ZnCl_2$ (6 g) as a catalyst at 80 °C under nitrogen environment for 6 h. The reaction progress was monitored by TLC, ATR-FTIR and ^{1}H NMR spectroscopies. Toluene was removed by rotary evaporator. Further purification was performed by column chromatography using silica gel as stationary phase and 10% ethylacetate in n-hexane as mobile phase.

Grafting of CNC was also conducted to optimize different parameters such as in the presence of buffers at pH 4, 7 and 10 at temperatures of 60, 80, and 100 °C for 24, 72 and 120 h. The progress of grafting reactions was monitored by ATR-FTIR and ^{1}H NMR spectroscopy. The molecular weights of synthesized CNC-grafted lipids were determined by gel permeation chromatography (GPC). Buffer solutions were prepared using Na_2HPO_4 and KH_2PO_4. On the basis of different reaction conditions, a temperature of 80 °C for 72 h reaction time and using buffer at pH 7 were used to synthesize the CNC-grafted precursor with a percentage yield of 64.37%. The experiments were performed in duplicate.

6.2.6. Acrylation of CNC-grafted spent hen oil using methacrylic anhydride (Monomer)

The monomer was synthesized by reacting 1000 mg of CNC-grafted oil (1 equivalent) with methacrylic anhydride 1695.32 mg (11 equivalents) in the presence of 1-methylimidazole (82.1 mg) as catalyst at 40 °C for 30 min. The reaction was monitored by TLC and ATR-FTIR and the obtained yield was 65.20%. The experiments were performed in duplicate.

6.2.7. Synthesis of composites

Styrene was added as a copolymer to enhance the strength of the composites because the homopolymers prepared were not strong enough for film preparation. The monomer and styrene (30% wt%) with the addition of different concentrations of modified nanoclay (1, 5 and 10%) were used to synthesize nanocomposites at 70 °C after purging the reaction mixture with nitrogen for 30 min. The composites were prepared in duplicate.

6.2.8. Characterizations

Attenuated total reflectance-Fourier transform infrared (ATR-FTIR) spectroscopy, proton nuclear magnetic resonance spectroscopy (^{1}H NMR), thermogravimetric analysis (TGA), differential scanning calorimetry (DSC), gel permeation chromatography (GPC), transmission electron microscopy (TEM), X-ray diffraction (XRD), and film thickness were performed according to the protocols described in Chapter 5 (Section 5.2).

6.2.9. Moisture uptake

To investigate the moisture uptake behavior of neat composite and nanoclay reinforced composites, the samples were first prepared following the standard protocol reported by (Arshad et al., 2016b) with slight modification. Briefly, the diameter of disc was 44.46 mm with 0.85 mm thickness. The discs were dried in an oven at a temperature of 100 °C until constant weight was achieved. A weighed quantity of all prepared composites, including neat polymer was conditioned

at room temperature (25 °C) and placed in a desiccator with 98% relative humidity (maintained by placing a saturated solution of $CuSO_4 \cdot 5H_2O$ overnight). The samples were taken out at specific intervals, initially at short intervals of 0.5, 1, 16, 24 h and then continued until it reached the plateau up to 160 h and weighed on an analytical balance to measure the gradual uptake of moisture. Equation (6.1) was used to calculate the moisture uptake (MU) of all samples:

$$MU\ (\%) = (\frac{Wt-W0}{W0})100 \qquad (6.1)$$

where W_0 is the initial weight of the sample and Wt is the weight of sample determined at specific time periods after exposure to 98% relative humidity.

6.3. Results and discussion

6.3.1. Composites preparation

The synthesis of monomer from spent hen lipids involved three steps as shown in Figure 6.1. In the first step, the double bonds of extracted TAGs were epoxidized in the presence of Amberlite-120 as ion exchange resin and in the second step the CNC was grafted using those epoxy rings in the presence of a buffer. Also, during the CNC grafting different parameters, i.e., temperature, pH and reaction time were studied to achieve the maximum level of CNC grafting. In the third step, the monomer was prepared by reacting CNC-grafted spent hen lipid with methacrylic anhydride in the presence of 1-methylimidazole as catalyst as shown in Figure 6.2. Finally, the composites were prepared by bulk polymerization method in the presence of AIBN as initiator, including copolymerization with 30% styrene and *in situ* addition of different proportions of modified nanoclay to evaluate the effect of nano reinforcement on thermal and water uptake properties of the composites. The proposed schemes for the synthesis of monomer and the corresponding composites are shown in Figures 6.1 and 6.2, respectively.

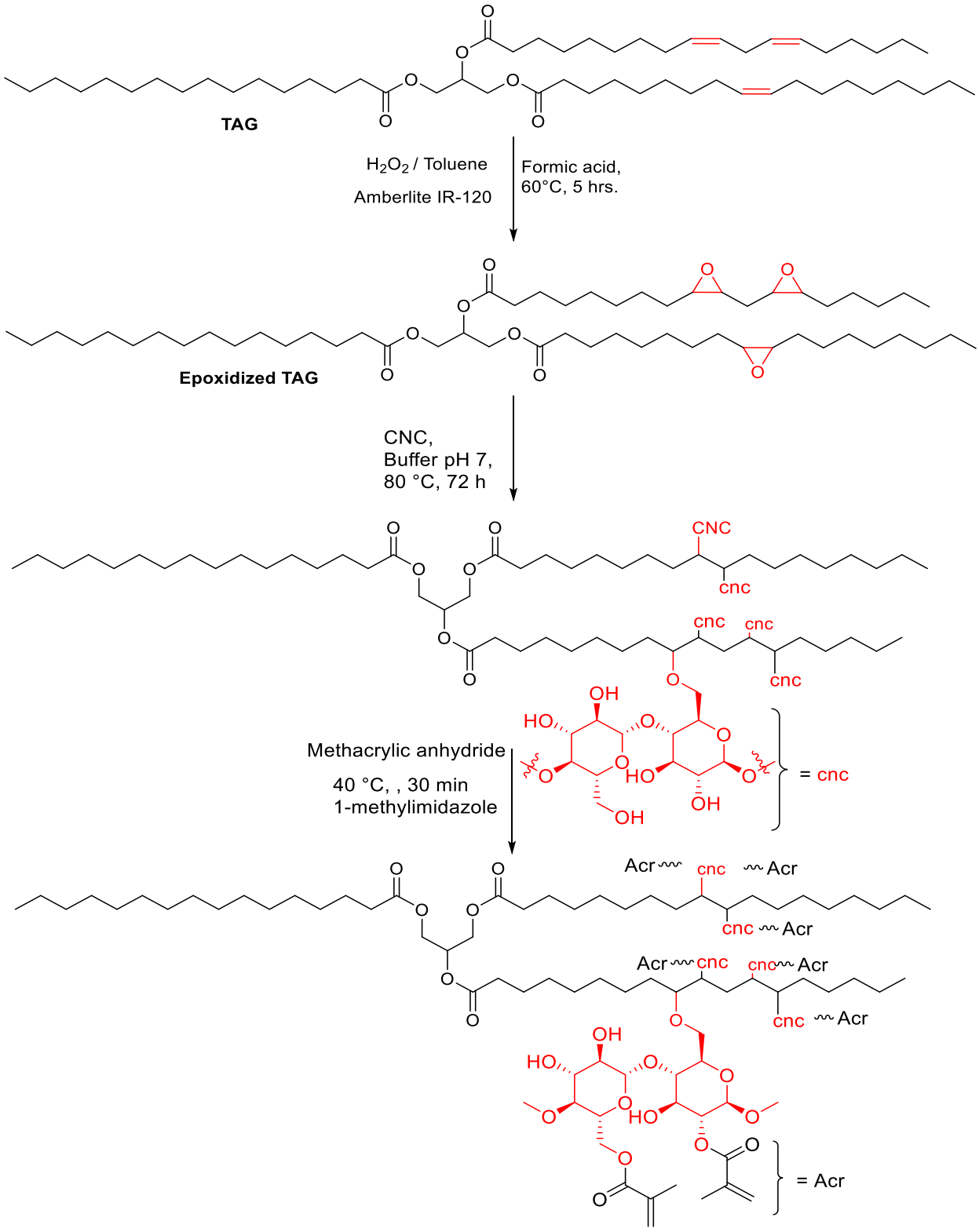

Figure 6.1: Preparation of monomer.

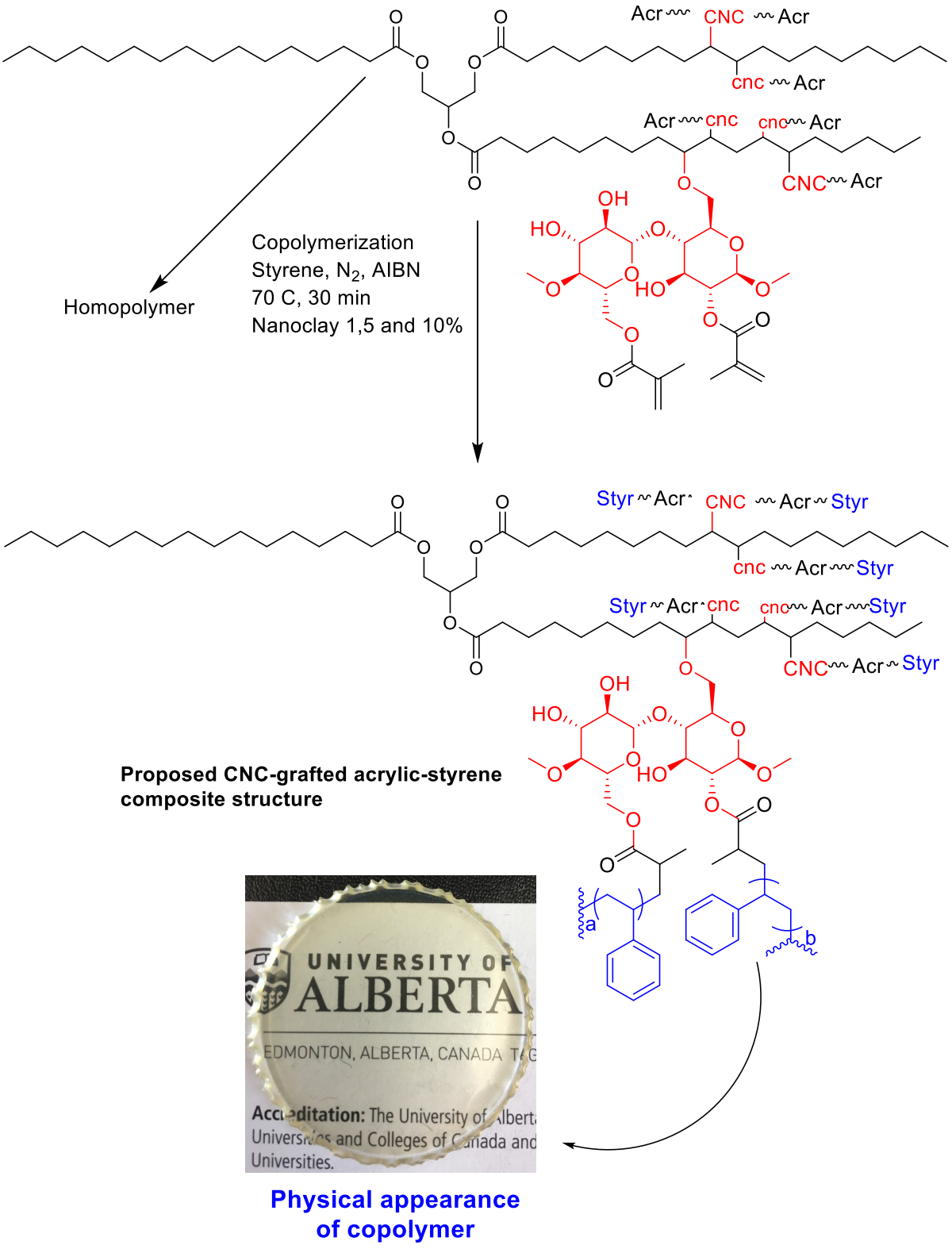

Figure 6.2: Preparation of copolymer composite from monomer and styrene.

6.3.2. ATR-FTIR analysis

ATR-FTIR spectra of extracted lipids from spent hens, epoxidized oil, CNC-grafted oil, monomer (CNC-grafted acrylated) and 10% nanoclay reinforced composite are shown in Figure 6.3. From the spectra, it was obvious that during the first step, the peak of double bonds at 3005 cm^{-1} disappeared and a new peak at 832 cm^{-1} of oxirane functionality appeared, which showed the epoxy ring formation of unsaturated part of extracted lipid in agreement with the previously reported data (Adhvaryu and Erhan, 2002). In the second step, the signal of epoxy ring disappeared and as a result a broad high intensity new peak at 3382 cm^{-1} of hydroxyl groups appeared, including several other peaks, i.e., 1418, 1173, and 1071 cm^{-1} in the fingerprint region, which indicated the grafting of CNC onto the epoxy rings. As well, the third step of monomer synthesis was also indicated by the disappearance or decrease in hydroxyl of CNC peak at 3382 cm^{-1}, introduction of a weak signal at 3001 cm^{-1} and a clear peak at 1634 cm^{-1} of terminal double bonds, which showed the successful formation of acrylated CNC-grafted monomer. These data were in agreement with the previously reported data (Abraham et al., 2016). A representative FTIR spectra for nanoclay reinforced composites shown in Figure 6.3 indicated the complete polymerization with the disappearance of double bond peaks together with the appearance of clay peaks at 1230 and 940 cm^{-1}, which were associated with Si-O bending and Si-O-Si stretching vibration, respectively.

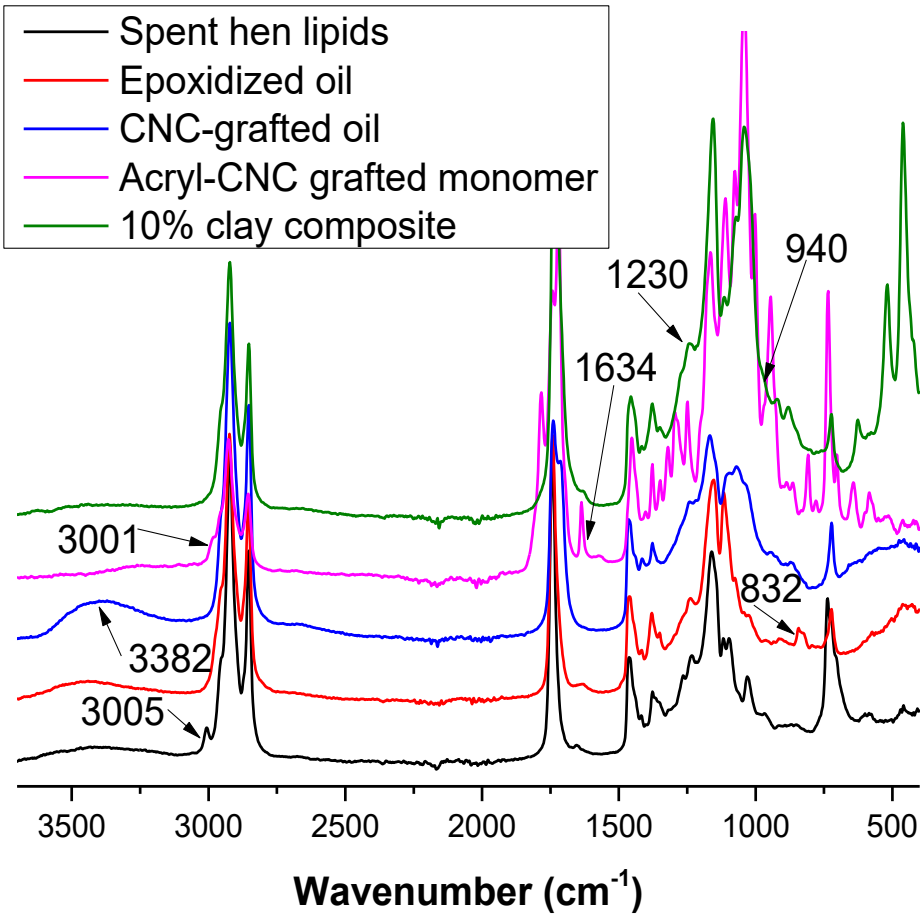

Figure 6.3: FTIR spectra of extracted lipids from spent hens, epoxidized oil, CNC-grafted oil, monomer (CNC-grafted acrylated) and 10% nanoclay reinforced composite.

6.3.3. Gel Permeation Chromatography (GPC)

To study the effect of pH, temperature and time on CNC grafting onto the spent hen epoxy TAGs on their molecular weights, the GPC was used. The average molecular weights of CNC-grafted TAGs at different reaction conditions are shown in Table 6.1. The molecular weight of spent hen epoxidized oil was 3026.4. The higher molecular weight of 4455.6 was obtained at a temperature of 60 °C, 72 h and at a pH of 7, which showed the grafting of CNC.

Table 6.1: Reaction conditions and average molecular weights obtained by GPC for CNC grafting

	pH	Temperature (°C)	Time (h)	MW
1	7	80	72	4228.7
2	7	100	72	3809.7
3	7	60	72	4205.5
4	7	80	72	4172.7
5	7	100	72	3923.2
6	10	60	72	3625.8
7	10	80	72	3590.5
8	10	100	72	3917.2
9	10	80	72	3780.2
11	10	100	72	3907.5
12	10	60	72	3276.3
13	10	80	72	3612.2
14	7	100	72	3116.8
15	7	60	72	4455.6
16	7	80	72	4373.9
17	4	100	72	2911.9
18	4	60	72	3251.9
19	4	80	72	4139.9

6.3.4. ^{1}H NMR analysis

The synthesis of acrylated CNC-grafted monomer from spent hen was confirmed by ^{1}H NMR spectroscopy. ^{1}H NMR spectra of extracted lipids from spent hens, epoxidized oil, CNC-grafted oil, and monomer (CNC-grafted acrylated) are shown in Figure 6.4. The epoxidation of extracted TAGs from spent hen was also confirmed by the disappearance of two peaks of olefinic

protons from the starting material at 5.37 and 2.02 ppm and appearance of two new characteristic peaks of oxirane protons at 1.50 and 2.92 ppm. In the second step of monomer preparation, which was grafting of CNC onto the epoxides, the peaks of oxirane protons disappeared. The third step of monomer synthesis was confirmed by proton signals associated to acrylic part resonating in the range of 5.97-6.55.

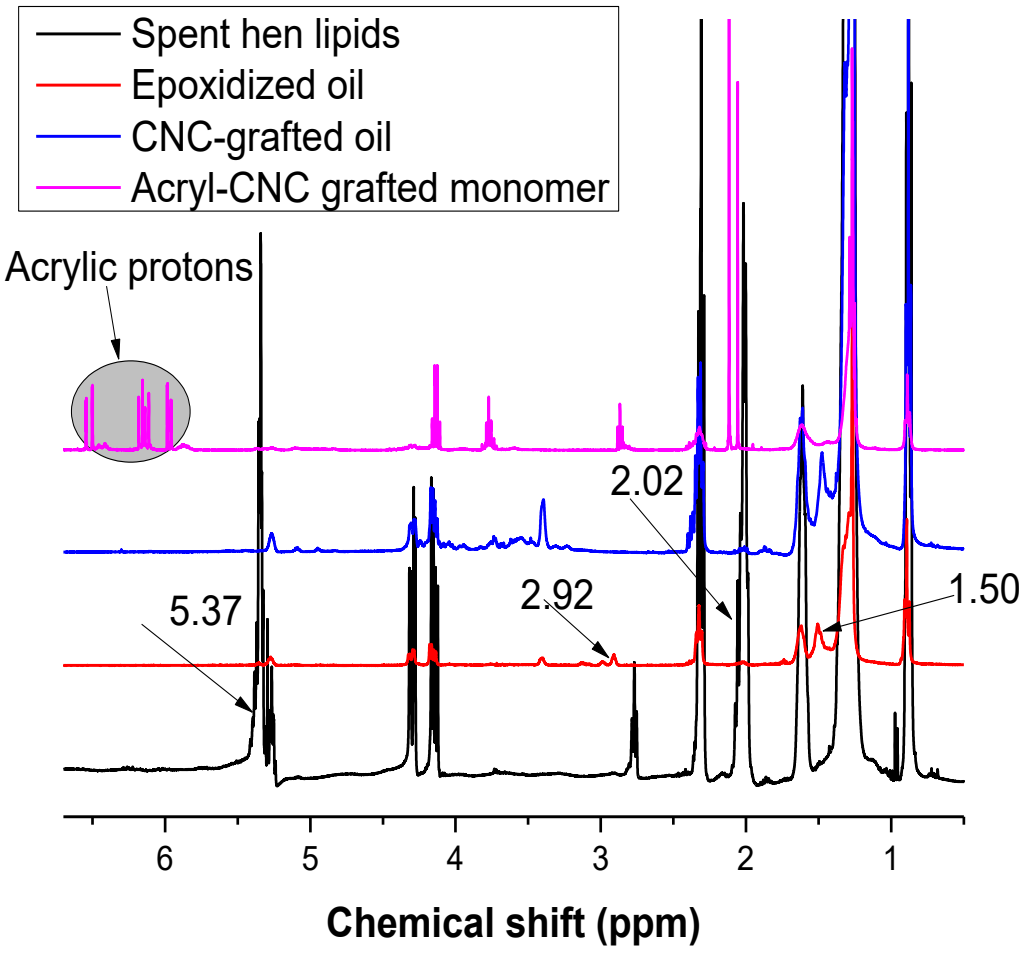

Figure 6.4: ^{1}H NMR spectra of extracted lipids from spent hens, epoxidized oil, CNC-grafted oil, and monomer (CNC-grafted acrylated).

6.3.5. XRD pattern analysis

The extent of *in situ* dispersion of nanoclay was studied by XRD pattern. Figure 6.5 shows the XRD patterns of the nanocomposites prepared with the addition of 1, 5, and 10% nanoclay. The nanoclay showed XRD peaks at a 2θ angle of 5.85°, 19.78°, 26.70°, 29.01°, 35.07°, 53.99°, 61.82°, and 73.09°, while the homopolymer showed a broad peak at 20.72°. All the characteristic peaks, assigned to the modified nanoclay (Jose et al., 2014), completely disappeared in the nanocomposites, which showed that the polymer composite developed interactions with the clay particles, and as a result, clay crystallinity was destroyed. The differences in XRD patterns are prominent with the appearance of some small new distinct peaks in samples containing 5% and 10% nanoclay at 40.54°, and 73.54°, which may be attributed to a new crystalline region created during *in situ* polymerization (Sahmani et al., 2018). These new peaks could be related to the formation of a new crystal pattern, which may be created during the dispersion, indicating that the nanoclay sheets were intercalated or exfoliated into the polymers or complete nanoclay dispersion/exfoliation was achieved, leading to greater inter layer spacing, as further confirmed by TEM analysis.

6.3.6. Thermogravimetric analysis (TGA)

The thermal stability and degradation behavior of nanoclay composites was studied by thermogravimetric analysis (TGA) and its derivative (DTG). Figures 6.6 and 6.7, respectively, show the TGA and DTG curves of the homopolymer and nanocomposites. The first stage of weight loss occurred from 120 °C to 235 °C, which could be due to the evaporation of some bound moisture from the homopolymer and nanocomposites. The second stage of major weight loss started at about 325-365 °C because of the thermal degradation of the homopolymer in nanocomposites. The added clay acts as a superior insulator and barrier to the volatile products

generated during decomposition. A prominent improvement in thermal stability was observed by the addition of nanoclay, and the char left as a residue after complete combustion up to 600 °C could be due to the presence of silica and alumina. Overall, the composites with 5 and 10% nanoclay showed less weight loss compared to the neat homopolymer. A 50% weight loss was observed around 389 to 400 ºC for all the composites. The copolymer showed 98.5% weight loss at 600 ºC while the composites with 5 and 10% nanoclay showed 94.6 and 94.2% weight loss, respectively, as shown in Table 6.2. The thermal transitions of the biopolymer and its nanocomposites were studied by DSC and are shown in Figure 6.8. The neat biopolymer exhibited a melting peak at around 150 °C and among the nanocomposites, the 5% clay containing bionanocomposite displayed a melting peak at around 160 °C.

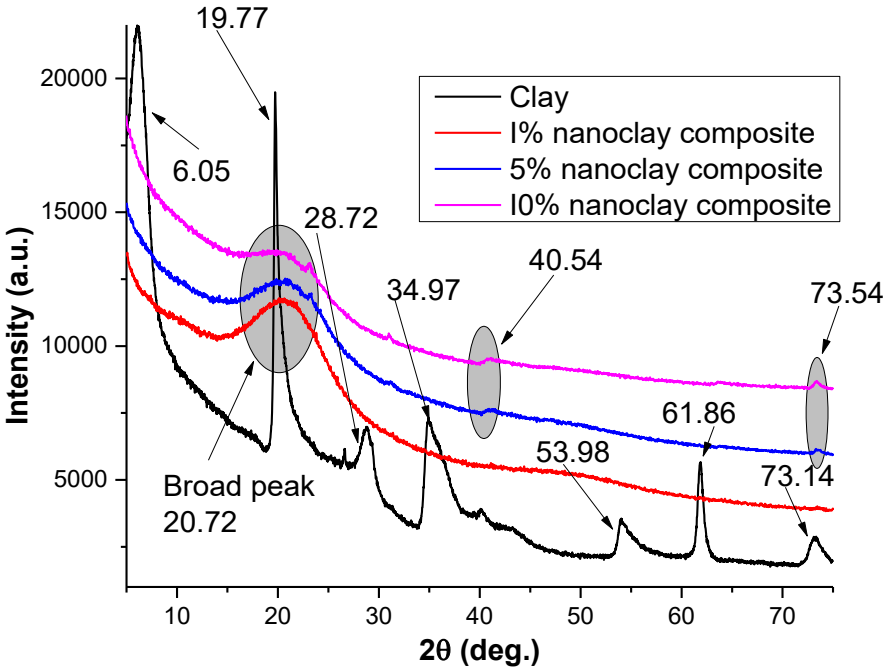

Figure 6.5: XRD patterns of nanoclay, 1% nanoclay composite, 5% nanoclay composite, and 10% nanoclay composite.

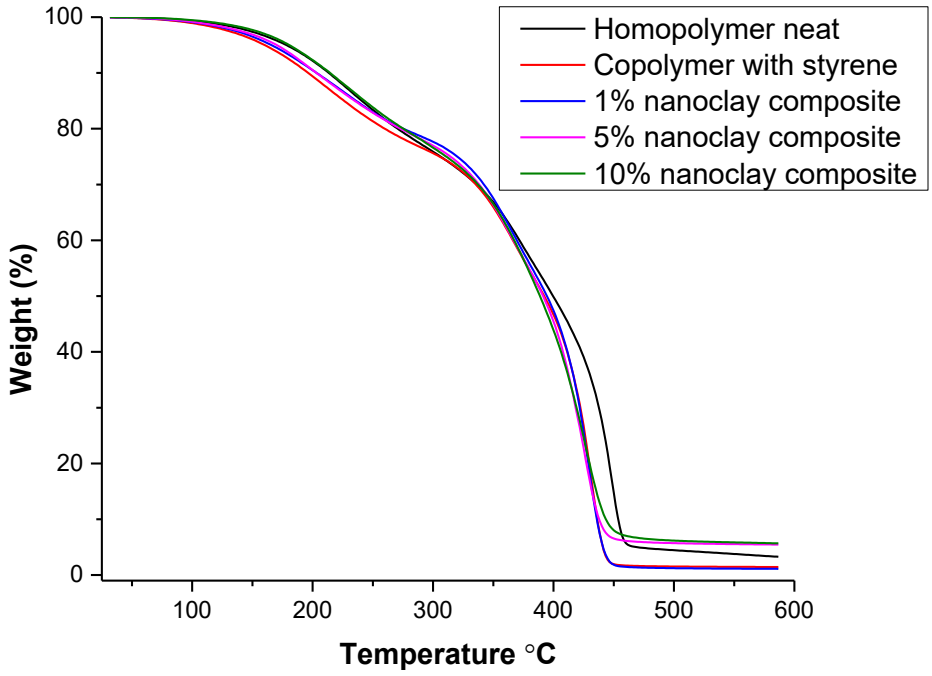

Figure 6.6: TGA curves of homopolymer, 1, 5, and 10% nanoclay composites.

Table 6.2: Thermal stability of nanoclay reinforced lipid-derived composites

Sample (% nanoclay)	Weight loss temperatures (˚C)				Char at 600 ˚C (%)
	5%	10%	50%	90%	
Homopolymer neat	176.9	212.6	399.3	453.7	3.3
Copolymer with styrene	158.9	196.1	392.2	436.6	1.5
1% nanoclay composite	165.3	203.4	394.7	435.7	1.2
5% nanoclay composite	169.4	203	391.3	438.1	5.4
10% nanoclay composite	179.3	214.1	388.8	443.1	5.8

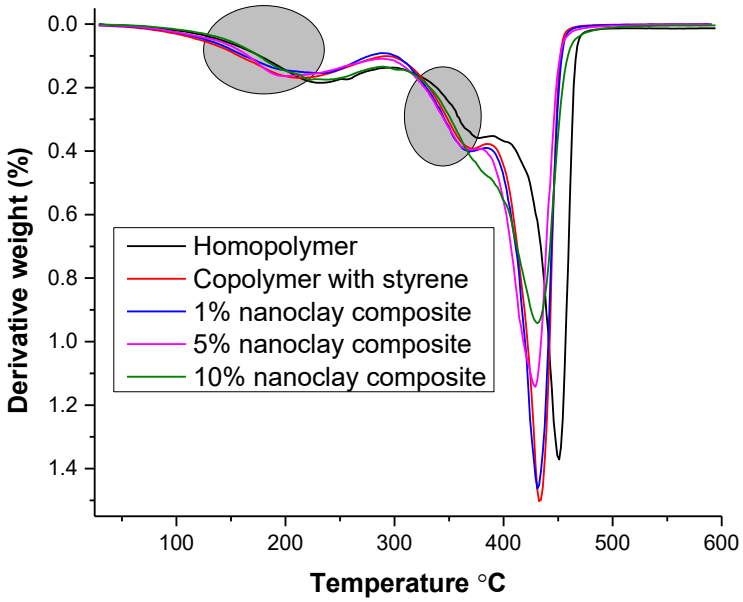

Figure 6.7: DTG curves of homopolymer, 1, 5, and 10% nanoclay composites.

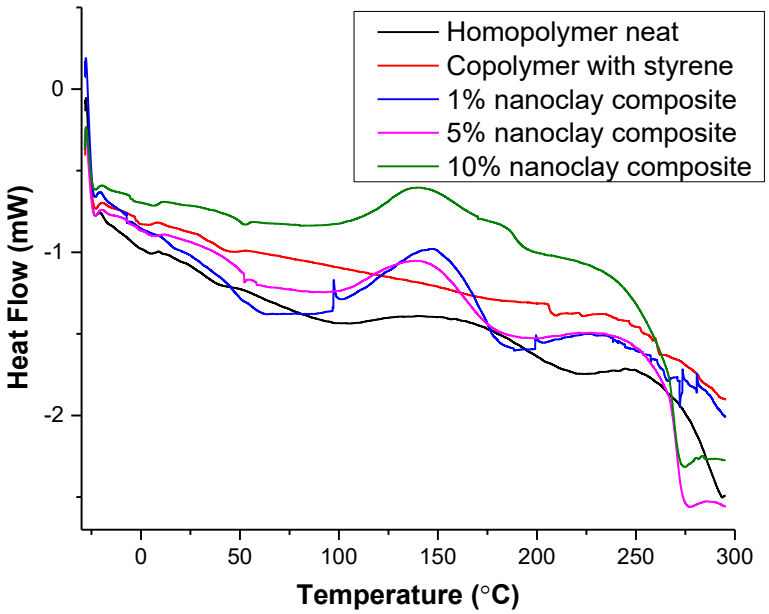

Figure 6.8: DSC curves of homopolymer, 1, 5, and 10% nanoclay composites.

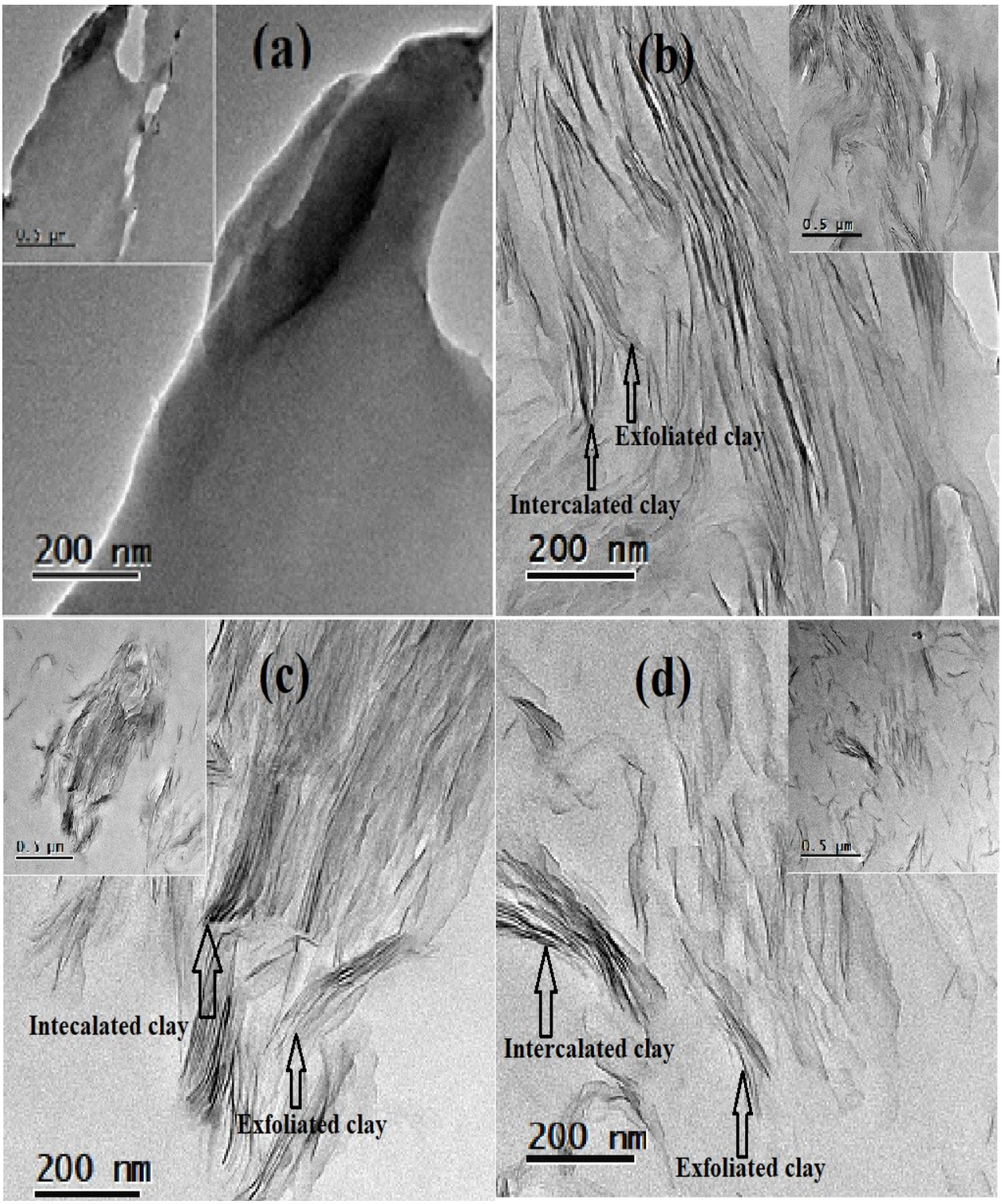

Figure 6.9: TEM images of (a) copolymer, (b) 1% nanoclay composite, (c) 5% nanoclay composite, and (d) 10% nanoclay composite.

6.3.7. TEM Analysis

TEM images gave additional information regarding the dispersion of nanoclay in the composites using 1, 5, and 10% nanoclay and copolymer as shown in Figure 6.9. In the TEM images, there is an embedded image with low magnification of 0.5 μm in the higher magnification of 200 nm (Figure 6.9). Intercalated and exfoliated clay sheets were observed in all the composites except for the copolymer where no nanoclay was added. More intercalated structures can be seen in 10% and 5% nanoclay composites as compared to 1% nanoclay composite where most of the nanoclays are exfoliated.

6.3.8. Moisture Uptake (MU)

The water molecules can be adsorbed directly by the polar groups on the surface of the composites. The moisture uptake behavior of neat polymer and nanoclay reinforced composites were carried out by placing the samples in a relative humidity (RH) of 98%. The moisture uptake behavior of neat and modified composites is shown in Figure 6.10. The rate of moisture uptake is high in the first few hours. The CNC-grafted and nanoclay reinforced composites absorbed more water as compared to the neat polymer without CNC and neat polymer with nanoclay reinforced composites. The neat homopolymer showed the least water absorption of 1% as compared to the composite (CNC-grafted polymer with 10% nanoclay addition), which absorbed 15.6% moisture. The lower water absorption in the case of neat polymer could be because of the nonpolar structure of neat polymer. In general, all the composites prepared from CNC-grafted monomer, including nanoclay reinforced composites absorbed water in the range of 15.6-17.1%, while the rest of the composites prepared from acrylated monomer without CNC absorbed less water, which was in the range of 1-14.4%. The higher absorption of water in the case of CNC-grafted composites could be attributed to the introduction of higher number of hydrophilic groups, which lead to higher uptake

of water molecules. The highest absorption of 17.1% in the case of neat homopolymer prepared from CNC-grafted lipid was due to hydrophilic hydroxyl groups, which lead to higher absorption of water uptake while in the case of monomer where there was no CNC-grafted, it absorbed the least water. Similarly, the presence of nanoclay (nonpolar in nature) in different proportions, i.e., 1, 5 and 10% in the composites and styrene copolymer composites resulted in less sorption of water molecules than the neat polymers.

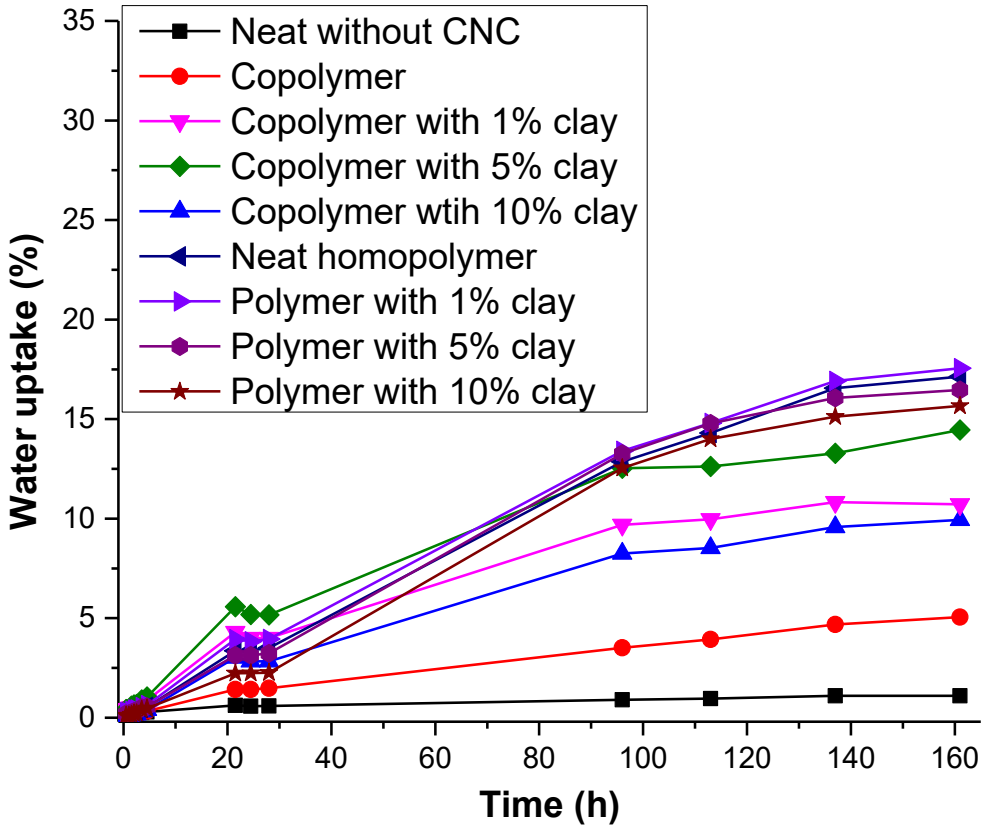

Figure 6.10. Moisture uptake behavior of homopolymer, copolymer with styrene and composites with 1, 5 and 10% nanoclay reinforcements during conditioning at RH of 98%.

6.4. Conclusions

A novel CNC-grafted acrylated monomer and the corresponding polymeric composites reinforced by different percentages of nanoclay were prepared from spent hen lipids and their chemical structures were characterized by FT-IR, ^{1}H NMR, and gel permeation chromatography (GPC). The monomer was synthesized in three steps, firstly via epoxidation of spent hen lipids, followed by grafting CNC and then acrylic groups onto spent hen lipid molecules. The bionanocomposites were prepared by *in situ* addition of modified nanoclay in 1, 5 and 10% proportions. Also, the nanocomposites were synthesized by copolymerization of spent hen lipid monomer and 30% styrene. The influence of experimental factors on thermomechanical properties of the cured bionanocomposites were evaluated to better understand structure–property relationships of the biomaterials and optimize experimental conditions. The obtained spent hen lipid monomer possessed a highly polymerizable C═C functionality, consequently resulting in rigid bioplastics. The synthesized cross-linked biomaterial from spent hen lipid provide an environmentally friendly material that can potentially be used in structural plastics.

6.5. References

Aerts, H.A., Jacobs, P.A. 2004. Epoxide yield determination of oils and fatty acid methyl esters using 1H NMR. *Journal of the American Oil Chemists' Society*, **81**(9), 841-846.

Andreeßen, C., Steinbüchel, A. 2019. Recent developments in non-biodegradable biopolymers: Precursors, production processes, and future perspectives. *Applied Microbiology and Biotechnology*, **103**(1), 143-157.

Arshad, M., Huang, L., Ullah, A. 2016. Lipid-derived monomer and corresponding bio-based nanocomposites. *Polymer International*, **65**(6), 653-660.

Bernhart, M., Fasina, O.O. 2009. Moisture effect on the storage, handling and flow properties of poultry litter. *Waste Management*, **29**(4), 1392-1398.

Bertolino, V., Cavallaro, G., Lazzara, G., Merli, M., Milioto, S., Parisi, F., Sciascia, L. 2016. Effect of the biopolymer charge and the nanoclay morphology on nanocomposite materials. *Industrial & Engineering Chemistry Research*, **55**(27), 7373-7380.

Brockhaus, S., Petersen, M., Kersten, W. 2016. A crossroads for bioplastics: exploring product developers' challenges to move beyond petroleum-based plastics. *Journal of Cleaner Production*, **127**, 84-95.

Cohen-Karni, D., Kovaliov, M., Ramelot, T., Konkolewicz, D., Graner, S., Averick, S. 2017. Grafting challenging monomers from proteins using aqueous ICAR ATRP under bio-relevant conditions. *Polymer Chemistry*, **8**(27), 3992-3998.

Dietrich, K., Dumont, M.-J., Del Rio, L.F., Orsat, V. 2017. Producing PHAs in the bioeconomy—Towards a sustainable bioplastic. *Sustainable Production and Consumption*, **9**, 58-70.

Forfang, K., Zimmermann, B., Kosa, G., Kohler, A., Shapaval, V. 2017. FTIR spectroscopy for evaluation and monitoring of lipid extraction efficiency for oleaginous fungi. *PloS one*, **12**(1), e0170611.

Garrison, T., Murawski, A., Quirino, R. 2016. Bio-based polymers with potential for biodegradability. *Polymers*, **8**(7), 262.

Giannakas, A.E., Leontiou, A.A. 2018. Montmorillonite composite materials and food packaging. *Composites Materials for Food Packaging*, 1-71.

He, M., Wang, X., Wang, Z., Chen, L., Lu, Y., Zhang, X., Li, M., Liu, Z., Zhang, Y., Xia, H. 2017. Biocompatible and biodegradable bioplastics constructed from chitin via a “green” pathway for bone repair. *ACS Sustainable Chemistry & Engineering*, **5**(10), 9126-9135.

Hong, H., Roy, B.C., Chalamaiah, M., Bruce, H.L., Wu, J. 2018. Pretreatment with formic acid enhances the production of small peptides from highly cross-linked collagen of spent hens. *Food Chemistry*, **258**, 174-180.

Jambeck, J.R., Geyer, R., Wilcox, C., Siegler, T.R., Perryman, M., Andrady, A., Narayan, R., Law, K.L. 2015. Plastic waste inputs from land into the ocean. *Science*, **347**(6223), 768-771.

Jiang, Y., Ding, D., Zhao, S., Zhu, H., Kenttämaa, H.I., Abu-Omar, M.M. 2018. Renewable thermoset polymers based on lignin and carbohydrate derived monomers. *Green Chemistry*, **20**(5), 1131-1138.

Jose, T., George, S.C., Maria, H.J., Wilson, R., Thomas, S. 2014. Effect of bentonite clay on the mechanical, thermal, and pervaporation performance of the poly (vinyl alcohol) nanocomposite membranes. *Industrial & Engineering Chemistry Research*, **53**(43), 16820-16831.

Khanra, S., Mondal, M., Halder, G., Tiwari, O., Gayen, K., Bhowmick, T.K. 2018. Downstream processing of microalgae for pigments, protein and carbohydrate in industrial application: A review. *Food and Bioproducts Processing*, **110**, 60-84.

Kondaiah, N., Panda, B. 1992. Processing and utilization of spent hens. *World's Poultry Science Journal*, **48**(3), 255-268.

Lambert, S., Wagner, M. 2017. Environmental performance of bio-based and biodegradable plastics: the road ahead. *Chemical Society Reviews*, **46**(22), 6855-6871.

Makaremi, M., Pasbakhsh, P., Cavallaro, G., Lazzara, G., Aw, Y.K., Lee, S.M., Milioto, S. 2017. Effect of morphology and size of halloysite nanotubes on functional pectin bionanocomposites for food packaging applications. *ACS Applied Materials & Interfaces*, **9**(20), 17476-17488.

Malinconico, M. 2017. *Soil degradable bioplastics for a sustainable modern agriculture*. Springer, Verlag GmbH Germany.

Mauck, S.C., Wang, S., Ding, W., Rohde, B.J., Fortune, C.K., Yang, G., Ahn, S.-K., Robertson, M.L. 2016. Biorenewable tough blends of polylactide and acrylated epoxidized soybean oil compatibilized by a polylactide star polymer. *Macromolecules*, **49**(5), 1605-1615.

Miller, S.A. 2013. Sustainable polymers: opportunities for the next decade, *ACS Macro Lett.*, **2**(6), 550-554.

Mohanty, A.K., Vivekanandhan, S., Pin, J.-M., Misra, M. 2018. Composites from renewable and sustainable resources: Challenges and innovations. *Science*, **362**(6414), 536-542.

Mousa, M.H., Dong, Y., Davies, I.J. 2016. Recent advances in bionanocomposites: Preparation, properties, and applications. *International Journal of Polymeric Materials and Polymeric Biomaterials*, **65**(5), 225-254.

Olkiewicz, M., Caporgno, M.P., Fortuny, A., Stüber, F., Fabregat, A., Font, J., Bengoa, C. 2014. Direct liquid–liquid extraction of lipid from municipal sewage sludge for biodiesel production. *Fuel Processing Technology*, **128**, 331-338.

Papanikolaou, S., Dimou, A., Fakas, S., Diamantopoulou, P., Philippoussis, A., Galiotou-Panayotou, M., Aggelis, G. 2011. Biotechnological conversion of waste cooking olive oil into lipid-rich biomass using Aspergillus and Penicillium strains. *Journal of Applied Microbiology*, **110**(5), 1138-1150.

Paul, D., Robeson, L.M. 2008a. Polymer nanotechnology: nanocomposites. *Polymer*, **49**(15), 3187-3204.

Qi, X., Zhang, Y., Chang, C., Luo, X., Li, Y. 2018. Thermal, mechanical, and morphological properties of rigid crude glycerol-based polyurethane foams reinforced with nanoclay and

microcrystalline cellulose. *European Journal of Lipid Science and Technology*, **120**(5), 1700413.

Ray, S.S., Bousmina, M. 2005. Biodegradable polymers and their layered silicate nanocomposites: in greening the 21st century materials world. *Progress in Materials Science*, **50**(8), 962-1079.

Sahmani, S., Shahali, M., Khandan, A., Saber-Samandari, S., Aghdam, M. 2018. Analytical and experimental analyses for mechanical and biological characteristics of novel nanoclay bio-nanocomposite scaffolds fabricated via space holder technique. *Applied Clay Science*, **165**, 112-123.

Salimon, J., Abdullah, B.M., Salih, N. 2011. Hydrolysis optimization and characterization study of preparing fatty acids from Jatropha curcas seed oil. *Chemistry Central Journal*, **5**(1), 67.

Schneiderman, D.K., Hillmyer, M.A. 2017. 50th anniversary perspective: There is a great future in sustainable polymers. *Macromolecules*, **50**(10), 3733-3749.

Souza, V.G.L., Fernando, A.L. 2016. Nanoparticles in food packaging: Biodegradability and potential migration to food—A review. *Food Packaging and Shelf Life*, **8**, 63-70.

Spurr, A.R. 1969. A low-viscosity epoxy resin embedding medium for electron microscopy. *Journal of Ultrastructure Research*, **26**(1-2), 31-43.

Tactacan, G.B., Guenter, W., Lewis, N.J., Rodriguez-Lecompte, J.C., House, J.D. 2009. Performance and welfare of laying hens in conventional and enriched cages. *Poultry Science*, **88**(4), 698-707.

Tuck, C.O., Pérez, E., Horváth, I.T., Sheldon, R.A., Poliakoff, M. 2012. Valorization of biomass: deriving more value from waste. *Science*, **337**(6095), 695-699.

Vlachos, N., Skopelitis, Y., Psaroudaki, M., Konstantinidou, V., Chatzilazarou, A., Tegou, E. 2006. Applications of Fourier transform-infrared spectroscopy to edible oils. *Analytica Chimica Acta*, **573**, 459-465.

Wang, H., Wu, J., Betti, M. 2013. Chemical, rheological and surface morphologic characterisation of spent hen proteins extracted by pH-shift processing with or without the presence of cryoprotectants. *Food Chemistry*, **139**(1), 710-719.

Wróblewska-Krepsztul, J., Rydzkowski, T., Borowski, G., Szczypiński, M., Klepka, T., Thakur, V.K. 2018. Recent progress in biodegradable polymers and nanocomposite-based packaging materials for sustainable environment. *International Journal of Polymer Analysis and Characterization*, **23**(4), 383-395.

Wu, S., Baskin, T.I., Gallagher, K.L. 2012. Mechanical fixation techniques for processing and orienting delicate samples, such as the root of *Arabidopsis thaliana*, for light or electron microscopy. *Nature Protocols*, **7**(6), 1113.

Yu, W., Field, C.J., Wu, J. 2018. Purification and identification of anti-inflammatory peptides from spent hen muscle proteins hydrolysate. *Food Chemistry*, **253**, 101-107.

Zhang, C., Garrison, T.F., Madbouly, S.A., Kessler, M.R. 2017. Recent advances in vegetable oil-based polymers and their composites. *Progress in Polymer Science*, **71**, 91-143.

Zhu, Y., Romain, C., Williams, C.K. 2016. Sustainable polymers from renewable resources. *Nature*, **540**(7633), 354.

Zubair, M., Wu, J., Ullah, A. 2019. Hybrid bionanocomposites from spent hen proteins. *ACS Omega*, **4**(2), 3772-3781.

Chapter 7-CONCLUSIONS AND RECOMMENDATIONS

7.1 Summary and conclusions

The spent hen is an untapped biomass source of lipid for producing a variety of lipid-derived materials. Approximately, over 2.6 billion spent hens are produced every year around the world and most of them are disposed of in landfills. Two main challenges associated with using this huge bioresource were targeted in this PhD research, first the extraction of lipid from spent hens using environmentally friendly techniques and second, value addition to extracted lipids in the form of bionanocomposite production. For the extraction of lipid, environmentally friendly technologies were used, i.e., microwave-assisted, and supercritical CO_2 (SC-CO_2) extraction and then the extracted lipids were converted to bionanocomposites using different approaches, i.e., epoxidation, monomer synthesis, *in situ* nanoclay addition and CNC-grafted composite formation.

In the first study (Chapter 3), the spent hen lipids were rapidly extracted using microwaves. The effects of extraction parameters such as the solvent-to-feed ratio, extraction time, and temperature on lipid extraction yield were studied and observed to be significant. The optimal yield was obtained using 2 mL/g solvent-to-feed ratio for 10 min at 80 °C. To account for the low sample size, parametric bootstrapping was used with a replacement approach, and data in all combinations were bootstrapped up to 10,000 times, which showed a decrease in standard deviation and p-value with an increase in sample size. The fatty acid composition of lipids predominantly had oleic, linoleic, and palmitic acids.

In the second study (Chapter 4), SC-CO_2 extraction was used to extract the lipids. A range of pressures and temperatures were investigated for the maximum extraction of lipids from spent hen. Over 92% of lipids were recovered at 50 MPa and 70 °C. Furthermore, the extracted lipids were epoxidized. The epoxidation of lipids was completed in less than 20 min under solvent-free

conditions and epoxidation conversion rates were calculated, resulting in conversion rates of 59.8, 84.2 and 100% at 5, 10, and 20 min, respectively.

To compare the two lipid extraction technologies investigated, the microwave-assisted method was rapid with 10 times reduction in organic solvent use and no need to remove moisture from the feed material; however, an extra step was involved to recover the lipid by evaporation of solvents. While in the case of SC-CO_2 extraction, there was no use of organic solvent and the obtained lipids were clean, but an extra step of moisture removal from the feed material was required for efficient lipid recovery. Considering all these factors, it is necessary to perform energy and cost analysis before a choice can be made between the two extraction techniques.

The interesting findings were observed during fatty acid compositional analysis of microwave-assisted and SC-CO_2 extractions. In case of microwave extraction, the C18:1 and C18:2 were in the ranges of 43.9-47.7 and 18.1-22.3% respectively. While in case of supercritical CO_2 extraction, the ranges of C18:1 and C18:2 were 50.07-59.96 and 4.04-19.73% respectively. The possible reason could be, as in case of SC-CO_2 only the CO_2 was used in extraction without any other organic solvent which extracted more nonpolar lipids, while in case of microwave assisted extraction dichloromethane-methanol (2:1, v/v) were used.

In the third study (Chapter 5), the extracted lipid was used in monomer synthesis. The bulk polymerization of the spent hen derived monomer at different temperatures and times showed that the highest molecular weight polymer was obtained at 70 ˚C for 24 h. The *in situ* addition of different proportions of nanoclay during the polymer formation resulted in significant improvement in the thermal properties. Specifically, the fire retardancy of the nanoclay reinforced films was substantially improved to double as compared to the homopolymer without the addition

of nanoclay, which suggests that the synthesized composites can be used in indoor applications such as switchboards where flame retardancy is a desirable attribute.

In the fourth study (Chapter 6), a novel CNC-grafted acrylated monomer and the corresponding polymeric composites reinforced by different percentages of nanoclay addition were prepared from the extracted lipid and their chemical structures were characterized by FT-IR, ^{1}H NMR, and gel permeation chromatography (GPC). The monomer was synthesized in three steps, firstly via epoxidation of spent hen lipids, followed by grafting CNC and subsequently acrylic groups onto the triacylglycerol molecules. The bionanocomposites were prepared by *in situ* addition of modified nanoclay at levels of 1, 5 and 10% (wt.%). As well, the nanocomposites were also synthesized by copolymerization of spent hen lipid monomer and 30% styrene. The synthesized cross-linked biomaterial from spent hen lipids provide a sustainable material for potential use in structural plastics.

In conclusion, it was demonstrated that the extracted lipids are suitable for biomaterial production. The rapid extraction of lipids from spent hen provides a unique and promising opportunity to produce lipid-based materials in subsequent stages of production. The environmentally friendly extraction of lipids and their subsequent conversion into epoxides under solvent-free conditions provide a promising green approach for the production of lipid-derived bio-epoxy materials from an unutilized sustainable resource. The spent hen lipids were successfully modified to nanoclay composites. The novelty in the approaches developed in this PhD research is that while preparing the bionanocomposites no extra step is required to purify the TAGs for monomer and subsequent composite synthesis, because all of the unreacted residual traces and other lipid components present in the extracts were removed during monomer purification using chromatography. Furthermore, the findings contribute to larger initiatives

towards complete utilization of spent hens where the protein-enriched residue after lipid extraction can also be used to prepare protein-derived hybrid bionanocomposites (Zubair et al., 2019). As well, keratin protein from feather can be used to prepare biosorbents for wastewater treatment and removal of heavy metals (Donner et al., 2019; Kaur et al., 2018; Khosa et al., 2013).

7.2. Recommendations

Spent hen lipids show great potential for use in different valuable applications. In the future, it would be worthwhile to study and enhance the thermal and mechanical properties of the lipid-derived composites because in general the bio-based composites show relatively poor properties as compared to their petroleum-based plastic competitors (Peelman et al., 2013). Firstly, cost analysis of both of the lipid extraction techniques used in this research, i.e., microwave-assisted, and SC-CO_2 extraction is recommended and then on the basis of economic efficiency, the feasible process can be scaled up for lipid production in the industry.

As the epoxidation reactions are exothermic, there is a need to cool and control the temperature variations in the reactor. Different approaches can be evaluated by increasing agitation rate, by adding additional heat exchange jacket, or by suspending a fluid around the reaction vessel that will boil at the required reaction temperature and the vapours could be condensed again and returned into the fluid. In addition, use of enzymes to catalyze this reaction at lower temperatures can be evaluated. Secondly, to improve the thermal and mechanical properties of the bionanocomposites different methods can be used. The controlled synthesis of polymer using controlled polymerization such as reversible addition fragmentation chain transfer (RAFT) polymerization to selectively polymerize terminal double bonds and then perform post polymerization modification to use internal double bonds in the unsaturated fatty acid chain can improve thermal and mechanical properties. Further, addition of small amount of copolymerizable

nanoparticles such as nano-POSS could substantially improve the final product properties. To get better homogenization of the particles, ultrasound technology is recommended.

The presence of nanofillers in the polymer matrix leads to significant modifications of the charge transport, and charge distribution due to the interfacial effects. Therefore, understanding surface charge distribution in nanocomposites is an important parameter for the design of nanocomposite materials with desired properties and the use of electrostatic voltmeter and Kelvin probe is recommended for that purpose.

Apparent surface color and transmittance of the composite film is greatly influenced by the type and amount of nanoparticle added, which can be measured for required properties by Chroma meter and spectrophotometer.

In composite materials, stresses are generated due to swelling with moisture uptake, so to study the water uptake behaviour, Fickian and non-Fickian analysis is suggested. Furthermore, it is recommended to perform biodegradability tests on the synthesized composites.

To prepare food packaging materials from spent hen lipids, it is recommended to comprehensively study their barrier properties as well as their thermal and mechanical properties for their long-term stability under the conditions of use. Furthermore, the prepared composite materials were rigid and brittle, so it is recommended to use plasticizers. The properties of nanocomposites are mainly dominated by the interfacial interactions between nanoclay and polymer, so it will be worthwhile to analyse these properties by combining broadband dielectric spectroscopy with small-angle X-ray scattering.

Bibliography:

Abraham, E., Kam, D., Nevo, Y., Slattegard, R., Rivkin, A., Lapidot, S., Shoseyov, O., 2016. Highly modified cellulose nanocrystals and formation of epoxy-nanocrystalline cellulose (CNC) nanocomposites. *ACS applied materials & interfaces* **8**(41), 28086-28095.

Adhvaryu, A., Erhan, S., 2002. Epoxidized soybean oil as a potential source of high-temperature lubricants. *Industrial Crops and Products* **15**(3), 247-254.

Aerts, H.A., Jacobs, P.A., 2004. Epoxide yield determination of oils and fatty acid methyl esters using 1H NMR. *Journal of the American Oil Chemists' Society* **81**(9), 841-846.

Aguilera, A.F., Tolvanen, P., Heredia, S., Muñoz, M.G.l., Samson, T., Oger, A., Verove, A., Eränen, K., Leveneur, S., Mikkola, J.-P., 2018. Epoxidation of Fatty Acids and Vegetable Oils Assisted by Microwaves Catalyzed by a Cation Exchange Resin. *Industrial & Engineering Chemistry Research* **57**(11), 3876-3886.

Ahn, B.K., Kraft, S., Wang, D., Sun, X.S., 2011. Thermally stable, transparent, pressure-sensitive adhesives from epoxidized and dihydroxyl soybean oil. *Biomacromolecules* **12**(5), 1839-1843.

Aigbodion, A., Okieimen, F., Obazee, E., Bakare, I., 2003. Utilisation of maleinized rubber seed oil and its alkyd resin as binders in water-borne coatings. *Progress in Organic Coatings* **46**(1), 28-31.

Alagi, P., Choi, Y.J., Seog, J., Hong, S.C., 2016. Efficient and quantitative chemical transformation of vegetable oils to polyols through a thiol-ene reaction for thermoplastic polyurethanes. *Industrial Crops and Products* **87**, 78-88.

Alam, M., Akram, D., Sharmin, E., Zafar, F., Ahmad, S., 2014. Vegetable oil based eco-friendly coating materials: A review article. *Arabian Journal of Chemistry* **7**(4), 469-479.

Álvarez-Díaz, P.D., Ruiz, J., Arbib, Z., Barragán, J., Garrido-Pérez, M.C., Perales, J.A., 2017. Freshwater microalgae selection for simultaneous wastewater nutrient removal and lipid production. *Algal Research* **24**(Part B), 477-485.

Amarni, F., Kadi, H., 2010. Kinetics study of microwave-assisted solvent extraction of oil from olive cake using hexane: Comparison with the conventional extraction. *Innovative Food Science & Emerging Technologies* **11**(2), 322-327.

Ammala, A., 2013. Biodegradable polymers as encapsulation materials for cosmetics and personal care markets. *International Journal of Cosmetic Science* **35**(2), 113-124.

Andreeßen, C., Steinbüchel, A., 2019. Recent developments in non-biodegradable biopolymers: Precursors, production processes, and future perspectives. *Applied Microbiology and Biotechnology* **103**(1), 143-157.

Aris, A., Shojaei, A., Bagheri, R., 2015. Cure kinetics of nanodiamond-filled epoxy resin: influence of nanodiamond surface functionality. *Industrial & Engineering Chemistry Research* **54**(36), 8954-8962.

Arrieta, M.P., Samper, M., Jiménez-López, M., Aldas, M., López, J., 2017. Combined effect of linseed oil and gum rosin as natural additives for PVC. *Industrial Crops and Products* **99**, 196-204.

Arshad, M., Huang, L., Ullah, A., 2016a. Lipid-derived monomer and corresponding bio-based nanocomposites. *Polymer International* **65**(6), 653-660.

Arshad, M., Kaur, M., Ullah, A., 2016b. Green biocomposites from nanoengineered hybrid natural fiber and biopolymer. *ACS Sustainable Chemistry & Engineering* **4**(3), 1785-1793.

Arshad, M., Saied, S., Ullah, A., 2014. PEG-lipid telechelics incorporating fatty acids from canola oil: synthesis, characterization and solution self-assembly. *RSC Advances* **4**(50), 26439-26446.

Auvergne, R., Caillol, S., David, G., Boutevin, B., Pascault, J.-P., 2013. Biobased thermosetting epoxy: present and future. *Chemical Reviews* **114**(2), 1082-1115.

Barnwal, B., Sharma, M., 2005. Prospects of biodiesel production from vegetable oils in India. *Renewable and Sustainable Energy Reviews* **9**(4), 363-378.

Bazou, D., Behan, G., Reid, C., Boland, J., Zhang, H., 2011. Imaging of human colon cancer cells using He-Ion scanning microscopy. *Journal of Microscopy* **242**(3), 290-294.

Beardmore, P., 1986. Composite structures for automobiles. *Composite Structures* **5**(3), 163-176.

Benaniba, M., Belhaneche-Bensemra, N., Gelbard, G., 2003. Stabilization of PVC by epoxidized sunflower oil in the presence of zinc and calcium stearates. *Polymer Degradation and Stability* 82(2), 245-249.

Bernhart, M., Fasina, O.O., 2009. Moisture effect on the storage, handling and flow properties of poultry litter. *Waste Management* **29**(4), 1392-1398.

Bertolino, V., Cavallaro, G., Lazzara, G., Merli, M., Milioto, S., Parisi, F., Sciascia, L., 2016. Effect of the biopolymer charge and the nanoclay morphology on nanocomposite materials. *Industrial & Engineering Chemistry Research* **55**(27), 7373-7380.

Bharti, S.K., Roy, R., 2012. Quantitative 1H NMR spectroscopy. *TrAC Trends in Analytical Chemistry* **35**, 5-26.

Binnig, G., Quate, C.F., Gerber, C., 1986. Atomic force microscope. *Physical review letters* **56**(9), 930.

Binnington, D.S., 1932. Improved soxhlet extraction apparatus. *Industrial & Engineering Chemistry Analytical Edition* **4**(1), 125-126.

Biswas, A., Sharma, B., Willett, J., Erhan, S., Cheng, H., 2008. Soybean oil as a renewable feedstock for nitrogen-containing derivatives. *Energy & Environmental Science* **1**(6), 639-644.

Bligh, E.G., Dyer, W.J., 1959. A rapid method of total lipid extraction and purification. *Canadian Journal of Biochemistry and Physiology* **37**(8), 911-917.

Boontawee, H., Nakason, C., Kaesaman, A., Thitithammawong, A., Chewchanwuttiwong, S., 2017. Benzyl Esters of Vegetable Oils as Processing Oil in Carbon Black–Filled SBR Compounding: Chemical Modification, Characterization, and Performance. *Advances in Polymer Technology* **36**(3), 320-330.

Bozan, B., Temelli, F., 2002. Supercritical CO2 extraction of flaxseed. *Journal of the American Oil Chemists' Society* **79**(3), 231-235.

Brennecke, J.F., 1997. Molecular trees for green chemistry. *Nature* 389, 333.

Brockhaus, S., Petersen, M., Kersten, W., 2016. A crossroads for bioplastics: exploring product developers' challenges to move beyond petroleum-based plastics. *Journal of Cleaner Production* **127**, 84-95.

Brunner, G., 2013. Gas extraction: an introduction to fundamentals of supercritical fluids and the application to separation processes. Springer Science & Business Media.

Bryant, J., Clausen, T., Reichardt, P., McCarthy, M., Werner, R., 1987. Effect of nitrogen fertilization upon the secondary chemistry and nutritional value of quaking aspen (Populus tremuloides Michx.) leaves for the large aspen tortrix (Choristoneura conflictana (Walker)). *Oecologia* **73**(4), 513-517.

Burch, M.J., Ievlev, A.V., Mahady, K., Hysmith, H., Rack, P.D., Belianinov, A., Ovchinnikova, O.S., 2017. Helium Ion Microscopy for Imaging and Quantifying Porosity at the Nanoscale. *Analytical chemistry* **90**(2), 1370-1375.

Byrne, J.M., Schmidt, M., Gauger, T., Bryce, C., Kappler, A., 2018. Imaging organic–mineral aggregates formed by Fe (II)-oxidizing bacteria using Helium ion microscopy. *Environmental Science & Technology Letters* **5**(4), 209-213.

Camel, V., 2000. Microwave-assisted solvent extraction of environmental samples. *TrAC Trends in Analytical Chemistry* **19**(4), 229-248.

Campanella, A., Rustoy, E., Baldessari, A., Baltanás, M.A., 2010. Lubricants from chemically modified vegetable oils. *Bioresource Technology* **101**(1), 245-254.

Carrapiso, A.I., García, C., 2000. Development in lipid analysis: some new extraction techniques and in situ transesterification. *Lipids* **35**(11), 1167-1177.

Chen, G., Guan, X., Xu, R., Tian, J., He, M., Shen, W., Yang, J., 2016. Synthesis and characterization of UV-curable castor oil-based polyfunctional polyurethane acrylate via photo-click chemistry and isocyanate polyurethane reaction. *Progress in Organic Coatings* **93**, 11-16.

Chen, L., Wang, C., Wang, W., Wei, J., 2013. Optimal conditions of different flocculation methods for harvesting Scenedesmus sp. cultivated in an open-pond system. *Bioresource Technology* **133**(Supplement C), 9-15.

Cho, H.G., Park, S.Y., Jegal, J., Song, B.K., Kim, H.J., 2010. Preparation and characterization of acrylic polymers based on a novel acrylic monomer produced from vegetable oil. *Journal of Applied Polymer Science* **116**(2), 736-742.

Cho, S.-C., Choi, W.-Y., Oh, S.-H., Lee, C.-G., Seo, Y.-C., Kim, J.-S., Song, C.-H., Kim, G.-V., Lee, S.-Y., Kang, D.-H., 2012. Enhancement of lipid extraction from marine microalga, Scenedesmus associated with high-pressure homogenization process. *BioMed Research International* 2012.

Cohen-Karni, D., Kovaliov, M., Ramelot, T., Konkolewicz, D., Graner, S., Averick, S., 2017. Grafting challenging monomers from proteins using aqueous ICAR ATRP under bio-relevant conditions. *Polymer Chemistry* **8**(27), 3992-3998.

Cravotto, G., Boffa, L., Mantegna, S., Perego, P., Avogadro, M., Cintas, P., 2008. Improved extraction of vegetable oils under high-intensity ultrasound and/or microwaves. *Ultrasonics Sonochemistry* **15**(5), 898-902.

Da Silva, T.L., Gouveia, L., Reis, A., 2014. Integrated microbial processes for biofuels and high value-added products: the way to improve the cost effectiveness of biofuel production. *Applied Microbiology and Biotechnology* **98**(3), 1043-1053.

De Castro, M.L., Priego-Capote, F., 2010. Soxhlet extraction: Past and present panacea. *Journal of Chromatography A* 1217(16), 2383-2389.

Deopura, B., Padaki, N., 2015. Synthetic textile fibres: polyamide, polyester and aramid fibres, Textiles and Fashion. Elsevier, pp. 97-114.

Desroches, M., Escouvois, M., Auvergne, R., Caillol, S., Boutevin, B., 2012. From vegetable oils to polyurethanes: synthetic routes to polyols and main industrial products. *Polymer Reviews* **52**(1), 38-79.

Devaraj, K., Aathika, S., Mani, Y., Thanarasu, A., Periyasamy, K., Periyaraman, P., Velayutham, K., Subramanian, S., 2018. Experimental investigation on cleaner process of enhanced fat-

oil extraction from alkaline leather fleshing waste. *Journal of Cleaner Production* **175**, 1-7.

Dietrich, K., Dumont, M.-J., Del Rio, L.F., Orsat, V., 2017. Producing PHAs in the bioeconomy—Towards a sustainable bioplastic. *Sustainable Production and Consumption* **9**, 58-70.

Do Valle, C.P., Rodrigues, J.S., Fechine, L.M.U.D., Cunha, A.P., Malveira, J.Q., Luna, F.M.T., Ricardo, N.M.P.S., 2018. Chemical modification of Tilapia oil for biolubricant applications. *Journal of Cleaner Production* **191**, 158-166.

Donner, M.W., Arshad, M., Ullah, A., Siddique, T., 2019. Unravelled keratin-derived biopolymers as novel biosorbents for the simultaneous removal of multiple trace metals from industrial wastewater. *Science of The Total Environment* **647**, 1539-1546.

Eskilsson, C.S., Björklund, E., 2000. Analytical-scale microwave-assisted extraction. *Journal of chromatography A* **902**(1), 227-250.

Espana, J., Sánchez-Nacher, L., Boronat, T., Fombuena, V., Balart, R., 2012. Properties of biobased epoxy resins from epoxidized soybean oil (ESBO) cured with maleic anhydride (MA). *Journal of the American Oil Chemists' Society* **89**(11), 2067-2075.

Fang, H., Zhao, C., Kong, Q., Zou, Z., Chen, N., 2016. Comprehensive utilization and conversion of lignocellulosic biomass for the production of long chain α,ω-dicarboxylic acids. *Energy* **116**(Part 1), 177-189.

Fauziah, S., Liyana, I., Agamuthu, P., 2015. Plastic debris in the coastal environment: The invincible threat? Abundance of buried plastic debris on Malaysian beaches. *Waste Management & Research* **33**(9), 812-821.

Feng, Y., Liang, H., Yang, Z., Yuan, T., Luo, Y., Li, P., Yang, Z., Zhang, C., 2017. A Solvent-Free and Scalable Method To Prepare Soybean-Oil-Based Polyols by Thiol–Ene Photo-

Click Reaction and Biobased Polyurethanes Therefrom. *ACS Sustainable Chemistry & Engineering* **5**(8), 7365-7373.

Fernandes, F.C., Kirwan, K., Lehane, D., Coles, S.R., 2017. Epoxy resin blends and composites from waste vegetable oil. *European Polymer Journal* **89**, 449-460.

Floros, M., Hojabri, L., Abraham, E., Jose, J., Thomas, S., Pothan, L., Leao, A.L., Narine, S., 2012. Enhancement of thermal stability, strength and extensibility of lipid-based polyurethanes with cellulose-based nanofibers. *Polymer degradation and stability* **97**(10), 1970-1978.

Folch, J., Lees, M., Stanley, G.S., 1957. A simple method for the isolation and purification of total lipides from animal tissues. *Journal of biological chemistry* **226**(1), 497-509.

Forfang, K., Zimmermann, B., Kosa, G., Kohler, A., Shapaval, V., 2017. FTIR spectroscopy for evaluation and monitoring of lipid extraction efficiency for oleaginous fungi. PloS one **12**(1), e0170611.

Galià, M., de Espinosa, L.M., Ronda, J.C., Lligadas, G., Cádiz, V., 2010. Vegetable oil-based thermosetting polymers. *European Journal of Lipid Science and Technology* **112**(1), 87-96.

García-Ayuso, L.E., Luque de Castro, M.D., 2001. Employing focused microwaves to counteract conventional Soxhlet extraction drawbacks. *TrAC Trends in Analytical Chemistry* **20**(1), 28-34.

Garrison, T., Murawski, A., Quirino, R., 2016. Bio-based polymers with potential for biodegradability. *Polymers* **8**(7), 262.

Gerken, H.G., Donohoe, B., Knoshaug, E.P., 2013. Enzymatic cell wall degradation of Chlorellavulgaris and other microalgae for biofuels production. *Planta* **237**(1), 239-253.

Giannakas, A.E., Leontiou, A.A., 2018. Montmorillonite Composite Materials and Food Packaging. *Composites Materials for Food Packaging*, 1-71.

Goodman, S.H., Hanna, D., 2014. Handbook of thermoset plastics, Elsevier, San Diego, CA , USA.

Greco, A., Ferrari, F., Maffezzoli, A., 2016. Effect of the epoxidation yield of a cardanol derivative on the plasticization and durability of soft PVC. *Polymer Degradation and Stability* **134**, 220-226.

Güçlü-Üstündağ, Ö., Temelli, F., 2006. Solubility behavior of ternary systems of lipids in supercritical carbon dioxide. *The Journal of Supercritical Fluids* **38**(3), 275-288.

Gupta, R.N., Harsha, A., 2017. Antiwear and extreme pressure performance of castor oil with nano-additives. Proceedings of the Institution of Mechanical Engineers, Part J: *Journal of Engineering Tribology*, **232**(9), 1055-67.

Halsey, L.G., Curran-Everett, D., Vowler, S.L., Drummond, G.B., 2015. The fickle P value generates irreproducible results. *Nature Methods* 12, 179.

Haq, M., Burgueño, R., Mohanty, A.K., Misra, M., 2008. Hybrid bio-based composites from blends of unsaturated polyester and soybean oil reinforced with nanoclay and natural fibers. *Composites Science and Technology* **68**(15-16), 3344-3351.

He, M., Wang, X., Wang, Z., Chen, L., Lu, Y., Zhang, X., Li, M., Liu, Z., Zhang, Y., Xia, H., 2017. Biocompatible and biodegradable bioplastics constructed from chitin via a “green” pathway for bone repair. *ACS Sustainable Chemistry & Engineering* **5**(10), 9126-9135.

Hong, H., Roy, B.C., Chalamaiah, M., Bruce, H.L., Wu, J., 2018. Pretreatment with formic acid enhances the production of small peptides from highly cross-linked collagen of spent hens. *Food Chemistry* **258**, 174-180.

Horwitz, W., Latimer, G.W., 2005. Official methods of analysis of AOAC International. AOAC International, Gaithersburg, Md.

Huang, K., Zhang, P., Zhang, J., Li, S., Li, M., Xia, J., Zhou, Y., 2013. Preparation of biobased epoxies using tung oil fatty acid-derived C21 diacid and C22 triacid and study of epoxy properties. *Green Chemistry* **15**(9), 2466-2475.

Indumathi, M., Rajarajeswari, G., 2019. Mahua oil-based polyurethane/chitosan/nano ZnO composite films for biodegradable food packaging applications. *International journal of biological macromolecules* **124**, 163-174.

Jambeck, J.R., Geyer, R., Wilcox, C., Siegler, T.R., Perryman, M., Andrady, A., Narayan, R., Law, K.L., 2015. Plastic waste inputs from land into the ocean. *Science* **347**(6223), 768-771.

Jensen, S.K., 2008. Improved Bligh and Dyer extraction procedure. *Lipid Technology* **20**(12), 280-281.

Jia, P., Ma, Y., Xia, H., Zheng, M., Feng, G., Hu, L., Zhang, M., Zhou, Y., 2018. Clean synthesis of epoxidized Tung oil derivatives via phase transfer catalyst and thiol–ene reaction: A Detailed Study. *ACS Sustainable Chemistry & Engineering* **6**(11), 13983-13994.

Jiang, Y., Ding, D., Zhao, S., Zhu, H., Kenttämaa, H.I., Abu-Omar, M.M., 2018. Renewable thermoset polymers based on lignin and carbohydrate derived monomers. *Green Chemistry* **20**(5), 1131-1138.

Jin, L., Zeng, H., Ullah, A., 2017. Rapid copolymerization of canola oil derived epoxide monomers with anhydrides and carbon dioxide (CO2). *Polymer Chemistry* **8**(41), 6431-6442.

Joens, M.S., Huynh, C., Kasuboski, J.M., Ferranti, D., Sigal, Y.J., Zeitvogel, F., Obst, M., Burkhardt, C.J., Curran, K.P., Chalasani, S.H., 2013. Helium Ion Microscopy (HIM) for the imaging of biological samples at sub-nanometer resolution. *Scientific reports* **3**, 3514.

John, J., Bhattacharya, M., Turner, R.B., 2002. Characterization of polyurethane foams from soybean oil. *Journal of Applied Polymer Science* **86**(12), 3097-3107.

Jose, T., George, S.C., Maria, H.J., Wilson, R., Thomas, S., 2014. Effect of bentonite clay on the mechanical, thermal, and pervaporation performance of the poly (vinyl alcohol) nanocomposite membranes. *Industrial & Engineering Chemistry Research* **53**(43), 16820-16831.

Kamarudin, S.H., Abdullah, L.C., Aung, M.M., Ratnam, C.T., Jusoh, E.R., 2018. A study of mechanical and morphological properties of PLA based biocomposites prepared with EJO vegetable oil based plasticiser and kenaf fibres. *Materials Research Express,* **368**, 12011.

Karlovic, D., Sovilj, M., Turkulov, J., 1992. Kinetics of oil extraction from corn germ. *Journal of the American Oil Chemists' Society* **69**(5), 471-476.

Katouzian, I., Faridi Esfanjani, A., Jafari, S.M., Akhavan, S., 2017. Formulation and application of a new generation of lipid nano-carriers for the food bioactive ingredients. *Trends in Food Science & Technology* **68**(Supplement C), 14-25.

Kaur, M., Arshad, M., Ullah, A., 2018. In-situ nanoreinforced green bionanomaterials from natural keratin and montmorillonite (MMT)/cellulose nanocrystals (CNC). *ACS Sustainable Chemistry & Engineering* **6**(2), 1977-1987.

Kawashima, H., Kijima, M., 2018. Selective Synthesis of Botryococcene Pentaepoxide-The Chemical Modifications of the Algal Biomass Oil. *ChemistrySelect* **3**(33), 9589-9591.

Kersey, J.H., Waldroup, P.W., 1998. Utilization of spent hen meal in diets for broiler chickens. *Poultry Science* **77**(9), 1377-1387.

Khanra, S., Mondal, M., Halder, G., Tiwari, O., Gayen, K., Bhowmick, T.K., 2018. Downstream processing of microalgae for pigments, protein and carbohydrate in industrial application: A review. *Food and Bioproducts Processing* **110**, 60-84.

Khosa, M.A., Wu, J., Ullah, A., 2013. Chemical modification, characterization, and application of chicken feathers as novel biosorbents. *Rsc Advances* **3**(43), 20800-20810.

Khundamri, N., Aouf, C., Fulcrand, H., Dubreucq, E., Tanrattanakul, V., 2019. Bio-based flexible epoxy foam synthesized from epoxidized soybean oil and epoxidized mangosteen tannin. *Industrial Crops and Products* **128**, 556-565.

King, J.W., Johnson, J.H., Friedrich, J.P., 1989. Extraction of fat tissue from meat products with supercritical carbon dioxide. *Journal of Agricultural and Food Chemistry* **37**(4), 951-954.

Kondaiah, N., Panda, B., 2007. Processing and utilization of spent hens. *World's Poultry Science Journal* **48**(3), 255-268.

Kumar, M., Ghosh, P., Khosla, K., Thakur, I.S., 2016. Biodiesel production from municipal secondary sludge. *Bioresource Technology* **216**(Supplement C), 165-171.

Lagaron, J.M., Lopez-Rubio, A., 2011. Nanotechnology for bioplastics: opportunities, challenges and strategies. *Trends in food science & technology* **22**(11), 611-617.

Lambert, S., Wagner, M., 2017. Environmental performance of bio-based and biodegradable plastics: the road ahead. *Chemical Society Reviews* **46**(22), 6855-6871.

Lee, I., Han, J.-I., 2015. Simultaneous treatment (cell disruption and lipid extraction) of wet microalgae using hydrodynamic cavitation for enhancing the lipid yield. *Bioresource technology* **186**, 246-251.

Leitner, W., 2000. Designed to dissolve. *Nature* **405**, 129.

Li, H., Pordesimo, L., Weiss, J., 2004. High intensity ultrasound-assisted extraction of oil from soybeans. *Food Research International* **37**(7), 731-738.

Li, P., Ma, S., Dai, J., Liu, X., Jiang, Y., Wang, S., Wei, J., Chen, J., Zhu, J., 2016. Itaconic acid as a green alternative to acrylic acid for producing a soybean oil-based thermoset: synthesis and properties. *ACS Sustainable Chemistry & Engineering* **5**(1), 1228-1236.

Liu, C., Shang, Q., Jia, P., Dai, Y., Zhou, Y., Liu, Z., 2016. Tung oil-based unsaturated co-ester macromonomer for thermosetting polymers: synergetic synthesis and copolymerization with styrene. *ACS Sustainable Chemistry & Engineering* **4**(6), 3437-3449.

Liu, W., Xie, T., Qiu, R., 2016. Biobased thermosets prepared from rigid isosorbide and flexible soybean oil derivatives. *ACS Sustainable Chemistry & Engineering* **5**(1), 774-783.

Lligadas, G., Ronda, J.C., Galià, M., Cádiz, V., 2006. Bionanocomposites from renewable resources: epoxidized linseed oil− polyhedral oligomeric silsesquioxanes hybrid materials. *Biomacromolecules* **7**(12), 3521-3526.

Loh, S.K., 2017. The potential of the Malaysian oil palm biomass as a renewable energy source. *Energy Conversion and Management* **141**, 285-298.

Loo, L., Maaten, B., Siirde, A., Pihu, T., Konist, A., 2015. Experimental analysis of the combustion characteristics of Estonian oil shale in air and oxy-fuel atmospheres. *Fuel Processing Technology* **134**(Supplement C), 317-324.

Luque de Castro, M.D., Castillo-Peinado, L.S., 2016. 3 - Microwave-Assisted Extraction of Food Components, Innovative Food Processing Technologies. Woodhead Publishing, pp. 57-110.

Makaremi, M., Pasbakhsh, P., Cavallaro, G., Lazzara, G., Aw, Y.K., Lee, S.M., Milioto, S., 2017. Effect of morphology and size of halloysite nanotubes on functional pectin

bionanocomposites for food packaging applications. *ACS applied materials & interfaces* **9**(20), 17476-17488.

Malinconico, M., 2017. Soil degradable bioplastics for a sustainable modern agriculture. Springer, Verlag GmbH Germany.

Mashhadi, F., Habibi, A., Varmira, K., 2018. Enzymatic production of green epoxides from fatty acids present in soapstock in a microchannel bioreactor. *Industrial Crops and Products* **113**, 324-334.

Mauck, S.C., Wang, S., Ding, W., Rohde, B.J., Fortune, C.K., Yang, G., Ahn, S.-K., Robertson, M.L., 2016. Biorenewable tough blends of polylactide and acrylated epoxidized soybean oil compatibilized by a polylactide star polymer. *Macromolecules* **49**(5), 1605-1615.

Maurin-Pasturel, G., Lemor, A., Robin, J.J., Lapinte, V., 2019. Preparation and spectroscopic characterization of Si-coated vegetable oils and their ppplication in *in situ* curing of hybrid coatings. *European Journal of Lipid Science and Technology* **121**(4), 1800231.

McMillan, J.R., Watson, I.A., Ali, M., Jaafar, W., 2013. Evaluation and comparison of algal cell disruption methods: Microwave, waterbath, blender, ultrasonic and laser treatment. *Applied Energy* **103**(Supplement C), 128-134.

Meier, M.A., 2019. Plant-oil-based polyamides and polyurethanes: Toward sustainable nitrogen-containing thermoplastic materials. *Macromolecular rapid communications*, **40***,* 1800524.

Meier, M.A., Metzger, J.O., Schubert, U.S., 2007. Plant oil renewable resources as green alternatives in polymer science. *Chemical Society Reviews* **36**(11), 1788-1802.

Mello, J.L.M., Souza, R.A., Paschoalin, G.C., Ferrari, F.B., Berton, M.P., Giampietro-Ganeco, A., Souza, P.A., Borba, H., 2017. Physical and chemical characteristics of spent hen breast meat aged for 7 days. *Animal Production Science* **57**(10), 2133-2140.

Meullemiestre, A., Breil, C., Abert-Vian, M., Chemat, F., 2016. Microwave, ultrasound, thermal treatments, and bead milling as intensification techniques for extraction of lipids from oleaginous Yarrowia lipolytica yeast for a biojetfuel application. *Bioresource Technology* **211**(Supplement C), 190-199.

Miao, S., Wang, P., Su, Z., Zhang, S., 2014. Vegetable-oil-based polymers as future polymeric biomaterials. *Acta biomaterialia* **10**(4), 1692-1704.

Migneco, F., Huang, Y.-C., Birla, R.K., Hollister, S.J., 2009. Poly (glycerol-dodecanoate), a biodegradable polyester for medical devices and tissue engineering scaffolds. *Biomaterials* **30**(33), 6479-6484.

Miller, S.A., 2013. Sustainable polymers: opportunities for the next decade. *ACS Macro Lett.*, **2**(6), 550-554.

Mohamed, H., Badran, B., Rabie, A., Morsi, S., 2014. Synthesis and characterization of aqueous (polyurethane/aromatic polyamide sulfone) copolymer dispersions from castor oil. *Progress in Organic Coatings* **77**(5), 965-974.

Mohanty, A.K., Vivekanandhan, S., Pin, J.-M., Misra, M., 2018. Composites from renewable and sustainable resources: Challenges and innovations. *Science* **362**(6414), 536-542.

Molina-Gutiérrez, S., Ladmiral, V., Bongiovanni, R., Caillol, S., Lacroix-Desmazes, P., 2019. Radical polymerization of biobased monomers in aqueous dispersed media. *Green Chemistry,* **21**, 36-53.

Mousa, M.H., Dong, Y., Davies, I.J., 2016. Recent advances in bionanocomposites: Preparation, properties, and applications. *International Journal of Polymeric Materials and Polymeric Biomaterials* **65**(5), 225-254.

Muise, I., Adams, M., Côté, R., Price, G., 2016. Attitudes to the recovery and recycling of agricultural plastics waste: A case study of Nova Scotia, Canada. Resources, *Conservation and Recycling* **109**, 137-145.

Mulakayala, N., Kumar, K.M., Rapolu, R.K., Kandagatla, B., Rao, P., Oruganti, S., Pal, M., 2012. Catalysis by Amberlite IR-120 resin: a rapid and green method for the synthesis of phenols from arylboronic acids under metal, ligand, and base-free conditions. *Tetrahedron Letters* **53**(45), 6004-6007.

Mulla, M., Ahmed, J., Al-Attar, H., Castro-Aguirre, E., Arfat, Y.A., Auras, R., 2017. Antimicrobial efficacy of clove essential oil infused into chemically modified LLDPE film for chicken meat packaging. *Food Control* **73**, 663-671.

Mungroo, R., Pradhan, N.C., Goud, V.V., Dalai, A.K., 2008. Epoxidation of canola oil with hydrogen peroxide catalyzed by acidic ion exchange resin. *Journal of the American Oil Chemists' Society* **85**(9), 887-896.

Nisha, A., Sankar, K.U., Venkateswaran, G., 2012. Supercritical CO_2 extraction of Mortierella alpina single cell oil: Comparison with organic solvent extraction. *Food chemistry* **133**(1), 220-226.

Okieimen, F.E., Pavithran, C., Bakare, I.O., 2005. Epoxidation and hydroxlation of rubber seed oil: one-pot multi-step reactions. *European Journal of Lipid Science and Technology* **107**(5), 330-336.

Olkiewicz, M., Caporgno, M.P., Fortuny, A., Stüber, F., Fabregat, A., Font, J., Bengoa, C., 2014. Direct liquid–liquid extraction of lipid from municipal sewage sludge for biodiesel production. *Fuel Processing Technology* **128**, 331-338.

Orellana, J.L., Smith, T.D., Kitchens, C.L., 2013. Liquid and supercritical CO2 extraction of fat from rendered materials. *The Journal of Supercritical Fluids* **79**, 55-61.

Orr, V.C.A., Plechkova, N.V., Seddon, K.R., Rehmann, L., 2016. Disruption and Wet Extraction of the Microalgae Chlorella vulgaris Using Room-Temperature Ionic Liquids. *ACS Sustainable Chemistry & Engineering* **4**(2), 591-600.

Osen, R., Toelstede, S., Wild, F., Eisner, P., Schweiggert-Weisz, U., 2014. High moisture extrusion cooking of pea protein isolates: Raw material characteristics, extruder responses, and texture properties. *Journal of Food Engineering* **127**(Supplement C), 67-74.

Pacheco-Torgal, F., Diamanti, M.V., Nazari, A., Goran-Granqvist, C., Pruna, A., Amirkhanian, S., 2018. Nanotechnology in eco-efficient construction: Materials, Processes and Applications. Woodhead Publishing.

Papanikolaou, S., Dimou, A., Fakas, S., Diamantopoulou, P., Philippoussis, A., Galiotou-Panayotou, M., Aggelis, G., 2011. Biotechnological conversion of waste cooking olive oil into lipid-rich biomass using Aspergillus and Penicillium strains. *Journal of Applied Microbiology* **110**(5), 1138-1150.

Parameswaranpillai, J., Sidhardhan, S.K., Jose, S., Hameed, N., Salim, N.V., Siengchin, S., Pionteck, J.r., Magueresse, A., Grohens, Y., 2016. Miscibility, phase morphology, thermomechanical, viscoelastic and surface properties of poly (ε-caprolactone) modified epoxy systems: effect of curing agents. *Industrial & Engineering Chemistry Research* **55**(38), 10055-10064.

Passos, M.L., Ribeiro, C.P., 2016. Innovation in food engineering: New techniques and products. CRC Press, New York, USA.

Patil, C.K., Jirimali, H.D., Paradeshi, J.S., Chaudhari, B.L., Gite, V.V., 2019. Functional antimicrobial and anticorrosive polyurethane composite coatings from algae oil and silver doped egg shell hydroxyapatite for sustainable development. *Progress in Organic Coatings* **128**, 127-136.

Paul, D., Robeson, L.M., 2008. Polymer nanotechnology: nanocomposites. *Polymer* **49**(15), 3187-3204.

Peelman, N., Ragaert, P., De Meulenaer, B., Adons, D., Peeters, R., Cardon, L., Van Impe, F., Devlieghere, F., 2013. Application of bioplastics for food packaging. *Trends in Food Science & Technology* **32**(2), 128-141.

Petrović, Z.S., 2008. Polyurethanes from vegetable oils. *Polymer Reviews* 48(1), 109-155.

Philp, J.C., Bartsev, A., Ritchie, R.J., Baucher, M.-A., Guy, K., 2013. Bioplastics science from a policy vantage point. *New biotechnology* **30**(6), 635-646.

Piker, A., Tabah, B., Perkas, N., Gedanken, A., 2016. A green and low-cost room temperature biodiesel production method from waste oil using egg shells as catalyst. *Fuel* **182**(Supplement C), 34-41.

Pueyo, E., Martínez-Rodríguez, A., Polo, M.C., Santa-María, G., Bartolomé, B., 2000. Release of lipids during yeast autolysis in a model wine system. *Journal of agricultural and food chemistry* **48**(1), 116-122.

Qadeer, S., Khalid, A., Mahmood, S., Anjum, M., Ahmad, Z., 2017. Utilizing oleaginous bacteria and fungi for cleaner energy production. *Journal of Cleaner Production* **168**, 917-928.

Qi, X., Zhang, Y., Chang, C., Luo, X., Li, Y., 2018. Thermal, Mechanical, and Morphological Properties of Rigid Crude Glycerol-Based Polyurethane Foams Reinforced With Nanoclay

and Microcrystalline Cellulose. *European journal of lipid science and technology* **120**(5), 1700413.

Radient, 2018, January 12. Radient technology. http://radientinc.com/index.php.

Ranjith Kumar, R., Hanumantha Rao, P., Arumugam, M., 2015. Lipid extraction methods from microalgae: a comprehensive review. *Frontiers in Energy Research* **2**, 61.

Rastegari, H., Jazini, H., Ghaziaskar, H.S., Yalpani, M., 2019. Applications of Biodiesel By-products, Biodiesel. Springer, pp. 101-125.

Raventós, M., Duarte, S., Alarcón, R., 2002. Application and possibilities of supercritical CO2 extraction in food processing industry: an overview. *Food Science and Technology International* **8**(5), 269-284.

Ray, S.S., Bousmina, M., 2005. Biodegradable polymers and their layered silicate nanocomposites: in greening the 21st century materials world. *Progress in materials science* **50**(8), 962-1079.

Rocha Garcia, C., Youssef, E., Souza, N., Matsushita, M., Figueiredo, E., Shimokomaki, M., 2003. Preservation of spent leghorn hen meat by a drying and salting process. *Journal of applied poultry research* **12**(3), 335-340.

Rwahwire, S., Tomkova, B., Periyasamy, A.P., Kale, B.M., 2019. Green thermoset reinforced biocomposites, Green Composites for Automotive Applications. Elsevier, pp. 61-80.

Sahmani, S., Shahali, M., Khandan, A., Saber-Samandari, S., Aghdam, M., 2018. Analytical and experimental analyses for mechanical and biological characteristics of novel nanoclay bio-nanocomposite scaffolds fabricated via space holder technique. *Applied Clay Science* **165**, 112-123.

Salimon, J., Abdullah, B.M., Salih, N., 2011. Hydrolysis optimization and characterization study of preparing fatty acids from Jatropha curcas seed oil. *Chemistry Central Journal* **5**(1), 67.

Sánchez-Camargo, A.P., Martinez-Correa, H.A., Paviani, L.C., Cabral, F.A., 2011. Supercritical CO2 extraction of lipids and astaxanthin from Brazilian redspotted shrimp waste (Farfantepenaeus paulensis). *The Journal of Supercritical Fluids* **56**(2), 164-173.

Satyanarayana, K.G., Arizaga, G.G., Wypych, F., 2009. Biodegradable composites based on lignocellulosic fibers—An overview. *Progress in polymer science* **34**(9), 982-1021.

Schneiderman, D.K., Hillmyer, M.A., 2017. 50th anniversary perspective: There is a great future in sustainable polymers. *Macromolecules* **50**(10), 3733-3749.

Sharma, B.K., Adhvaryu, A., Liu, Z., Erhan, S.Z., 2006. Chemical modification of vegetable oils for lubricant applications. *Journal of the American Oil Chemists' Society* **83**(2), 129-136.

Sharmin, E., Zafar, F., Akram, D., Alam, M., Ahmad, S., 2015. Recent advances in vegetable oils based environment friendly coatings: A review. *Industrial Crops and Products* **76**, 215-229.

Sinadinović-Fišer, S., Janković, M., Borota, O., 2012. Epoxidation of castor oil with peracetic acid formed in situ in the presence of an ion exchange resin. *Chemical Engineering and Processing: Process Intensification* **62**, 106-113.

Soh, L., Zimmerman, J., 2011. Biodiesel production: the potential of algal lipids extracted with supercritical carbon dioxide. *Green Chemistry* **13**(6), 1422-1429.

Song, L., Wang, Z., Lamm, M.E., Yuan, L., Tang, C., 2017. Supramolecular polymer nanocomposites derived from plant oils and cellulose nanocrystals. *Macromolecules* **50**(19), 7475-7483.

Souza, V.G.L., Fernando, A.L., 2016. Nanoparticles in food packaging: Biodegradability and potential migration to food—A review. *Food Packaging and Shelf Life* 8, 63-70.

Spurr, A.R., 1969. A low-viscosity epoxy resin embedding medium for electron microscopy. *Journal of Ultrastructure Research* **26**(1-2), 31-43.

Srivastava, A., Prasad, R., 2000. Triglycerides-based diesel fuels. *Renewable and sustainable Energy Reviews* **4**(2), 111-133.

Stephen, J.L., Periyasamy, B., 2018. Innovative developments in biofuels production from organic waste materials: A review. *Fuel* **214**, 623-633.

Sun, M., Temelli, F., 2006. Supercritical carbon dioxide extraction of carotenoids from carrot using canola oil as a continuous co-solvent. *The Journal of supercritical fluids* **37**(3), 397-408.

Sun, S., Yang, G., Bi, Y., Liang, H., 2011. Enzymatic epoxidation of corn oil by perstearic acid. *Journal of the American Oil Chemists' Society* **88**(10), 1567-1571.

Suzuki, A.H., Botelho, B.G., Oliveira, L.S., Franca, A.S., 2018. Sustainable synthesis of epoxidized waste cooking oil and its application as a plasticizer for polyvinyl chloride films. *European Polymer Journal* **99**, 142-149.

Tactacan, G.B., Guenter, W., Lewis, N.J., Rodriguez-Lecompte, J.C., House, J.D., 2009. Performance and welfare of laying hens in conventional and enriched cages. *Poultry Science* **88**(4), 698-707.

Tao, B.Y., 2007. Chapter 24 - Industrial Applications for Plant Oils and Lipids A2 - Yang, Shang-Tian, Bioprocessing for Value-Added Products from Renewable Resources. Elsevier, Amsterdam, pp. 611-627.

Teles dos Santos, M., Gerbaud, V., Le Roux, G.A.C., 2012. Comparison of predicted and experimental DSC curves for vegetable oils. *Thermochimica Acta* **545**(Supplement C), 96-102.

Temelli, F., 1992. Extraction of triglycerides and phospholipids from canola with supercritical carbon dioxide and ethanol. *Journal of Food Science* **57**(2), 440-443.

Temelli, F., 2009. Perspectives on supercritical fluid processing of fats and oils. *The Journal of Supercritical Fluids* **47**(3), 583-590.

Tharanathan, R., 2003. Biodegradable films and composite coatings: past, present and future. *Trends in food science & technology* **14**(3), 71-78.

Tuck, C.O., Pérez, E., Horváth, I.T., Sheldon, R.A., Poliakoff, M., 2012. Valorization of biomass: deriving more value from waste. *Science* **337**(6095), 695-699.

Ullah, A., Vasanthan, T., Bressler, D., Elias, A.L., Wu, J., 2011. Bioplastics from feather quill. *Biomacromolecules* **12**(10), 3826-3832.

Ullah, A., Wu, J., 2013. Feather fiber-based thermoplastics: effects of different plasticizers on material properties. *Macromolecular Materials and Engineering* **298**(2), 153-162.

Viner, K., Champagne, P., Jessop, P.G., 2018. Comparison of cell disruption techniques prior to lipid extraction from Scenedesmus sp. slurries for biodiesel production using liquid CO_2. *Green Chemistry* **20**(18), 4330-4338.

Vlachos, N., Skopelitis, Y., Psaroudaki, M., Konstantinidou, V., Chatzilazarou, A., Tegou, E., 2006. Applications of Fourier transform-infrared spectroscopy to edible oils. *Analytica Chimica Acta* **573**, 459-465.

Wahidin, S., Idris, A., Shaleh, S.R.M., 2014. Rapid biodiesel production using wet microalgae via microwave irradiation. *Energy Conversion and Management* **84**(Supplement C), 227-233.

Wang, C., Qian, L., Wang, W., Wang, T., Deng, Z., Yang, F., Xiong, J., Feng, W., 2017. Exploring the potential of lipids from black soldier fly: New paradigm for biodiesel production (I). *Renewable Energy* **111**(Supplement C), 749-756.

Wang, H., Wu, J., Betti, M., 2013. Chemical, rheological and surface morphologic characterisation of spent hen proteins extracted by pH-shift processing with or without the presence of cryoprotectants. *Food Chemistry* **139**(1), 710-719.

Wróblewska-Krepsztul, J., Rydzkowski, T., Borowski, G., Szczypiński, M., Klepka, T., Thakur, V.K., 2018. Recent progress in biodegradable polymers and nanocomposite-based packaging materials for sustainable environment. *International Journal of Polymer Analysis and Characterization* **23**(4), 383-395.

Wu, C.-S., 2012. Characterization and biodegradability of polyester bioplastic-based green renewable composites from agricultural residues. *Polymer degradation and stability* **97**(1), 64-71.

Wu, S., Baskin, T.I., Gallagher, K.L., 2012. Mechanical fixation techniques for processing and orienting delicate samples, such as the root of Arabidopsis thaliana, for light or electron microscopy. *Nature Protocols* **7**(6), 1113.

Wu, T., Xue, Q., Li, X., Tao, Y., Jin, Y., Ling, C., Lu, S., 2016. Extraction of kerogen from oil shale with supercritical carbon dioxide: Molecular dynamics simulations. *The Journal of Supercritical Fluids* **107**, 499-506.

Wu, Y., Ni, G., Yang, F., Li, C., Dong, G., 2012. Modified maleic anhydride co-polymers as pour-point depressants and their effects on waxy crude oil rheology. *Energy & Fuels* **26**(2), 995-1001.

Xia, W., Budge, S.M., Lumsden, M.D., 2016. ^{1}H-NMR Characterization of epoxides derived from polyunsaturated fatty acids. *Journal of the American Oil Chemists' Society* **93**(4), 467-478.

Xia, Y., Larock, R.C., 2010. Vegetable oil-based polymeric materials: synthesis, properties, and applications. *Green Chemistry* **12**(11), 1893-1909.

Xiao, W., Han, L., Shi, B., 2008. Microwave-assisted extraction of flavonoids from Radix Astragali. *Separation and Purification Technology* **62**(3), 614-618.

Xu, J., Wu, H.-C., Zhu, C., Ehrlich, A., Shaw, L., Nikolka, M., Wang, S., Molina-Lopez, F., Gu, X., Luo, S., 2019. Multi-scale ordering in highly stretchable polymer semiconducting films. *Nature materials* **18**(6), 594.

Xu, X., Sun, L., Dong, J., Zhang, H., 2009. Breaking the cells of rape bee pollen and consecutive extraction of functional oil with supercritical carbon dioxide. *Innovative food science & emerging technologies* **10**(1), 42-46.

Yan, M., Huang, Y., Lu, M., Lin, F.-Y., Hernández, N.B., Cochran, E.W., 2016. Gel point suppression in RAFT polymerization of pure acrylic cross-linker derived from soybean oil. *Biomacromolecules* **17**(8), 2701-2709.

Yanık, D.K., 2017. Alternative to traditional olive pomace oil extraction systems: Microwave-assisted solvent extraction of oil from wet olive pomace. *LWT - Food Science and Technology* **77**(Supplement C), 45-51.

Yu, L., Dean, K., Li, L., 2006. Polymer blends and composites from renewable resources. *Progress in polymer science* **31**(6), 576-602.

Yu, W., Field, C.J., Wu, J., 2018. Purification and identification of anti-inflammatory peptides from spent hen muscle proteins hydrolysate. *Food Chemistry* **253**, 101-107.

Zhang, B., Wang, Q., 2012. Development of highly ordered nanofillers in zein nanocomposites for improved tensile and barrier properties. *Journal of agricultural and food chemistry* **60**(16), 4162-4169.

Zhang, C., Garrison, T.F., Madbouly, S.A., Kessler, M.R., 2017. Recent advances in vegetable oil-based polymers and their composites. *Progress in Polymer Science* **71**, 91-143.

Zhang, P., Zhang, J., 2013. One-step acrylation of soybean oil (SO) for the preparation of SO-based macromonomers. *Green Chemistry* **15**(3), 641-645.

Zhao, L., Temelli, F., Curtis, J.M., Chen, L., 2015. Preparation of liposomes using supercritical carbon dioxide technology: Effects of phospholipids and sterols. *Food Research International* **77**(Part 1), 63-72.

Zheng, H., Yin, J., Gao, Z., Huang, H., Ji, X., Dou, C., 2011. Disruption of *Chlorella vulgaris* cells for the release of biodiesel-producing lipids: a comparison of grinding, ultrasonication, bead milling, enzymatic lysis, and microwaves. *Applied biochemistry and biotechnology* **164**(7), 1215-1224.

Zhu, Y., Romain, C., Williams, C.K., 2016. Sustainable polymers from renewable resources. *Nature* **540**(7633), 354.

Zubair, M., Ullah, A., 2019. Recent advances in protein derived bionanocomposites for food packaging applications. *Critical reviews in food science and nutrition,* 1-29.

Zubair, M., Wu, J., Ullah, A., 2019. Hybrid Bionanocomposites from Spent hen proteins. *ACS Omega* **4**(2), 3772-3781.